

Central Laser Facility Annual Report

2018–2019



Science and
Technology
Facilities Council



Central Laser Facility
Science & Technology Facilities Council
Rutherford Appleton Laboratory
Harwell Campus
Didcot, Oxfordshire OX11 0QX
T: +44 (0)1235 445603
E: clfannrep@stfc.ac.uk
W: www.clf.stfc.ac.uk
Front cover design: Helen Towrie
ISBN: 978-0-9574402-7-2

The production team for this Annual Report was as follows:

Editor: Raoul Trines

Production: Tracey Burge, Lizzie Henderson and Raoul Trines

Section Editors: David Carroll, Richard Chapman, Ian Clark, Dave Clarke, Rob Clarke, James Green, Chris Hooker, Ian Musgrave, David Neely, Rajeev Pattathil, Jonathan Phillips, Dan Symes, Martin Tolley, Raoul Trines, Christopher Tynan, Adam Wyatt

This report is available on the CLF website at www.clf.stfc.ac.uk

Design, layout and production: UKRI Creative Services (JRS)

Thanks to all of the above for their contribution towards producing this report and, of course, to all of the authors for their submissions.

Contents

Foreword	4
Overview of the Central Laser Facility	6
Industry Engagement and Innovation	10
Communication and Outreach Activities within the CLF	12
High Energy Density & High Intensity Physics	16
Laser Science & Development	27
Theory & Computation	37
Plasma Diagnostics	38
Ultrafast & XUV Science	41
Imaging & Dynamics for Physical & Life Sciences	43
Appendices	57
Operational Statistics	57
Publications	65
Panel Membership and CLF Structure	74

Foreword

John Collier

Director, Central Laser Facility, STFC Rutherford Appleton Laboratory, Harwell Campus, Didcot, UK
Email address: john.collier@stfc.ac.uk Website: www.clf.stfc.ac.uk



This annual report for the Central Laser Facility (CLF) at the STFC Rutherford Appleton Laboratory provides highlights of scientific and technical research that has been carried out by users of the Facility and its staff over the financial year 2018-19.

The CLF and its community have continued to deliver scientific output and technical development of the highest order.

Vulcan – has progressed the design of a new short-pulse beamline for the Vulcan TAP (Target Area Petawatt) area. Based on the OPCPA technique that the CLF has pioneered, this will deliver a petawatt level pulse (30 J in 30 fs) in addition to the existing petawatt (500 J, 500 fs) and long pulse (250 J) capabilities. This beamline will enable new areas of imaging and combined proton/electron interactions to take place. Tenders for the main equipment have been started and work to transform the old Target Area East into the new laser area for the beamline is nearing completion.

Gemini – discovered a potential solution for one of the perennial problems with pointing jitter, affected by vibrations. This solution, based on stabilising a back-propagating beam from the focus, was successfully tested and put into effect in an experiment in Gemini. We also took a great stride towards implementing machine learning algorithms for plasma-based accelerators. An experiment in Gemini's Astra target area used a genetic algorithm to apply active feedback to optimise laser-driven electron acceleration, the results of which were published in *Physical Review Accelerators and Beams*.

Artemis – has moved across campus to the Research Complex at Harwell as part of a major upgrade. The upgraded Artemis will include a new laser system – a mid-IR system running at 100 kHz – which is a joint development with Ultra. This year saw the building and installation of new laboratories, which will re-open in 2020. These laboratories will hold three dedicated XUV beamlines for imaging, photoemission from condensed matter, and gas-phase photoelectron spectroscopy.

Target Fabrication – has maintained delivery of high specification targets to the internal user programme, including development of multi-element assemblies with high alignment tolerances and novel coil geometries for ion acceleration experiments. Target delivery has been achieved using the highly specialist equipment available within the CLF and more widely across STFC. The investments in x-ray computed tomography (CT) for characterisation have allowed Target Fabrication to provide user groups with increased data on targets, while the further development of single point diamond turning for precision machining has allowed new targets to be fielded. High repetition rate targetry developments include robotic assembly and tape targets. Scitech Precision Limited (the spin out from CLF Target Fabrication) has provided microtargets to many national and university laboratories across the world, in addition to supplying precision laser machining services to support the high-tech businesses on the wider campus.

Plasma Physics Group – has improved its provision of codes, cluster resources, and direct user support. The group is in the process of obtaining a replacement for the computer cluster SCARF-Lexicon-2, namely SCARF-DeMagnet, which will be of comparable specification.

The CLF's *Ultra* and *Octopus* facilities in the Research Complex at Harwell continue to serve a multidisciplinary community, with user programmes in areas ranging from fundamental chemistry and materials science to biomedical and environmental research.

Ultra – delivered 60 weeks of access to the academic community and two weeks to industrial users. The changes in the structure of proteins and DNA underpin their function in nature; to study the dynamics of these changes, Ultra has developed a unique two-dimensional infrared (2DIR) spectrometer with 1 ns high intensity laser that induces bimolecular change by creating temperature jumps in the sample. A new programme, “Structural dynamics and photoinduced electron transfer”, will deliver new understanding on the mechanisms of electron transfer. This research will impact the development of photocatalysts and light energy harvesting and chemical synthesis.

Octopus – delivered 100 weeks of access to the user community. This included 10 weeks of proof of concept access, enabling prospective users to make short visits for feasibility studies. In addition to this, the facility has delivered industrial access to a number of companies, through paid access, collaboration with academia, and the Bridging for Innovators (B4I) funding programme. Development on correlative light and electron microscopy (CLEM) continues. The most recent development, funded jointly by BBSRC’s 18ALERT scheme and the CLF, was the installation of a cryo focused ion-beam scanning electron microscope that will be used for both imaging and preparation of samples for transmission electron microscopy, as part of a CLEM workflow involving other Octopus microscopes.

Following delivery of the first 1 kW DiPOLE system to the HiLASE Centre in Dolní Břežany, Czech Republic, the CLF’s Centre for Advanced Laser Technology and Applications (**CALTA**) has made significant progress on the construction of a second system destined for the European XFEL in Hamburg. Funded through a joint STFC / EPSRC research grant, this “DiPOLE 100” will be used to drive materials to high pressure states to be diagnosed using the XFEL x-ray beam. A unique temporal pulse shaping capability, developed specifically for the XFEL application, will enable precise control of the pressure produced, while the high repetition rate will enable rapid accumulation of data for improved measurement accuracy. The system build is nearing completion and commissioning of the first stage of amplification is underway.

Further development of the DiPOLE Diode Pumped Solid State Laser (DPSSL) technology is an essential element of a Widespread Teaming collaboration between STFC and the HiLASE Centre. The €50M project to establish HiLASE as a Centre of Excellence is jointly funded by the EC and the

Czech Ministry of Science. STFC is assisting in the establishment of the Centre and is playing a leading role in the development of advanced DPSSL technology. This includes the design and construction of a 100 Hz version of the DiPOLE 10 J laser, increasing the pulse energy of the DiPOLE architecture and developing efficient second and third harmonic generation at 10 Hz. This will extend STFC’s lead at the forefront of DPSSL technology.

Industry Partnerships and Innovation Group

has been established to build and manage the CLF’s partnerships with industry, deliver contract access to our capabilities and expertise, and oversee the innovation activities within the department. The CLF continues to participate in the STFC Bridging For Innovators funding programme, which offers businesses access to STFC facilities for projects that fast-track solutions to industrial challenges. For example, OxSyBio, a University of Oxford spin out developing adipose models for testing new drugs, accessed microscopy techniques in Octopus to validate their 3D printed cell structures. *“It is a powerful platform for potentially identifying new therapeutic interventions for metabolic diseases. This achievement has only been possible through a multi-institutional collaboration between a broad range of specialists at OxSyBio, MRC Harwell Institute and the Central Laser Facility.”* Dr Alex Graham (MRC-Harwell).

Dr Chris Thornton at the CLF was successful in his application for a three-year UKRI-EPSRC Innovation Fellowship, in partnership with Johnson Matthey, the Manufacturing Technology Centre and Warwick Manufacturing Group. The Fellowship is hosted at the CLF and is focused on laser-driven x-ray techniques for advanced micro-CT imaging and x-ray absorption spectroscopy.

I do hope that you enjoy reading this selection of abstracts. Please visit the CLF website to access the full papers and find out more about the exciting times ahead at the CLF!



Professor John Collier FLSW
Director, Central Laser Facility

Overview of the Central Laser Facility (CLF)

Cristina Hernandez-Gomez

Central Laser Facility, STFC Rutherford Appleton Laboratory, Harwell Campus, Didcot, UK
Email address: cristina.hernandez-gomez@stfc.ac.uk Website: www.clf.stfc.ac.uk

The CLF is a world leading centre for research using lasers in a wide range of scientific disciplines. This section provides an overview of the capabilities offered to our international academic and industrial community.

Vulcan

Vulcan is a versatile high power laser system that is composed of Nd:glass amplifier chains capable of delivering up to 2.6 kJ of laser energy in long pulses (nanosecond duration) and up to 1 PW peak power in a short pulse (500 fs duration) at 1053 nm.

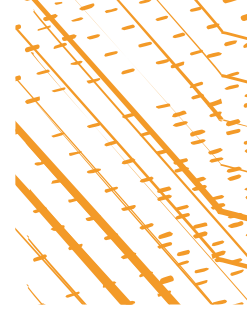
It currently has eight beam lines. Two of these beam lines can operate in either short pulse mode or long pulse mode, while the remaining six normally operate in a long pulse mode. The short-pulse and long-pulse systems operating jointly can be directed to two different target areas, enabling sophisticated interaction and probing experiments.

We have continued the design of a new short-pulse beamline for the Vulcan TAP area based on the technique of OPCPA which the CLF has pioneered. The upgrade will deliver a PW level pulse (30 J in 30 fs) in addition to the existing PW (500 J, 500 fs) and long pulse (250 J) capabilities. This will enable new areas of imaging and combined proton/electron interactions to take place. Designs for the main compressor and turning chambers are complete and in the process of procurement. At the same time, the refurbishment of the old Target Area East is nearing completion – transforming the area into a new laser bay for the new beamline front end and main amplifiers.

Gemini

Gemini is a Titanium-Sapphire based dual-beam high power laser system with two synchronised Petawatt-class beams, enabling pump-probe studies at extreme light intensities ($>10^{21}$ Wcm⁻²). In recent years, Gemini has emerged as one of the preeminent centres in the world for laser-driven acceleration. This year, Gemini performed some highly complicated experiments ranging from medical applications of laser-driven ion beams to implementing new techniques for laser-plasma electron accelerators. Experiments studied the biological effectiveness of laser-accelerated ions for cancer therapy, and ultrafast pulsed ion radiolysis with much better time resolution than previously possible. Progress towards operating laser-driven sources at higher repetition rates has included using a train of pulses in Target Area 3 to excite wakefields, thus lowering the demand on laser energy in the future. Operating Target Area 2 at 5 Hz allowed the implementation of feedback techniques that directly optimised secondary sources generated in the plasma. These developments, including machine learning methods, will be crucial to fully exploit upcoming high repetition rate petawatt laser facilities.

An important facility development has been progress towards active stabilisation of the laser beam onto target – for a consistent interaction between the laser pulse and the plasma, fluctuations in beam pointing must be minimised. This is particularly the case in dual beam experiments when the pulses need to be well overlapped both spatially and temporally. A beam stabilisation system was trialled consisting of a fibre-coupled pilot laser back-propagated from a gas cell target. Measurements of the position of this beam fed into a piezo-electrically driven mirror in the laser system that corrected pointing fluctuations at high frequency. This improved laser pointing jitter by a factor of 2.5 and in initial tests reduced electron beam jitter by 20%.



Artemis

Artemis is the CLF's facility for ultrafast laser and XUV science. It offers ultrashort pulses at high repetition-rate, spanning the spectral range from the XUV to the far-infrared. The facility is configured flexibly for pump-probe experiments. Tuneable or few-cycle pulses can be used as pump and probe pulses, or to generate ultrafast, coherent XUV pulses through high harmonic generation. XUV beamlines lead to end-stations for time-resolved photoelectron spectroscopy (for both gas-phase and condensed matter experiments) and coherent lensless XUV imaging.

Artemis has received funding for a major upgrade, and has re-located across campus to the Research Complex at Harwell (RCaH), adding a new laser system and a third XUV beamline. The new 100 kHz laser system operates at 1700 nm and 3000 nm, and is a joint purchase with Ultra. It will complement the existing 1 kHz Ti:Sapphire system, which has been updated with a new amplifier to increase the energy available for XUV generation. Over 2018-19, building work to upgrade the labs has been carried out, for re-opening of the upgraded facility in 2020.

Target Fabrication

The Target Fabrication Group makes the majority of the solid targets shot on the CLF's high-power lasers and also supports micro-assembly and characterisation in the wider CLF. The Group is also responsible for the production of targets for academic access shots on the Orion Facility at AWE. Commercial access to target fabrication capabilities is available to external laboratories and experimentalists via the spin-out company Scitech Precision Ltd.

A wide variety of microtarget types are produced to enable the exploration of many experimental regimes. Fabrication techniques include thin film coating, precision micro

assembly, laser micromachining, and chemistry processes, all verified by sophisticated characterisation. STFC's advanced capabilities in both high precision micro machining and MEMS microfabrication are also utilised. The Group is ISO9001 accredited and has been awarded the latest ISO9001:2015 standard for its process management, providing a high level of traceability for all supplied microtargets.

This year, work has continued to implement robotic assembly for simple target geometries, to facilitate the production of array targets for high rep rate experiments. In collaboration with Scitech Precision, a high stability, high rep-rate (HRR) tape drive has been tested, to deliver targets to the Gemini laser and to other HRR facilities at up to 10 Hz. This work to produce complex tapes will open up new experimental regimes for the user community.

The Group remains at the leading edge of target fabrication technology, collaborating with universities in areas such as nanowire growth, thin diamond production, and advanced micro machining. Work with the LSF on the assembly of advanced micro optics has enabled a number of high profile publications.

Theory and Modelling

The Plasma Physics Group supports scheduled experiments throughout the design, analysis and interpretation phases, as well as users who need theoretical support in matters relating to CLF science. We support principal investigators using radiation hydrodynamics, particle-in-cell, hybrid and Vlasov-Fokker-Planck codes, as well as by providing access to large-scale computing. Access to the PRISM suite has been renewed for a further year, as endorsed by the CLF User Forum. Support for student training in plasma physics, computational methods and opportunities for networking with colleagues will continue to be provided. Extended collaborative placements within the group are particularly encouraged.

In 2018 the group started replacing the SCARF-Lexicon-2 cluster with an up-to-date replacement, SCARF-DeMagnet which we hope will be operational in 2019.

Octopus and Ultra (Research Complex at Harwell)

The CLF operates two facilities in the RCaH: Ultra, for ultrafast molecular dynamics measurements in chemistry and biology, and Octopus, a cluster of advanced laser microscopes for life science research.

In the molecular and materials dynamics area, Ultra offers state-of-the-art high power high repetition rate fs / ps systems to generate pulses for a range of highly sensitive pump and probe vibrational spectroscopy techniques. These capture “movies” of the atomic and molecular dynamics used to study processes ranging from reactions in nature, energy capture and storage, catalysis and fundamental quantum level research on molecular and bio-molecular electronics, probes, therapeutics, enzymes and DNA. Kerr gated time resolved resonance Raman (TR^3) is unique in enabling highly fluorescent samples to be studied. Time-Resolved Multiple-Probe Spectroscopy (TR^MPS) captures reactions from their earliest beginning on femtosecond timescales to completion on milliseconds timescales. Fast scanning ultrafast 2DIR spectroscopies capture intra- and inter-molecular vibrational coupling and energy transport applied in fundamental molecular dynamics research and in pharmaceutical analytical research. Broad spectral band surface sum frequency generation provides insights into the chemical changes that occur at interfaces and surfaces where many reactions in nature and industry occur.

In the imaging area, the Octopus cluster offers a range of microscopy stations linked to a central core of pulsed and CW lasers offering “tailor-made” illumination for imaging. Microscopy techniques offered include total internal reflection (TIRF) and multi-wavelength single-molecule

imaging, confocal microscopy (including multiphoton), fluorescence energy transfer (FRET) and fluorescence lifetime imaging (FLIM). Super-resolution techniques available are Stochastic Optical Reconstruction Microscopy (STORM) with adaptive optics, Photoactivated Localization Microscopy (PALM), Structured Illumination Microscopy (SIM) and Stimulated Emission Depletion Microscopy (STED), Light Sheet Microscopy, and super-resolution cryo-microscopy. Laser tweezers are available for combined manipulation/trapping and imaging with other Octopus stations, and can also be used to study Raman spectra and pico-Newton forces between particles in solution for bioscience and environmental research. Current developments include 3D super-resolution microscopy using point spread function engineering, and a cryo focussed ion beam scanning electron microscope (FIB-SEM) has recently been commissioned with the aim of developing a workflow for correlative light and electron microscopy (CLEM).

Chemistry, biology, and spectroscopy laboratories support the laser facilities, and the CLF offers access to a multidisciplinary team providing advice to users on all aspects of imaging and spectroscopy, including specialised biological sample preparation, data acquisition, and advanced data analysis techniques. Access is also available to shared facilities in the Research Complex, including cell culture, scanning and transmission electron microscopy, NMR, and x-ray diffraction.

Engineering Services

Engineering is fundamental to all the operations and developments in the CLF. The engineering team operates across all of the CLF’s facilities, and endeavours to continually improve and expand the capabilities and reliability of the CLF. Mechanical, electrical and software support is provided for the operation of the laser facilities, for the experimental programmes on these facilities, and for the CLF’s research and development activities. These developments can range from small-scale modifications to existing equipment to improve its performance, through to larger scale projects, such as the design and development of commercial projects. In addition, we have active engineering collaborations with regional and international partners such as, HiLASE (Prague, Czech Republic), XFEL (Hamburg, Germany) and TIFR (Hyderabad, India).

Over the last year the Mechanical Engineering Section has seen significant growth. The mechanical workshop is now fully staffed, and new machinery is in place to expand its capabilities. The workshop and storage area for the Experimental Support Technicians has also been regenerated to provide a purpose-built assembly area.

Centre for Advanced Laser Technology and Applications (CALTA)

CALTA's mission is to deliver societal, scientific and economic impact from developments in the CLF. Hosting CALTA at the CLF enables novel technology and associated applications to be developed in the shortest possible time. Access to the CLF infrastructure and expertise (cleanrooms, optical metrology and advanced diagnostics, etc.), STFC's capability in cryogenics and high performance computing, and commercial connections within the Business and Innovation Department is key to its present and future success.

CALTA has successfully developed a new class of lasers capable of delivering high energy, high peak power pulses at high repetition rate and high efficiency. This DiPOLE Diode Pumped Solid State Laser (DPSSL) architecture is driving new applications in advanced imaging, materials processing, non-destructive testing and fundamental science.

The first 1 kW DiPOLE system was developed under a commercial contract for the HiLASE Centre in the Czech Republic. Following delivery and installation, a joint CLF/HiLASE team commissioned the laser to its full design specification in December 2016, producing 100 J in 10 ns pulses at 10 Hz. This performance gives DiPOLE an enduring world lead in this area of laser technology.

Construction of a second 1 kW laser, destined for the European XFEL in Hamburg in late 2019, is well underway. Funded through a joint STFC / EPSRC research grant, the "DiPOLE 100" will be used to drive materials to high energy density states to be diagnosed using the XFEL x-ray beam. A unique temporal pulse shaping capability will enable precise control of the material energetic states produced while the high repetition rate will enable rapid accumulation of data for improved measurement accuracy.

The development of advanced DPSSL technology forms an essential element of a Widespread Teaming collaboration between STFC and the HiLASE Centre. The €50M project to establish HiLASE as a Centre of Excellence is jointly funded by the EC and the Czech Ministry of Science. STFC input includes the design and construction of a 100 Hz version of the DiPOLE 10 J laser, increasing the output power of the DiPOLE architecture and developing efficient second and third harmonic generation at 10 Hz. This work will extend STFC's lead at the forefront of DPSSL technology.

Economic impact

The CLF completed eight contract-access projects with industrial users, delivering experimental access to Gemini, Ultra, and Octopus, and access to expertise in target fabrication and CALTA.

The CLF-Johnson Matthey partnership continues, led by Dr Kathryn Welsby as the CLF-JM industry research fellow, with a series of access projects and iCASE studentships. Other ongoing CLF-industry partnerships include Dstl, Sellafield and AstraZeneca.

Three new proof-of-concept projects were funded and started, while four were completed. From target fabrication techniques, to microscopy optics, to detector readout solutions, the range of innovations coming from CLF expertise has the potential to impact on many sectors. The CLF filed two new patent families this year, giving a current total of 19 active patent families.

Access to Facilities

Calls for access are made twice a year, with applications peer reviewed by external Facility Access Panels.

The CLF operates "free at the point of access", available to any UK academic or industrial group engaged in open scientific research, subject to external peer review. European collaboration is fully open for the high power lasers, whilst European and International collaborations are also encouraged across the CLF suite for significant fractions of the time. Dedicated access to CLF facilities is awarded to European researchers via the LaserLab-Europe initiative (www.laserlab-europe.net) funded by the European Commission.

Hiring of the facilities and access to CLF expertise is also available on a commercial basis for proprietary or urgent industrial research and development.

Please visit www.clf.stfc.ac.uk for more details on all aspects of the CLF.

Industry Engagement and Innovation

Ceri Brenner

Central Laser Facility, STFC Rutherford Appleton Laboratory, Harwell Campus, Didcot, UK
Email address: ceri.brenner@stfc.ac.uk

This article highlights the industrial user engagement, industry partnerships, and innovation activities of the Central Laser Facility for the reporting period April 2018 to March 2019.

Industrial users and engagement

The CLF completed eight commercial contract access projects with industrial users this year, delivering experimental access to Gemini, Ultra and Octopus, and access to expertise in target fabrication and CALTA. From fluorescence microscopy for tracking intracellular pathways in drug development, to laser-driven accelerators for development of defence sector technologies, to spectroscopy to support novel catalyst development, the CLF's expertise in combination with its world-class capabilities and laser-based techniques continue to make an impact on a wide variety of industrial science themes and R&D areas.

The CLF continues to participate in the STFC Bridging For Innovators (B4I) programme – a funding scheme that has been introduced to boost industrial collaboration with national facilities. B4I is supported by the Industrial Strategy Challenge Fund and provides UK industry with access to expertise and capabilities for projects that boost productivity on existing products, rather than for early-stage research and development. This year's B4I projects include supporting validation measurements for graphene manufacture and for novel 3D cell structure manufacture (see below).

University of Oxford spinout company OxSyBio collaborated with MRC-Harwell and CLF microscopy experts to access CLF's Octopus imaging cluster, to examine their innovative 3D drug-responsive adipose models and assist in the validation of their manufacturing process. Dr Alex Graham (MRC-Harwell) said about the research, "It is a powerful platform for potentially identifying new therapeutic interventions for metabolic

diseases. This achievement has only been possible through a multi-institutional collaboration between a broad range of specialists at OxSyBio, MRC Harwell Institute and the Central Laser Facility."

Industry Partnerships

The CLF's partnership with Johnson Matthey (JM) continues, with Dr Kathryn Welsby appointed as a CLF-JM research fellow to solve industrial challenges and add insight into fundamental R&D, through the application of advanced laser spectroscopy and laser microscopy techniques on Ultra and Octopus. Regions of scientific interest for JM include next generation battery technology, fuel cell characterisation and catalytic science of zeolites for clean air applications.

The CLF's Dr Chris Thornton was successful in his application for a three-year UKRI-EPSC Innovation Fellowship. The fellowship is in partnership with JM, Manufacturing Technology Centre and Warwick Manufacturing Group. The fellowship is hosted at the CLF and is focused on laser-driven x-ray techniques for advanced micro-CT imaging and x-ray absorption spectroscopy.

Professor Marisa Martin-Fernandez at the CLF has secured development funding to prototype an integrated and cost-effective device, that exploits the STFC proprietary method to stratify cancer patients. This is a three-year project in partnership with Kings College London and AstraZeneca.

The Defence Science and Technology Laboratory (Dstl) counter terrorism and security group continue their long-standing collaboration with the CLF, which assists their programme of R&D focusing on advanced inspection and disruption technologies for defence applications. Applications of high peak power lasers and laser-driven secondary sources were explored during contracted experimental access time to the Gemini laser this year.

The collaboration between the CLF, University of Bristol, Queen's University Belfast and Sellafield Ltd continues in the exploration and development of laser-driven x-rays and neutrons for inspection and waste assay applications. Pulsed Laser Accelerators for The Inspection of Nuclear Materials (PLATINUM) is a three-year project, funded by the STFC Innovation Partnership Scheme.

The CLF hosts EPSRC iCASE studentships that are part-funded by industry partners, including two studentships partnered with Dstl and two studentships partnered with JM.

International Impact

The CLF's partnership with the HiLASE facility in Czech Republic continues under the European Commission's Widespread Teaming programme – one of the first projects within this Horizon 2020 programme to be funded. Scientists from the Czech Institute of Physics and HiLASE are working with the CLF on a "Centre of Excellence" for the industrial exploitation of new laser technology. The project is further developing the CLF's DiPOLE technology towards 100 Hz repetition rate, and strengthening collaboration in industrial engagement and technology transfer.

Build and delivery of the DiPOLE D100X system, 100 J at 10 Hz, to the high-energy density end station of the European XFEL facility remains on track for delivery in late 2019. This is the second build contract for the CLF's world leading 100 J level high peak power and high average power laser system, and paves the way for more interest from international facilities for this innovative technology.

Innovation

We constantly scan for innovation and technology transfer opportunities across the whole of the CLF, as an ongoing activity with a view to capturing and driving forward the most impactful ideas and inventions.

During this year three new proof-of-concept projects were funded and started, while four were completed. From target fabrication techniques, to microscopy optics, to detector readout solutions, the range of innovations coming from CLF expertise has the potential to impact on many sectors. Two projects funded through the Challenge Led Applied Systems Programme, related to advanced solutions for waste remediation and targeted therapeutics, continue to develop CLF know-how and inventions towards commercialisation, and an STFC Innovation Partnership Scheme project is exploring applications in nuclear waste management.

This year the CLF filed two new patent families, giving a current total of 19 active patent families, and nine invention disclosure forms were submitted for consideration for future patent filing. This year, the CLF has also licenced technologies to Ximbio, the world's largest non-profit reagent technology transfer service, and to Scitech Precision, the CLF's spinout company providing advanced target fabrication and precision engineering to customers worldwide.

Communication and Outreach Activities within the CLF

Helen Towrie, Emma Springate

Central Laser Facility, STFC Rutherford Appleton Laboratory, Harwell Campus, Didcot, UK

Email address: helen.towrie@stfc.ac.uk, emma.springate@stfc.ac.uk Website: www.clf.stfc.ac.uk

CLF's Communication Strategies

The CLF recognises the importance of communication with current and potential users, STFC, UKRI and other funders, new industry partners, the wider scientific community, and the general public. Outreach activities raise the profile of our world-class research and may inspire the next generation, while communication activities help to publicise the high-impact and inspiring science that the CLF delivers. Over the past year, the CLF has embarked on several exciting projects to help achieve its strategy of finding new and innovative ways to communicate what we do. This has involved working directly with STFC communications team members, hosting and involving ourselves in events that increase our visibility, and exploring new media as a vessel for communication.

Exploiting social media

Since its establishment in February 2018, the CLF Twitter account continues to be regularly maintained. By March 2019, it had almost 400 followers, including a number of Principal Investigators and users with whom we regularly interact via the account. The Twitter account has several purposes: to gain the attention of audiences we may not otherwise reach; to interact with the scientific community in a casual setting; and to create another channel back to the CLF website, where we have more stories, information, and the opportunity to apply for access.

Popular tweets tend to include job adverts, details of staff achievements, and tweets with illustrations, GIFs or videos attached.

Over the past six months, the CLF website has attracted over 12,500 users, with almost 49,000 unique page views. Excluding approximately 1500 users based at Harwell, this corresponds to 60 external users per day. This is 1,500 more users than last year and five more users a day. Out of 12,500 users, 129 came from twitter, 83 from Facebook, 20 Youtube, nine LinkedIn and four Others.

In order to get the most out of the CLF Twitter account, the CLF Communications Team holds monthly meetings with the STFC social media team and account owners from the other STFC facilities. This regular communication keeps the CLF up to date with STFC social media schemes, and enables us to tie them into our own projects and ideas.

Capturing science in action

In 2018, STFC hired a new videographer, Raquel Taylor, who has already worked on several exciting projects with the CLF. She has currently published five professional videos for social media about experiments, our lasers, and the scientists and engineers who work at the CLF. This is a large proportion of the 23 videos she has produced in total for RAL and DL. The CLF Communications Team continues to drive this work, as they understand how eye-catching and engaging videos can be, especially on social media; according to Twitter¹, tweets with videos garner around ten-times more interaction than those without.

Attracting a wider audience

As part of the Communications Team's initiative to develop new and innovative ways to communicate the CLF to the public, we secured Simon Clark, a physics YouTuber with over 200k subscribers, to visit the CLF site to film. He published two videos - one on the extreme power of lasers, and the other on our specialist imaging techniques, which featured an interview with Prof. Pavel Matousek.

These videos have together had around 27k views; moreover, they have reached an international audience, with the high volume of viewers far greater than what would be attracted to CLF-only videos. Comments from viewers have also been extremely positive, in particular from those saying that they now have a better understanding of this area of physics or that they feel inspired to do physics.

¹ <https://business.twitter.com/en/blog/creating-video-content-with-your-phone.html>

Another exciting moment for us was when CLF Engineer Steph Tomlinson was interviewed on BBC Radio Oxford. During her appearance she talked about her background, her engineering career, and the daily enjoyment she gets from working in a dynamic and innovative job. Recent data indicates that BBC Radio Oxford has an average of 82,000 listeners per week, which is a huge audience for the CLF to reach, raising our profile in the local area.

In February 2019, the CLF's Gemini Laser was featured in New Scientist magazine. The article, entitled "What's inside nothing? This laser will rip it up to find out," featured a Gemini experiment colliding electron beams with lasers to explore the limits of quantum electrodynamics (QED).

The art of science

The use of art to communicate our science has continued. A general audience-focused [infographic](#) was designed to show how our lasers are being used to shape the future. This infographic gained almost 130 interactions on Twitter, and the information and images have been reused multiple times.

As part of our public engagement strategy, we produced a series of postcards using illustrations depicting high power laser highlights. These postcards carried an image on one side with a summary of the science on the other, and they have proved very popular with both staff and the public. At the UK Research and Innovation Conference in June 2018, many people asked to take postcards home for a variety of reasons – some liked the artwork, others thought the science highlight was intriguing, while a few mentioned taking them home to show their children



QR code to download the infographic



The printed postcards (left) and CLF Impact and Engagement Officer Helen Towrie at the UKRI Conference in Swindon

Linking in to global science highlights

This year was a big year for lasers globally, as Donna Strickland and Gérard Mourou won half the Nobel Prize in Physics for inventing Chirped Pulse Amplification (CPA). All of the lasers at the CLF use this technique in some capacity.

The other half of the Nobel Prize in Physics was awarded to Arthur Ashkin for his invention of Optical Tweezers, a technique where tiny droplets of substances such as oil or glass can be held between beams of light. This technique is used in Octopus, and has enabled a wide range of studies including trapping individual solid particles of asthma inhaler drugs, and cloud chemistry.

The CLF marked the Nobel Prize with news stories and tweets highlighting the links to our work.

Organising user events

Several CLF-organised events have taken place over the past year. Perhaps most notable is the annual Christmas meeting of the High Power Laser (HPL) User Community, which over the years has grown from a small meeting to a huge, three-day event comprising talks, poster sessions and fantastic networking opportunities.



People gathering at the Christmas meeting of the HPL User Community

The annual Target Area Operator (TAO) training weeks, organised by Dr David Carroll, took place in the summer. These courses cover TAO responsibilities when leading a research team during an experiment and explain how the role fits within the safe working culture of the CLF. Specific aspects of health and safety related to experiments on high power laser facilities are also explored, including vacuum and gases, ionising radiation, and laser safety. Although these courses are tailored to meet the needs of the CLF's HPL facilities, they help to develop skills and knowledge that are applicable to experiments at other laser facilities, and also provide an opportunity for the attending scientists to network with each other.



Delegates on the annual Target Area Operator (TAO) training weeks.



Delegates on the annual Target Area Operator (TAO) training weeks.

Maintaining all avenues of communication

Alongside discovering new and innovative ways to communicate our science, the Communications Team continues to maintain existing methods of communication.

Outreach within local and wider communities is of great importance to the CLF, and includes interactions with schools across the country to highlight our areas of expertise. We have hosted around 80 tours of the Facility, around 27 of them for school children and those in higher education, along with a high number of general visits. At a recent visit from young students, we demonstrated how to freeze boiling water in a vacuum and explained the science. Such visual demonstrations are intended to foster engagement with students, and inspire them to consider a career in science and engineering.

RAL also hosts a bi-annual stargazing event, which is a fantastic way to interact with families from our local community. The CLF Visitor Centre has always proved a very popular destination at these events, and we ensure that the displays raise awareness of what we do and get people interested to find out more.

In order to keep CLF staff up-to-date with what is happening across the whole of the CLF, the Communications Team maintains a bi-monthly E-newsletter that shares science highlights, conferences, and events across the breadth of our various departments.

A total of 25 news articles have also been published online, across the CLF website and the STFC website.

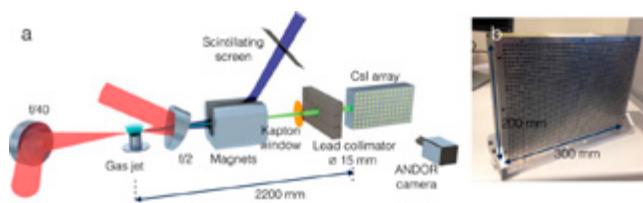
High Energy Density & High Intensity Physics

A spectrometer for ultrashort gamma-ray pulses with photon energies greater than 10 MeV

K.T. Behm, K. Krushelnick (Center for Ultrafast Optical Science, University of Michigan, Ann Arbor, USA)
J.M. Cole, E. Gerstmayr, J.C. Wood, K. Poder, S.P.D. Mangles, Z. Najmudin (The John Adams Institute for Accelerator Science, Imperial College London, UK)
A.S. Joglekar (Physics and Astronomy, University of California, Los Angeles, USA; Electrical Engineering, University of California, Los Angeles, USA)
C.D. Baird, C.D. Murphy, C.P. Ridgers (York Plasma Institute, Department of Physics, University of York, UK)
T.G. Blackburn, C. Harvey, M. Marklund (Department of Physics, Chalmers University of Technology, Gothenburg, Sweden)
M. Duff, P. McKenna (SUPA Department of Physics, University of Strathclyde, Glasgow, UK)

S. Kuschel (Institut für Optik und Quantenelektronik, Friedrich-Schiller-Universität, Jena, Germany)
G. Sarri, G.M. Samarín, J. Warwick (School of Mathematics and Physics, Queen's University Belfast, UK)
D. Symes (Central Laser Facility, STFC Rutherford Appleton Laboratory, Harwell Campus, Didcot, UK)
A. Ilderton (Department of Physics, Chalmers University of Technology, Gothenburg, Sweden; Centre for Mathematical Sciences, University of Plymouth, UK)
M. Zepf (Institut für Optik und Quantenelektronik, Friedrich-Schiller-Universität, Jena, Germany; School of Mathematics and Physics, Queen's University Belfast, UK)
A.G.R. Thomas (Center for Ultrafast Optical Science, University of Michigan, Ann Arbor, USA; Physics Department, Lancaster University, UK)

We present a design for a pixelated scintillator based gamma-ray spectrometer for non-linear inverse Compton scattering experiments. By colliding a laser wakefield accelerated electron beam with a tightly focused, intense laser pulse, gamma-ray photons up to 100 MeV energies and with few femtosecond duration may be produced. To measure the energy spectrum and angular distribution, a 33×47 array of caesium-iodide crystals was oriented such that the 47 crystal length axis was parallel to the gamma-ray beam and the 33 crystal length axis was oriented in the vertical direction. Using an iterative deconvolution method similar to the YOGI code, modelling of the scintillator response using GEANT4 and fitting to a quantum Monte Carlo calculated photon spectrum, we are able to extract the gamma ray spectra generated by the inverse Compton interaction



(a) Experimental setup of the Compton scattering experiment, including the γ -ray spectrometer. (b) Photograph of the CsI scintillator array used as the detector.

Reprinted from K.T. Behm et al., *Rev. Sci. Instrum.* 89, 113303 (2018); <https://doi.org/10.1063/1.5056248>, with the permission of AIP Publishing.

Contact: A.G.R. Thomas (agrt@umich.edu)

Debris studies for high-repetition rate and high-power laser experiments at the Central Laser Facility

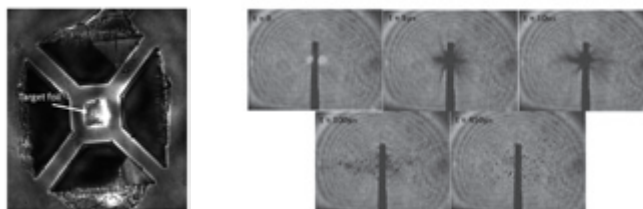
N. Booth, S. Astbury, E. Bryce, R.J. Clarke, C.D. Gregory, J.S. Green, D. Haddock, R.I. Heathcote, C. Spindloe (Central Laser Facility, STFC Rutherford Appleton Laboratory, Harwell Campus, Didcot, UK)

Many of the new large European facilities that are in the process of coming online will be operating at high power and high repetition rates. The ability to operate at high repetition rates is important for studies including secondary source generation and inertial confinement fusion research. In these interaction conditions, with solid targets, debris mitigation for the protection of beamline and diagnostic equipment becomes of the utmost importance. These facilities have the potential to take hundreds, if not thousands, of shots every day, creating massive volumes of debris and shot materials.

In recent testing of the Central Laser Facility's High Accuracy Microtargetry Supply (HAMS) system on the mid-repetition rate Gemini facility (15 J, 40 fs, 1 shot every 20 seconds), diagnostics were deployed to specifically look at the debris emitted from targets designed for high repetition rate experiments. By using a high frame rate camera, it has been possible to observe and characterize some of the debris production, whilst also looking at target fratricide.

Alongside these results from Gemini, we also present results of static debris measurements undertaken on the Vulcan Petawatt high energy, high power facility, where the

cumulative effects of debris produced by high power laser experiments have been observed.



Left: On shot rear surface probe data showing the laser clipping the target frame of a 100 nm-thick silicon nitride target suspended on a silicon frame of $300 \times 300 \mu\text{m}^2$.

Right: High frame rate camera images (210k fps) at $t=0, 5, 10, 100$ and $450 \mu\text{s}$ from the arrival of the laser pulse on a silicon nitride target with a $300 \mu\text{m}$ diameter aperture. At $t=0$ the initial plasma flash at the interaction point can be seen.

Reprinted from N. Booth, S. Astbury, E. Bryce, R. J. Clarke, C. D. Gregory, J. S. Green, D. Haddock, R. I. Heathcote, and C. Spindloe "Debris studies for high-repetition rate and high-power laser experiments at the Central Laser Facility", *Proc. SPIE 10763, Radiation Detectors in Medicine, Industry, and National Security XIX, 107630S* (11 September 2018); <https://doi.org/10.1117/12.2318946>. Copyright (2018) Society of Photo-Optical Instrumentation Engineers (SPIE).

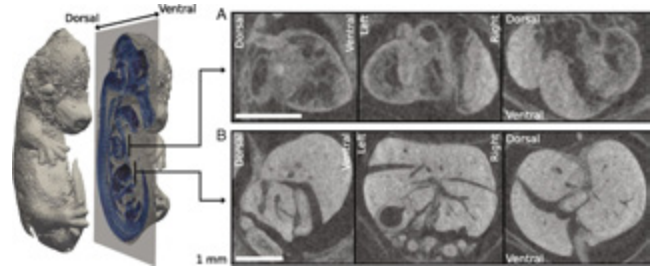
Contact: N. Booth (nicola.booth@stfc.ac.uk)

High-resolution μ CT of a mouse embryo using a compact laser-driven X-ray betatron source

J.M. Cole, K. Poder, N.C. Lopes, J.C. Wood, S. Alatabi, C. Kamperidis, S.P.D. Mangles, Z. Najmudin (The John Adams Institute for Accelerator Science, Blackett Laboratory, Imperial College London, UK)
D.P. Norris, J. Sanderson, H. Westerberg, M. Sandholzer (Medical Research Council (MRC) Harwell Institute, Harwell Campus, Didcot, UK)
S. Johnson, Z. Szoke-Kovacs, L. Teboul (The Mary Lyon Centre, MRC Harwell Institute, Harwell Campus, Didcot, UK)

M.A. Hill, M. De Lazzari, J. Thomson (CRUK/MRC Oxford Institute for Radiation Oncology, University of Oxford, UK)
D.R. Symes, D. Rusby, P.S. Foster, S. Botchway, S. Gratton (Central Laser Facility, STFC Rutherford Appleton Laboratory, Harwell Campus, Didcot, UK)
C.A.J. Palmer, O. Kononenko (Deutsches Elektronen-Synchrotron (DESY), Hamburg, Germany)
J.R. Warwick, G. Sarri (School of Mathematics and Physics, Queen's University Belfast, UK)

In the field of X-ray microcomputed tomography (μ CT) there is a growing need to reduce acquisition times at high spatial resolution (approximate micrometres) to facilitate in vivo and high-throughput operations. The state of the art represented by synchrotron light sources is not practical for certain applications, and therefore the development of high-brightness laboratory-scale sources is crucial. We present here imaging of a fixed embryonic mouse sample using a compact laser-plasma-based X-ray light source and compare the results to images obtained using a commercial X-ray μ CT scanner. The radiation is generated by the betatron motion of electrons inside a dilute and transient plasma, which circumvents the flux limitations imposed by the solid or liquid anodes used in conventional electron-impact X-ray tubes. This X-ray source is pulsed (duration <30 fs), bright ($>10^{10}$ photons per pulse), small (diameter <1 μ m), and has a critical energy >15 keV. Stable X-ray performance enabled tomographic imaging of equivalent quality to that of the μ CT scanner, an important confirmation of the suitability of the laser-driven source for applications. The X-ray flux achievable with this approach scales with the laser repetition rate without compromising the source size, which will allow the recording of high-resolution μ CT scans in minutes.



An isosurface rendering of the reconstruction from the laser source is depicted in gray. A sagittal slice of the reconstruction is overlaid in blue. Enlarged sections of sagittal, coronal, and transverse slices around the heart and liver are plotted in A and B, respectively. (Scale bars, 1 mm.)

Reprinted from J. M. Cole et al., PNAS 115(25), 6335-6340 (2018), published by PNAS under the Creative Commons Attribution-NonCommercial-NoDerivatives License 4.0 (CC BY-NC-ND).

Contact: D.R. Symes (dan.symes@stfc.ac.uk)

Observation of ultrafast proton interactions in water using the Gemini Laser Facility

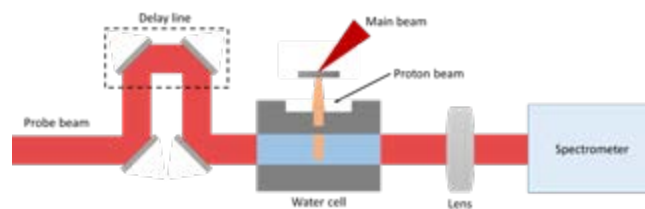
M. Coughlan, N. Breslin, M. Yeung, C. Arthur, H. Donnelly, S. White, B. Dromei (Department of Physics and Astronomy, Queen's University Belfast, UK)

R. Yang, M. Speicher, J. Schreiber (Lehrstuhl für Medizinphysik, Fakultät für Physik, Ludwig-Maximilians-Universität München, Germany)

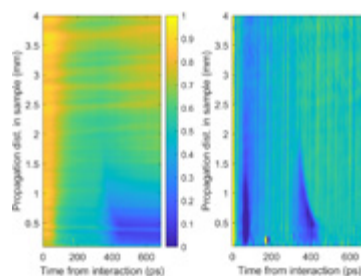
The solvated electron has been extensively studied in many areas of radiation chemistry. A large focus of this research has been in radiation biology, as solvated electrons are a product of ionising radiation reacting with water molecules that can cause damage to DNA. Many of these studies employ chemical scavenging techniques, where a chemical is added to the water that reacts in some measurable way to the ionising radiation.

Using an optical streaking technique with a high degree of synchronicity, and measuring changes in transmission of the pristine water sample, we use laser-driven protons to generate solvated electrons in water, whilst simultaneously probing their evolution on a sub-nanosecond (10^{-9} s) timescale.

Contact: M. Coughlan (m.coughlan@qub.ac.uk)



Above: Sketch of the experimental setup



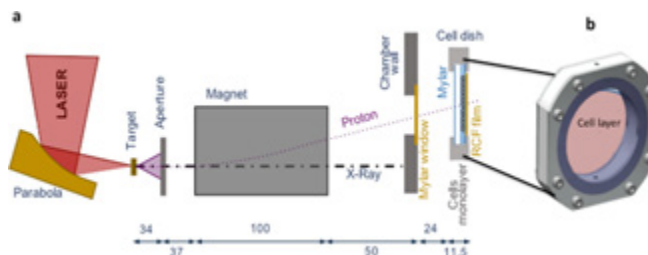
Left: Experimentally obtained optical streak showing the response of H_2O to protons produced by Target Normal Sheath Acceleration. The x-axis represents the temporal evolution of the opacity from time of the laser-foil interaction. The y-axis shows the spatial evolution along the central axis of the proton burst. Right: Differentiated image showing the rate of change of transmission with respect to time, highlighting the region of the streak where the ion pulse is depositing energy the subsequent electron solvation process.

DNA DSB Repair Dynamics following Irradiation with Laser-Driven Protons at Ultra-High Dose Rates

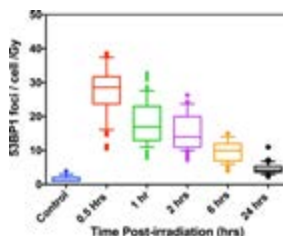
F. Hanton, D. Doria, D. Gwynne, C. Scullion, H. Ahmed, K. Naughton, S. Kar, M. Borghesi (Centre for Plasma Physics, School of Mathematics and Physics, Queen's University Belfast, UK)
P. Chaudhary, C. Maiorino, T. Marshall, K.M. Prise (Centre for Cancer Research & Cell Biology, Queen's University Belfast, UK)
D. Doria (Extreme Light Infrastructure – Nuclear Physics (ELI-NP), Horia Hulubei Institute for Nuclear Physics (IFIN-HH), Bucharest, Romania)

L. Romagnani (Laboratoire pour l'Utilisation des Lasers Intenses (LULI), Ecole Polytechnique, Palaiseau Cedex, France)
G. Schettino (National Physical Laboratory, Teddington, UK)
P. McKenna (Department of Physics, SUPA, University of Strathclyde, Glasgow, UK)
S. Botchway, D.R. Symes, P.P. Rajeev (Central Laser Facility, STFC Rutherford Appleton Laboratory, Harwell Campus, Didcot, UK)

Proton therapy has emerged as more effective in the treatment of certain tumours than photon-based therapies. However, significant capital and operational costs make proton therapy less accessible. This has stimulated interest in alternative proton delivery approaches, and, in this context, the use of laser-based technologies for the generation of ultra-high dose rate ion beams has been proposed as a prospective route. A better understanding of the radiobiological effects at ultra-high dose-rates is important for any future clinical adoption of this technology. In this study, we irradiated human skin fibroblasts-AG01522B cells with laser-accelerated protons at a dose rate of 10^9 Gy/s, generated using the Gemini laser system at the Rutherford Appleton Laboratory, UK. We studied DNA double strand break (DSB) repair kinetics using the p53 binding protein-1 (53BP1) foci formation assay and observed a close similarity in the 53BP1 foci repair kinetics in the cells irradiated with 225 kVp X-rays and ultra- high dose rate protons for the initial time points. At the microdosimetric scale, foci per cell per track values showed a good correlation between the laser and cyclotron-accelerated protons indicating similarity in the DNA DSB induction and repair, independent of the time duration over which the dose was delivered.



Above: (a) Schematic of the experimental set up for irradiation of AG01522 cells with 10MeV laser accelerated protons (b) Design of the dish where cells were grown as monolayers on $3 \mu\text{m}$ thin Mylar.



Left: Quantitative analysis of the variations in 53BP1 foci per cell per Gy in AG01522B cells after exposure to 10 MeV ($\text{LET}-4.6 \text{ keV}/\mu\text{m}$) laser-accelerated protons shown as whisker box plots generated using Prism 6 software.

Reprinted from Hanton, F., Chaudhary, P., Doria, D. et al. DNA DSB Repair Dynamics following Irradiation with Laser-Driven Protons at Ultra-High Dose Rates. *Sci Rep* 9, 4471 (2019) doi:10.1038/s41598-019-40339-6 published by Springer Nature, under the Creative Commons Attribution 4.0 International License.

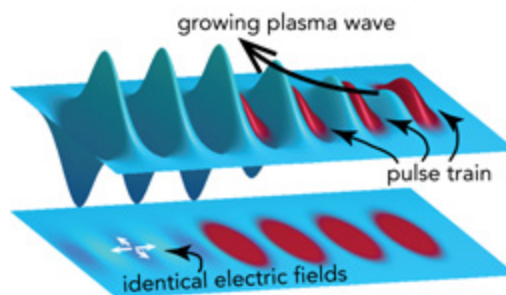
Contact: M. Borghesi (M.Borghesi@qub.ac.uk)

Measurement of the decay rate of laser-driven linear wakefields

J. Jonnerby, J. Holloway, A.V. Boettcher, A. Picksley, A.J. Ross, C. Arran, R.J. Shalloo, R. Walczak, S.M. Hooker (John Adams Institute, University of Oxford, UK)
L. Corner (Cockcroft Institute, University of Liverpool, UK)

N. Bourgeois, C. Thornton, S.J. Hawkes, C.J. Hooker (Central Laser Facility, STFC Rutherford Appleton Laboratory, Harwell Campus, Didcot, UK)

In the multi-pulse laser wakefield acceleration scheme (MP-LWFA), a train of laser pulses propagating through a plasma excites a plasma wakefield, which could be used to accelerate charged particles to GeV energies at a rate of several kHz. If the distance between the laser pulses is equal to the plasma wavelength, the wake amplitude is amplified by each subsequent laser pulse. We have performed an experiment to measure the lifetime, T_{wf} of the plasma wakes, in order to determine the maximum number of laser pulses that can be used to amplify these wakes.



A simulation of four laser pulses, separated by the plasma wavelength, driving a plasma wakefield through resonance.

In this report, we describe the method for determining T_{wf} using Temporally Encoded Spectral Shifting (TESS). Preliminary analysis confirms that measured values agree with theory. Further results will be reported in future publications. These advances in MP-LWFA could pave the way towards high-repetition rate laser-plasma accelerators.

Contact: J. Jonnerby (jakob.jonnerby@physics.ox.ac.uk)

Investigations of Optical Guiding through Hydrodynamic Optical-Field Ionised Plasma Channels

A. Picksley, A. Alejo, J. Cowley, J. Jonnerby, A.J. Ross, J. Holloway, A. Boetticher, R. Walczak, S.M. Hooker (John Adams Institute, University of Oxford, UK)
L. Feder, H.M. Milchberg (University of Maryland, USA)

H. Jones, L. Reid, L. Corner (Cockcroft Institute, University of Liverpool, UK)
N. Bourgeois, C.J. Hooker, S.J. Hawkes (Central Laser Facility, STFC Rutherford Appleton Laboratory, Harwell Campus, Didcot, UK)

Long, low-density plasma channels can be generated by Hydrodynamic Optical-Field-Ionisation (HOFI) and are capable of operating at kilohertz repetition rates, making them ideal waveguides for multi-GeV laser-plasma accelerators. In this report, the effects of spatial offset at the entrance of the channel are investigated.

Stability of the $f/40$ beam far-field was characterised by a leak inside the South compressor in LA3, and by a focus camera inside TA3. These measurements indicated that pointing jitter of the Gemini South F/40 beam was dominated by contributions from LA3. As the spatial offset at the channel entrance increased, an increase in guided spot size and reduction of energy transmission of the $f/40$ pulse was observed. The plasma channel acceptance angle was found to be approximately $3.7 \mu\text{rad}$, which can inform future experiments of the same type.

Contact: A. Picksley (alexander.picksley@physics.ox.ac.uk)

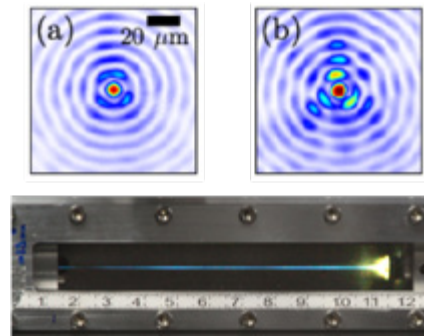


Figure 1: Transverse intensity profile of the channel-forming beam at the start of the line focus (a) and 100 mm downstream (b). (c) SLR image of a hydrogen plasma column ionised by the channel-forming beam.

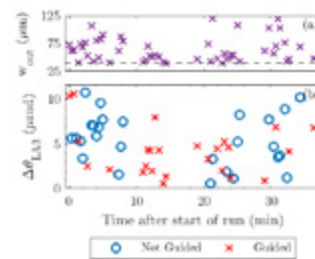


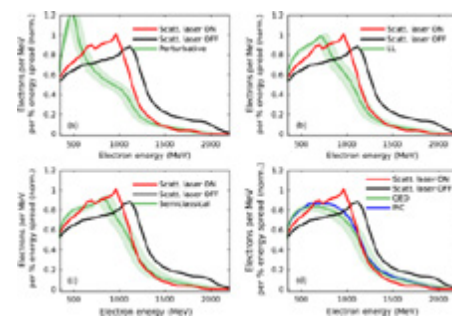
Figure 2: (a) Variation in the guided spot size w_{out} . (b) Graph showing how guiding quality is correlated with time and the LA3 leakage position for 50 consecutive shots.

Experimental Signatures of the Quantum Nature of Radiation Reaction in the Field of an Ultraintense Laser

K. Poder, J.M. Cole, E. Gerstmayr, S.P.D. Mangles, Z. Najmudin (The John Adams Institute for Accelerator Science, Blackett Laboratory, Imperial College London, UK)
M. Tamburini, A. Di Piazza, C.H. Keitel (Max-Planck-Institut für Kernphysik, Heidelberg, Germany)
G. Sarri, J. Warwick, D.J. Corvan, G.M. Samarín (School of Mathematics and Physics, Queen's University Belfast, UK)
S. Kuschel (Helmholtz Institute Jena, Germany; Institut für Optik und Quantenelektronik, Friedrich-Schiller-Universität Jena, Germany)
C.D. Baird, C.D. Murphy, C.P. Ridgers (Department of Physics, University of York, UK)
K. Behm, K. Krushelnick (Center for Ultrafast Optical Science, University of Michigan, Ann Arbor, USA)

S. Böhlen (Deutsches Elektronen Synchrotron DESY, Hamburg, Germany)
M. Duff, P. McKenna (Department of Physics, SUPA, University of Strathclyde, Glasgow, UK)
D.R. Symes (Central Laser Facility, STFC Rutherford Appleton Laboratory, Harwell Campus, Didcot, UK)
A.G.R. Thomas (Center for Ultrafast Optical Science, University of Michigan, Ann Arbor, USA; Lancaster University, UK)
M. Zepf (School of Mathematics and Physics, Queen's University Belfast, UK; Helmholtz Institute Jena, Germany; Institut für Optik und Quantenelektronik, Friedrich-Schiller-Universität Jena, Germany)

The description of the dynamics of an electron in an external electromagnetic field of arbitrary intensity is one of the most fundamental outstanding problems in electrodynamics. Remarkably, to date, there is no unanimously accepted theoretical solution for ultrahigh intensities, and little or no experimental data. The basic challenge is the inclusion of the self-interaction of the electron with the field emitted by the electron itself – the so-called radiation reaction force. We report here on the experimental evidence of strong radiation reaction, in an all-optical experiment, during the propagation of highly relativistic electrons (maximum energy exceeding 2 GeV) through the field of an ultraintense laser (peak intensity of $4 \times 10^{20} \text{ W/cm}^2$). In their own rest frame, the highest-energy electrons experience an electric field as high as one quarter of the critical field of quantum electrodynamics and are seen to lose up to 30% of their kinetic energy during the propagation through the laser field. The experimental data show signatures of quantum effects in the electron dynamics in the external laser field, potentially showing departures from the constant cross field approximation.



Experimentally measured electron spectrum without the scattering laser (black line) and the spectrum of scattered electrons (red line) compared to (a) the theoretical prediction assuming a model only based on the Lorentz force, (b) the Landau-Lifshitz equation, (c) a semiclassical model of radiation reaction, and (d) the quantum model of radiation reaction.

Reprinted figure from K. Poder et al., Phys. Rev. X 8, 031004 (2018) published by the American Physical Society, under the Creative Commons Attribution 4.0 International License.

Contact: Contact: G. Sarri (g.sarri@qub.ac.uk)

Making pions with laser light

W. Schumaker (SLAC National Accelerator Laboratory, Stanford University, California, USA; Center for Ultrafast Optical Science, University of Michigan, Ann Arbor, USA)

T. Liang (SLAC National Accelerator Laboratory, Stanford University, California, USA)

A.G.R. Thomas, M. Vargas, K. Krushelnick (Center for Ultrafast Optical Science, University of Michigan, Ann Arbor, USA)

R. Clarke, D. Symes (Central Laser Facility, STFC Rutherford Appleton Laboratory, Harwell Campus, Didcot, UK)

J.M. Cole, S.P.D. Mangles, Z. Najmudin, K. Poder (The John Adams Institute for Accelerator Science, Blackett Laboratory, Imperial College London, UK)

G. Grittani (Institute of Physics ASCR, v.v.i. (FZU), ELI Beamlines Project, Prague, Czechia; Czech Technical University in Prague, Czechia)

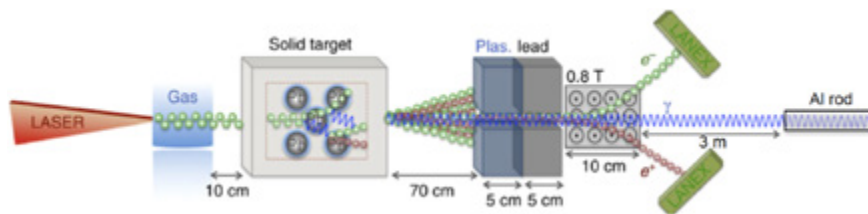
S. Kuschel (Helmholtz Institute Jena, Germany)

G. Sarri (School of Mathematics and Physics, Queen's University Belfast, UK)

M. Zepf (Czech Technical University in Prague, Czechia; School of Mathematics and Physics, Queen's University Belfast, UK)

The interaction of high intensity, short pulse laser beams with plasmas can accelerate electrons to energies in excess of a GeV. These electron beams can subsequently be used to generate short-lived particles, such as positrons, muons, and pions. In recent experiments, we have made the first measurements of pion production using 'all optical' methods. In particular, we have demonstrated that the interaction of bremsstrahlung generated by laser-driven electron beams with aluminium atoms can produce the

long-lived isotope of magnesium (^{27}Mg) which is a signature for pion (π^+) production and subsequent muon decay. Using a 300 TW laser pulse, we have measured the generation of 150 ± 50 pions per shot. We also show that the energetic electron beam is a source of an intense, highly directional neutron beam resulting from (γ, n) reactions which contributes to the ^{27}Mg measurement as background via the (n, p) process.



Experimental geometry for measuring pion/neutron production.

Reprinted from W Schumaker et al. 2018 New J. Phys. 20 073008 published by IOP Publishing Ltd, under the Creative Commons Attribution 3.0 License.

Contact: K. Krushelnick (kmr@umich.edu)

Experimental Testing of Targets for a High Accuracy Microtarget Supply (HAMS) System on the Gemini Laser System

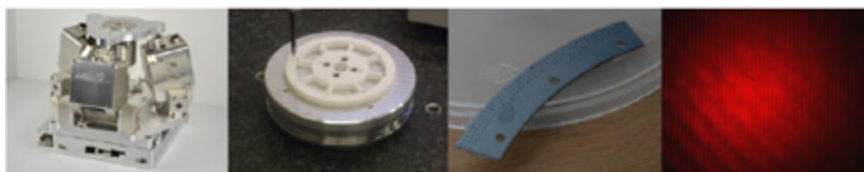
C. Spindloe, M.K. Tolley (Central Laser Facility, STFC Rutherford Appleton Laboratory, Harwell Campus, Didcot, UK; Scitech Precision Ltd, Rutherford Appleton Laboratory, Harwell Campus, Didcot, UK)

N. Booth, S. Astbury, C. Gregory, E. Bryce, S. Tomlinson, R. Heathcote, D. Haddock (Central Laser Facility, STFC Rutherford Appleton Laboratory, Harwell Campus, Didcot, UK)

G. Arthur (Scitech Precision Ltd, Rutherford Appleton Laboratory, Harwell Campus, Didcot, UK)

It is widely understood within the high-power laser community that recent developments in diode-pumped and high repetition rate laser systems will give unprecedented access to laser shots. This will provide a challenge for target fabrication in making enough experimental samples. While in the past access to facilities and shot rates during access periods have been the limiting factor for high power laser experiments, this will soon not be the case. There has already been a shift in development of the user base from fundamental science experiments to industrial applications, using the laser experiment as a reliable source for secondary aims. The Gemini laser system has been operating at a high repetition rate for high intensity (0.5 PW) experiments for a number of years, and the Central Laser

Facility has developed a target methodology to deliver to the user community the maximum number of solid targets and to fully utilise the available time on the laser. Targets for the High Accuracy Microtarget Supply (HAMS) system have been tested and have been proven to survive in a manner to allow shot rates comparable with the available laser repetition rate (0.1 Hz). Investigations into target geometry have been carried out and debris production has been studied by high frame rate camera imaging. The study of the relationship between target geometry and debris production has allowed the design of optimal target support infrastructure, such as aperture size and structure, for high repetition rate experiments on the Gemini system.



The four physical integrated parts of the HAMS system, which will allow for automated target alignment after integration of feedback programming.

Reprinted from C. Spindloe et al. 2018 J. Phys.: Conf. Ser. 1079 012014, published by IOP Publishing Ltd, under the Creative Commons Attribution 3.0 License.

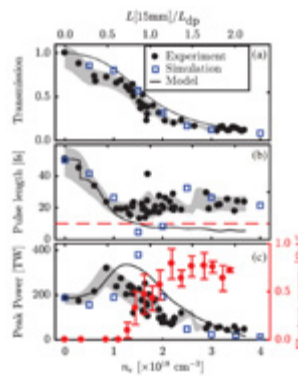
Contact: C. Spindloe (christopher.spindloe@stfc.ac.uk)

Observation of Laser Power Amplification in a Self-Injecting Laser Wakefield Accelerator

M.J.V. Streeter (The Cockcroft Institute, Daresbury, UK; Physics Department, Lancaster University, UK; The John Adams Institute for Accelerator Science, Blackett Laboratory, Imperial College London, UK)
S. Kneip, M.S. Bloom, A.E. Dangor, H. Nakamura, S.P.D. Mangles, Z. Najmudin (The John Adams Institute for Accelerator Science, Blackett Laboratory, Imperial College London, UK)
R.A. Bendoyro, J. Jiang (GoLP/Instituto de Plasmas e Fusão Nuclear, Instituto Superior Técnico, Universidade de Lisboa, Portugal)
O. Chekhlov, C.J. Hooker, P.A. Norreys, P.P. Rajeev, D.R. Symes (Central Laser Facility, STFC Rutherford Appleton Laboratory, Harwell Campus, Didcot, UK)

A. Döpp (The John Adams Institute for Accelerator Science, Blackett Laboratory, Imperial College London, UK; Fakultät für Physik, Ludwig-Maximilians-Universität München, Germany; Max-Planck-Institut für Quantenoptik, Garching, Germany)
J. Holloway, M. Wing (High Energy Physics Group, University College London, UK)
N.C. Lopes (The John Adams Institute for Accelerator Science, Blackett Laboratory, Imperial College London, UK; GoLP/Instituto de Plasmas e Fusão Nuclear, Instituto Superior Técnico, Universidade de Lisboa, Portugal)
C.A.J. Palmer (The Cockcroft Institute, Daresbury, UK; Physics Department, Lancaster University, UK)
J. Schreiber (Fakultät für Physik, Ludwig-Maximilians-Universität München, Garching, Germany; Max-Planck-Institut für Quantenoptik, Garching, Germany)

We report on the depletion and power amplification of the driving laser pulse in a strongly driven laser wakefield accelerator. Simultaneous measurement of the transmitted pulse energy and temporal shape indicate an increase in peak power from 187 ± 11 TW to a maximum of 318 ± 12 TW after 13 mm of propagation in a plasma density of $0.9 \times 10^{18} \text{ cm}^{-3}$. The power amplification is correlated with the injection and acceleration of electrons in the non-linear wakefield. This process is modelled by including a localized redshift and subsequent group delay dispersion at the laser pulse front.



Experimental and simulated (a) transmitted laser energy fraction, (b) pulse duration (FWHM), and (c) peak pulse power and maximum observed electron beam energy (red circles) versus plasma density for a 15 mm nozzle diameter. The grey shaded regions indicate rms error (statistical and measurement errors) of a moving average of the data points. The red dashed line in (b) is the instrument limit of the FROG for time-bandwidth limited pulses. The solid black lines are calculated from our pulse evolution model.

Reprinted figure with permission from M.J.V. Streeter et al., Phys. Rev. Lett. 120, 254801 (2018). Copyright (2018) by the American Physical Society.

Contact: Z. Najmudin (z.najmudin@imperial.ac.uk)

Temporal feedback control of high-intensity laser pulses to optimize ultrafast heating of atomic clusters

M.J.V. Streeter, S.J.D. Dann, J.D.E. Scott (The Cockcroft Institute, Daresbury, UK)
A.G.R. Thomas (The Cockcroft Institute, Daresbury, UK; Center for Ultrafast Optical Science, University of Michigan, Ann Arbor, USA)
C.D. Baird, C.D. Murphy (York Plasma Institute, Department of Physics, University of York, UK)
S. Eardley, R.A. Smith (Blackett Laboratory, Imperial College London, UK)
S. Rozario, J.-N. Gruse, S.P.D. Mangles, Z. Najmudin (The John Adams Institute for Accelerator Science, Imperial College London, UK)
S. Tata, M. Krishnamurthy (Tata Institute of Fundamental Research, Mumbai, India)

S.V. Rahul (TIFR Centre for Interdisciplinary Sciences, Hyderabad, India)
D. Hazra (Laser Plasma Section, Raja Ramanna Centre for Advanced Technology, Indore, India)
P. Pourmoussavi, J. Osterhoff (Deutsches Elektronen-Synchrotron DESY, Hamburg, Germany)
J. Hah (Center for Ultrafast Optical Science, University of Michigan, Ann Arbor, USA)
N. Bourgeois, C. Thornton, C.D. Gregory, C.J. Hooker, O. Chekhlov, S.J. Hawkes, B. Parry, V.A. Marshall, Y. Tang, E. Springate, P.P. Rajeev, D.R. Symes (Central Laser Facility, STFC Rutherford Appleton Laboratory, Harwell Campus, Didcot, UK)

We describe how active feedback routines can be applied at a limited repetition rate (5 Hz) to optimize high-power (>10 TW) laser interactions with clustered gases. Optimization of x-ray production from an argon cluster jet, using a genetic algorithm, approximately doubled the measured energy through temporal modification of the 150 mJ driving laser pulse. This approach achieved an increased radiation yield through exploration of a multi-dimensional parameter space, without requiring detailed a priori knowledge of the complex cluster dynamics. The optimized laser pulses exhibited a slow rising edge to the intensity profile, which enhanced the laser energy coupling into the cluster medium, compared to the optimally compressed FWHM pulse (40 fs). Our work suggests that this technique can be more widely utilized for control of intense pulsed secondary radiation from petawatt-class laser systems.

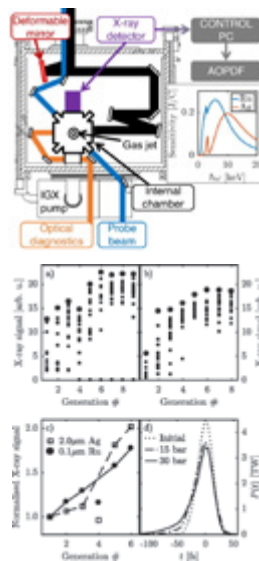


Figure 1: The gas jet target is housed in an internal differentially pumped chamber. Diagnostic output is fed into the control PC that applies settings to the acousto-optic programmable dispersive filter in an optimization feedback loop. Sensitivity for the $0.1 \mu\text{m}$ Ru and $2 \mu\text{m}$ Ag filtered PIN diodes is shown.

Figure 2: Optimization of Ru-filtered PIN diode X-ray flux with backing pressures of (a) 30 bar and (b) 15 bar. Each point is the average of 50 shots, with the best individual of each generation shown as a larger point. Error bars are omitted for visual clarity. (c) Improvement of the X-ray signal through the $0.1 \mu\text{m}$ Ru and $2 \mu\text{m}$ Ag filters, normalized to their starting values with the unmodified laser pulse (Generation 1) for a backing pressure of 30 bar. (d) Power profiles of the initial and optimized pulses from the 15 bar and 30 bar runs.

Contact: D.R. Symes (dan.symes@stfc.ac.uk)

Reprinted from M.J.V. Streeter et al. Appl. Phys. Lett. 112, 244101 (2018), with the permission of AIP Publishing.

Processing of Gemini betatron images for biological tomography

D.R. Symes, S. Botchway, D. Rusby, P.S. Foster, S. Gratton (Central Laser Facility, STFC Rutherford Appleton Laboratory, Harwell Campus, Didcot, UK)

J.M. Cole, J.C. Wood, K. Poder, S. Alatabi, C. Kamperidis, N.C. Lopes, S.P.D. Mangles, Z. Najmudin (The John Adams Institute for Accelerator Science, Blackett Laboratory, Imperial College London, UK)

S. Johnson, Z. Szoke-Kovacs, L. Teboul (The Mary Lyon Centre, MRC Harwell Institute, Harwell Campus, Didcot, UK)

J. Sanderson, M. Sandholzer, H. Westerberg, D.P. Norris (MRC Harwell Institute, Harwell Campus, Didcot, UK)

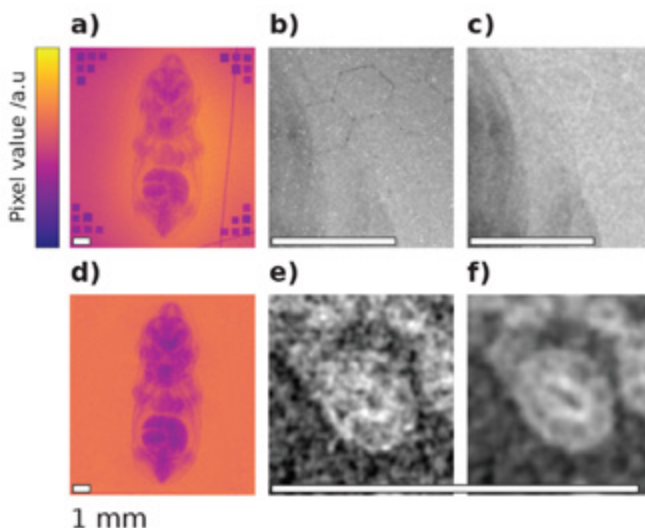
M. De Lazzari, J.M. Thompson, M.A. Hill (CRUK/MRC Oxford Institute for Radiation Oncology, University of Oxford, UK)

O. Kononenko, C.A.J. Palmer (Deutsches Elektronen-Synchrotron (DESY), Hamburg, Germany)

J.R. Warwick, G. Sarri (School of Mathematics and Physics, Queen's University Belfast, UK)

X-rays generated through betatron oscillations of electrons in laser wakefield accelerators have ideal properties for biological imaging. In recent years, experiments on Gemini have increased the flux and critical energy of betatron x-rays into the 10s keV regime that is needed to penetrate cm-scale objects, such as bone samples, mouse embryos, and soft tissue biopsies. Data analysis is complicated by fluctuations in x-ray profile, spectrum and brightness. In this report, we discuss the image quality and processing steps taken to perform tomographic reconstruction on a dataset obtained using Gemini.

(a) Raw image of mouse embryo detected by the x-ray CCD, wires are placed as fiducials for tomographic reconstruction. (b) Region of image showing hot and cold pixels and (c) the result of applying a selective median filter. (d) Processed version of the image in (a). (e) Zoomed region showing remaining noise and (f) the result of applying a non-local-denoising technique.



Contact: D.R. Symes (dan.symes@stfc.ac.uk)

Comparison of the properties of bright compact x-ray sources

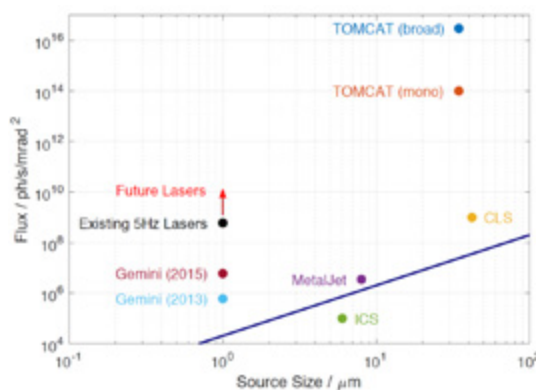
D.R. Symes (Central Laser Facility, STFC Rutherford Appleton Laboratory, Harwell Campus, Didcot, UK)

J.M. Cole, J.C. Wood, S.P.D. Mangles, Z. Najmudin (The John Adams Institute for Accelerator Science, Blackett Laboratory, Imperial College London, UK)

N. C. Lopes (The John Adams Institute for Accelerator Science, Blackett Laboratory, Imperial College London, UK; GoLP/Instituto de Plasmas e Fusao Nuclear, Instituto Superior Tecnico, Lisboa, Portugal)

Compact x-ray sources with much higher brightness than conventional electron-impact x-ray tubes are being developed to translate the advanced techniques achievable at synchrotron beamlines to laboratory settings. The benefits for biological research will be faster scanning at very high resolution for rapid microtomography and in vivo studies. X-ray sources based on relativistic electron beams produced in miniature plasma accelerators driven by high power lasers have ideal properties for these applications of micron-scale source size, extreme brightness and ultrashort image exposure time. The lateral coherence of the beam enables phase contrast imaging, providing superior contrast between soft tissues compared to traditional absorption-based radiography. The purpose of this report is to compare the performance of plasma accelerator based x-ray technology to other options available to researchers, and to discuss future capabilities.

Contact: D.R. Symes (dan.symes@stfc.ac.uk)



Flux of compact x-ray sources plotted against the x-ray source size. Values for the MetalJet (purple circle) and the Compact Light Source (yellow circle); parameters of the TOMCAT beamline (broad bandwidth: blue circle, 2% bandwidth: brown circle); simulated limit to solid anode tungsten sources (blue line); laser-based ICS source (green circle) and laser-betatron source. Existing lasers operating at 5 Hz could increase betatron flux to $6 \times 10^8 \text{ ph s}^{-1} \text{ mrad}^{-2}$ and developments in the near future could reach $>10^{10} \text{ ph s}^{-1} \text{ mrad}^{-2}$.

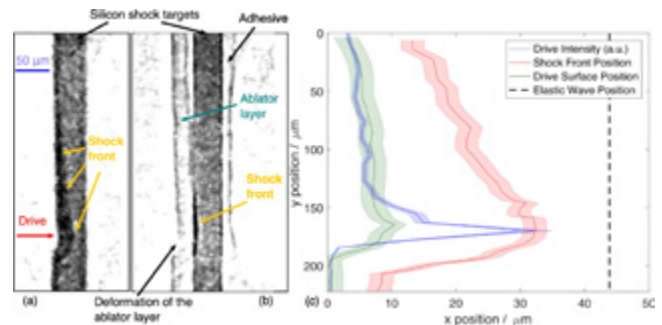
Ultrafast Imaging of Laser Driven Shock Waves using Betatron X-rays from a Laser Wakefield Accelerator

J.C. Wood, J.S.J. Bryant, K. Pöder, Z. Najmudin, S.P.D. Mangles (The John Adams Institute for Accelerator Science, Blackett Laboratory, Imperial College London, UK)
D.J. Chapman (Institute of Shock Physics, Blackett Laboratory, Imperial College London, UK)
N.C. Lopes (The John Adams Institute for Accelerator Science, Blackett Laboratory, Imperial College London, UK; GoLP/Instituto de Plasmas e Fusão Nuclear, Instituto Superior Técnico, Lisboa, Portugal)
M.E. Rutherford, D.E. Eakins (Institute of Shock Physics, Blackett Laboratory, Imperial College London, UK; Solid Mechanics and Materials Engineering, Department of Engineering Science, University of Oxford, UK)

T.G. White (Department of Physics, University of Nevada, Reno, USA)
F. Albert, B.B. Pollock (Lawrence Livermore National Laboratory, California, USA)
K.T. Behm, K. Krushelnick, A.G.R. Thomas, Z. Zhao (Center for Ultrafast Optical Science, University of Michigan, Ann Arbor, USA)
N. Booth, P.S. Foster, R.H.H. Scott (Central Laser Facility, STFC Rutherford Appleton Laboratory, Harwell Campus, Didcot, UK)
S. Glenzer, W. Schumaker (SLAC, California, USA)
E. Hill, S. Rose, M. Sherlock (Blackett Laboratory, Imperial College London, UK)

Betatron radiation from laser wakefield accelerators is an ultrashort pulsed source of hard, synchrotron-like x-ray radiation. It emanates from a centimetre-scale plasma accelerator producing GeV level electron beams. In recent years, betatron radiation has been developed as a unique source capable of producing high resolution x-ray images in compact geometries. However, until now, the short pulse nature of this radiation has not been exploited. This report details the first experiment to utilize betatron radiation to image a rapidly evolving phenomenon, by using it to radiograph a laser-driven shock wave in a silicon target. The spatial resolution of the image is comparable to what has been achieved in similar experiments at conventional synchrotron light sources. The intrinsic temporal resolution of betatron radiation is below 100 fs, indicating that significantly faster processes could be probed in future without compromising spatial resolution. Quantitative measurements of the shock velocity and material density were made from the radiographs recorded during shock compression, and were consistent with the established shock response of silicon, as determined with traditional velocimetry approaches. This suggests that future compact betatron imaging beamlines could be useful in the imaging and diagnosis of high-energy-density physics experiments.

Contact: J.C. Wood (jonathan.wood08@imperial.ac.uk)



X-ray images of shocked silicon targets taken with betatron radiation. (a) Radiograph of a laser driven shock in silicon at 5.2 ns after the start of the interaction. The shock driving laser travelled from left to right. The geometric magnification of the images was 30. (b) Radiograph of a shock wave in silicon with a 25 μm CH ablator layer on the drive surface taken at $\Delta t = 6.5$ ns. Also visible is adhesive at the rear of the target, which did not participate in the interaction. (c) Drive laser intensity (blue), shock front position (red) and drive surface position (green) as a function of y found from the image of the untamped silicon sample, where the shaded area indicates the error. The black dashed line shows the position that the elastic wave, which was not observed in this experiment, would have reached after 5.2 ns (travelling at 8.43 km s⁻¹).

Reprinted from Wood, J.C., Chapman, D.J., Pöder, K. et al. Ultrafast Imaging of Laser Driven Shock Waves using Betatron X-rays from a Laser Wakefield Accelerator. *Sci Rep* 8, 11010 (2018) doi:10.1038/s41598-018-29347-0, published by Springer Nature, under the Creative Commons Attribution 4.0 International License.

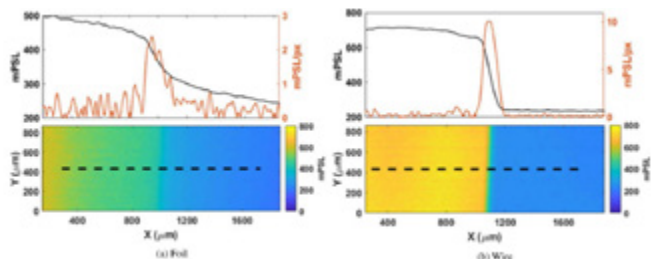
Bremsstrahlung emission from high power laser interactions with constrained targets for industrial radiography

C.D. Armstrong (Department of Physics SUPA, University of Strathclyde, Glasgow, UK; Central Laser Facility, STFC Rutherford Appleton Laboratory, Harwell Campus, Didcot, UK)
C.M. Brenner, D.R. Rusby, J. Wragg, S. Richards, C. Spindloe, P. Oliveira, M. Notley, R. Clarke, D. Neely (Central Laser Facility, STFC Rutherford Appleton Laboratory, Harwell Campus, Didcot, UK)
C. Jones, T. Scott (Interface Analysis Centre, HH Wills Physics Laboratory, Bristol, UK)
Z.E. Davidson, P. McKenna (Department of Physics SUPA, University of Strathclyde, Glasgow, UK)

Y. Zhang (Central Laser Facility, STFC Rutherford Appleton Laboratory, Harwell Campus, Didcot, UK; Beijing National Laboratory for Condensed Matter Physics, Institute of Physics, Chinese Academy of Sciences, Beijing, China)
Y. Li (Beijing National Laboratory for Condensed Matter Physics, Institute of Physics, Chinese Academy of Sciences, Beijing, China)
S.R. Mirfayzi, S.Kar (Centre for Plasma Physics, Queen's University Belfast, UK)

Laser–solid interactions are highly suited as a potential source of high energy X-rays for non-destructive imaging. A bright, energetic X-ray pulse can be driven from a small source, making it ideal for high resolution X-ray radiography. By limiting the lateral dimensions of the target we are able to confine the region over which X-rays are produced, enabling imaging with enhanced resolution and contrast. Using constrained targets we demonstrate experimentally a (20 ± 3) μm X-ray source, improving the image quality compared to unconstrained foil targets. Modelling demonstrates that a larger sheath field envelope around the perimeter of the constrained targets increases the proportion of electron current that recirculates through the target, driving a brighter source of X-rays.

Contact: C.D. Armstrong (chris.armstrong@stfc.ac.uk)



Penumbral radiograph, scale in mPSL (unit of flux for IP), and lineout for (a) foil and (b) wire targets. The dashed line in each radiograph is where the lineout is determined.

Reprinted from Armstrong, C. et al. High Power Laser Science and Engineering, 7, E24 (2019) doi: 10.1017/hpl.2019.8, under the terms of the Creative Commons Attribution 4.0 International License

Bremsstrahlung emission profile from intense laser-solid interactions as a function of laser focal spot size

C.D. Armstrong, E. Zemaityte (Department of Physics SUPA, University of Strathclyde, Glasgow, UK; Central Laser Facility, STFC Rutherford Appleton Laboratory, Harwell Campus, Didcot, UK)

C.M. Brenner, P. Oliveira, C. Spindloe, D. Neely, G.G. Scott, D.R. Rusby (Central Laser Facility, STFC Rutherford Appleton Laboratory, Harwell Campus, Didcot, UK)

G. Liao (Key Laboratory for Laser Plasmas (Ministry of Education) and School of Physics and Astronomy, Shanghai Jiao Tong University, Shanghai, China)

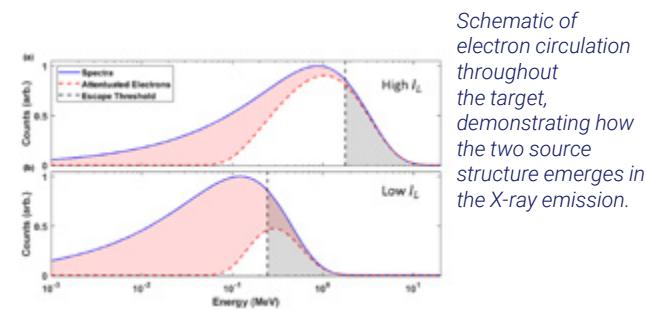
H. Liu, Y. Zhang (Central Laser Facility, STFC Rutherford Appleton Laboratory, Harwell Campus, Didcot, UK; Beijing National Laboratory for Condensed Matter Physics, Institute of Physics, Chinese Academy of Sciences, Beijing, China)

Y. Li, Z. Zhang, B. Zhu, W. Wang (Beijing National Laboratory for Condensed Matter Physics, Institute of Physics, Chinese Academy of Sciences, Beijing, China)

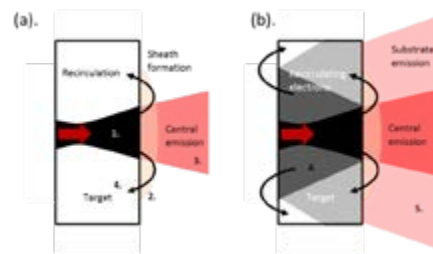
P. Bradford, N.C. Woolsey (Department of Physics, York Plasma Institute, University of York, UK) **P. McKenna** (Department of Physics SUPA, University of Strathclyde, Glasgow, UK)

The bremsstrahlung X-ray emission profile from high intensity laser-solid interactions provides valuable insight into the internal fast electron transport. Using penumbral imaging, we characterise the spatial profile of this bremsstrahlung source as a function of laser intensity by incrementally increasing the laser focal spot size on target. The experimental data shows a dual-source structure; one from the central channel of electrons, the second a larger substrate source from there circulating electron current. The results demonstrate that an order of magnitude improvement in the intensity contrast between the two X-ray sources is achieved with a large focal spot, indicating preferable conditions for applications in radiography. An

analytical model is derived to describe the transport of supra-thermal electron populations that contribute to substrate and central channel sources through a target. The model is in good agreement with the experimental results presented here and furthermore is applied to predict laser intensities for achieving optimum spatial contrast for a variety of target materials and thicknesses.



Schematic of electron circulation throughout the target, demonstrating how the two source structure emerges in the X-ray emission.



Maxwellian distribution for electrons with temperature at two different laser intensities, top for 10^{20} Wcm^{-2} and bottom for $4 \times 10^{18} \text{ Wcm}^{-2}$, this correlates to the laser at best focus and $150 \mu\text{m}$ defocus. The red dashed line indicates electron transmission through the target, black dashed line is the escape energy cut-off. The population of electrons between these two lines contributes to the substrate source (unshaded), the other two (red—collisional, grey—escaping) can only contribute to the central source.

Reprinted from C D Armstrong et al. (2019) Bremsstrahlung emission profile from intense laser-solid interactions as a function of laser focal spot size, *Plasma Phys. Control. Fusion* 61 034001, doi: 10.1088/1361-6587/aaf596, under the terms of the Creative Commons Attribution 3.0 Licence

Contact: C.D. Armstrong (chris.armstrong@stfc.ac.uk)

EMP control and characterization on high-power laser systems

P. Bradford, N.C. Woolsey (Department of Physics, York Plasma Institute, University of York, UK)

G.G. Scott, S. Astbury, C. Brenner, P. Brummitt, I. East, D. Haddock, P.J.R. Jones, E. Montgomery, P. Oliveira, D.R. Rusby, C. Spindloe, I. Musgrave, B. Summers (Central Laser Facility, STFC Rutherford Appleton Laboratory, Harwell Campus, Didcot, UK)

G. Liao (Key Laboratory for Laser Plasmas (Ministry of Education) and School of Physics and Astronomy, Shanghai Jiao Tong University, Shanghai, China)

H. Liu, Y. Zhang, B. Zhu, Y. Li (Beijing National Laboratory for Condensed Matter Physics, Institute of Physics, Chinese Academy of Sciences, Beijing, China; School of Physical Sciences, University of Chinese Academy of Sciences, Beijing, China)

C. Armstrong, R. Gray, E. Zemaityte, P. McKenna (Department of Physics SUPA, University of Strathclyde, Glasgow, UK)

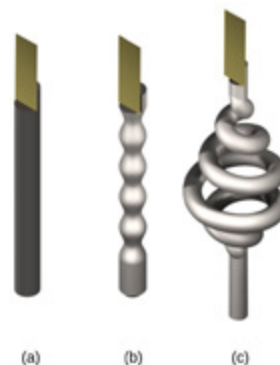
F. Consoli (ENEA - C.R. Frascati - Dipartimento FSN, Frascati, Italy)

P. Huggard (Space Science Department, STFC Rutherford Appleton Laboratory, Harwell Campus, Didcot, UK)

Z. Zhang (Beijing National Laboratory for Condensed Matter Physics, Institute of Physics, Chinese Academy of Sciences, Beijing, China)

D. Neely (Department of Physics SUPA, University of Strathclyde, Glasgow, UK; Central Laser Facility, STFC Rutherford Appleton Laboratory, Harwell Campus, Didcot, UK)

Electromagnetic pulses (EMP) generated during the interaction of high-power lasers with solid targets can seriously degrade electrical measurements and equipment. EMP emission is caused by the acceleration of hot electrons inside the target, which produce radiation across a wide band from DC to terahertz frequencies. Improved understanding and control of EMP is vital as we enter a new era of high repetition rate, high intensity lasers (e.g. the Extreme Light Infrastructure). We present recent data from the Vulcan laser facility that demonstrates how EMP emission can be significantly reduced. We show that target holder (stalk) geometry, material composition, geodesic path length and foil surface area can all play a significant role in the reduction of EMP. A combination of electromagnetic wave and 3D particle-in-cell simulations is used to inform our conclusions about the effects of stalk geometry on EMP, providing an opportunity for comparison with existing models of laser-target charging.



Three different stalk designs used to support the laser target: (a) cylinder (b) sinusoidally modulated stalk (c) spiral stalk. A significant reduction in EMP amplitude was observed for plastic stalks of all stalk designs compared with a metallic stalk of type (a). The biggest overall reduction was seen for a plastic spiral stalk design

Reprinted from Bradford, P. et al. (2018). EMP control and characterization on high-power laser systems. *High Power Laser Science and Engineering*, 6, E21. doi:10.1017/hpl.2018.21, under the terms of the Creative Commons Attribution 4.0 International License

Contact: P. Bradford (philip.bradford@york.ac.uk)

An optically multiplexed single-shot time-resolved probe of laser–plasma dynamics

Z.E. Davidson, B. Gonzalez-Izquierdo, A. Higginson, S.D.R. Williamson, M. King, P. McKenna, R.J. Gray (Department of Physics, SUPA, University of Strathclyde, Glasgow, UK)
K.L. Lancaster, D. Farley (Department of Physics, University of York, UK)

D. Neely (Central Laser Facility, STFC Rutherford Appleton Laboratory, Harwell Campus, Didcot, UK; Department of Physics, SUPA, University of Strathclyde, Glasgow, UK)

We introduce a new approach to temporally resolve ultrafast micron-scale processes via the use of a multi-channel optical probe. We demonstrate that this technique enables highly precise time-resolved, two-dimensional spatial imaging of intense laser pulse propagation dynamics, plasma formation and laser beam filamentation within a single pulse over four distinct time frames. The design, development and optimization of the optical probe system is presented, as are representative experimental results from

the first implementation of the multi-channel probe with a high-power laser pulse interaction with a helium gas jet target. The probe has also uncovered interesting, evolving front surface dynamics on solid targets. The novel concept presented here has the potential to be extended and adapted for cross-disciplinary research interests that could benefit from temporally resolving ultrafast processes, particularly in cases where the underlying dynamics appear stochastic.

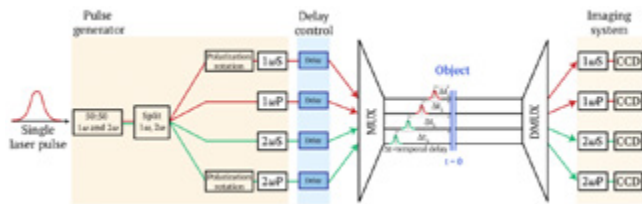


Figure 1: Process flow diagram of multiplexed optical probe concept. A single ultrashort laser pulse is divided into four separate laser pulses which are uniquely encoded by frequency and polarization. The four pulses are independently delayed in time and then spatially multiplexed (MUX) to propagate co-linearly in order to optically probe a given point in space and time. The inverse process (DMUX) is then applied to spatially separate and form an image for each of the channels. This enable 2D spatial and picosecond temporal resolution over multiple frames with a single laser pulse.

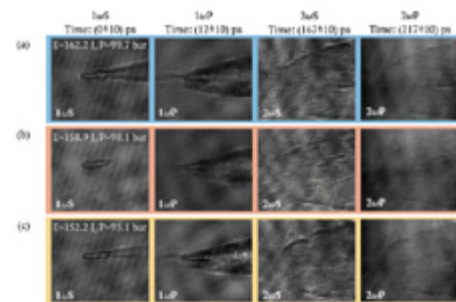


Figure 2: Shadowgraphy measurements of each probe output channel from the experiment for (a) $E = 162.2 \text{ J}$, $P = 99.7 \text{ bar}$ (b) $E = 158.9 \text{ J}$, $P = 98.1 \text{ bar}$ and (c) $E = 152.2 \text{ J}$, $P = 95.1 \text{ bar}$.

Reproduced from Z. E. Davidson et al. An optically multiplexed single-shot time-resolved probe of laser–plasma dynamics, *Opt. Express* 27, 4416–4423 (2019) doi: 10.1364/OE.27.004416, copyright OSA

Contact: Z.E. Davidson (zoe.e.davidson@strath.ac.uk)

Dual Ion Species Plasma Expansion from Isotopically Layered Cryogenic Targets

G.G. Scott, D.C. Carroll, S. Astbury, R.J. Clarke, C. Hernandez-Gomez, I.Y. Arteaga, S. Hook, D.R. Rusby, M.P. Selwood, C. Spindloe, M.K. Tolley, E. Zemaityte, D. Neely (Central Laser Facility, STFC Rutherford Appleton Laboratory, Harwell Campus, Didcot, UK)
M. King, R.J. Dance, A. Higginson, P. McKenna (Department of Physics SUPA, University of Strathclyde, Glasgow, UK)
A. Alejo, S. R. Mirfayzi, S. Kar, M. Borghesi (Department of Pure and Applied Physics, Queen's University Belfast, UK)

G. Liao (Key Laboratory for Laser Plasmas (Ministry of Education) and School of Physics and Astronomy, Shanghai Jiao Tong University, Shanghai, China)
H. Liu, Y. Li (Beijing National Laboratory for Condensed Matter Physics, Institute of Physics, Chinese Academy of Sciences, Beijing, China)
F. Wagner (PHELIX Group, GSI Helmholtzzentrum für Schwerionenforschung GmbH, Darmstadt, Germany)
M. Roth (Fachbereich Physik, Technische Universität Darmstadt, Germany)

In this study we utilise the state-of-the-art cryogenic targetry capability, jointly developed by the Central Laser Facility and A-SAIL consortium, to freeze nanometre-thick layers of solid density deuterium onto the rear surface of a target substrate, on which hydrogen rich monolayers are present.

In this unique target configuration, a heavier (deuteron) ion species exists as a separate layer between the target vacuum interface and a lighter (proton) ion species, and we show that this results in the ability to control the acceleration of the heavier ion population expansion dynamics, resulting in a spectrally peaked, directional beam.

In the full article^[1], we present the first theoretical consideration and experimental demonstration of a plasma expansion scheme of this nature.

This article was featured as a CLF [highlight](#).



Part of the experimental team alongside the CLF/A-SAIL cryogenic targetry apparatus

[1] G.G. Scott et al., *Phys. Rev. Lett.* 120, 20480, 2018

Contact: G.G. Scott (scott110@lnl.gov)

Supersonic Turbulence in the Laboratory

T.G. White (University of Nevada, Reno, USA)

M.T. Oliver, P. Mabey, A.F.A. Bott, A.R. Bell, M. Kühn-Kauffeldt, J. Meinecke, F. Miniati, S. Sarkar, A.A. Schekochihin, G. Gregori (University of Oxford, UK)

L.N.K. Döhl, N. Woolsey (University of York, UK)

R. Bingham, R. Clarke, R. Heathcote, M. Notley, M.P. Selwood, R.H.H. Scott (Central Laser Facility, STFC Rutherford Appleton Laboratory, Harwell Campus, Didcot, UK)

J. Foster, P. Graham (AWE, UK)

G. Giacinti (Max-Planck-Institut für Kernphysik, 69029 Heidelberg, Germany)

M. Koenig, Th. Michel (LULI-CNRS, Ecole Polytechnique, France)

Y. Kuramitsu (Osaka University, Japan)

D.Q. Lamb, P. Tzeferacos (University of Chicago, USA)

B. Reville (Queens University Belfast, UK)

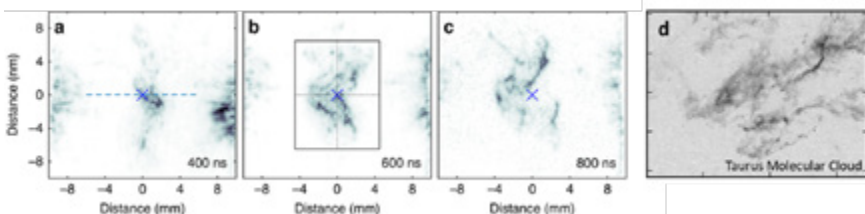
D. Ryu (School of Natural Sciences, UNIST, Korea)

Y. Sakawa (Institute of Laser Engineering, Osaka, Japan)

J. Squire (California Institute of Technology, USA)

The properties of supersonic, compressible plasma turbulence determine the behaviour of many terrestrial and astrophysical systems. In the interstellar medium and molecular clouds, compressible turbulence plays a vital role in star formation and the evolution of our galaxy. Observations of the density and velocity power spectra in the Orion B and Perseus molecular clouds show large deviations from those predicted for incompressible turbulence. Hydrodynamic simulations attribute this to the high Mach number in the interstellar medium (ISM), although the exact

details of this dependence are not well understood. Here we investigate experimentally the statistical behaviour of boundary-free supersonic turbulence created by the collision of two laser-driven high-velocity turbulent plasma jets. The Mach number dependence of the slopes of the density and velocity power spectra agree with astrophysical observations and support the notion that the turbulence transitions from being Kolmogorov-like at low Mach number to being more Burgers-like at higher Mach numbers.



Schlieren images showing the region between two colliding supersonic jets taken at (a) 400 ns, (b) 600 ns, and (c) 800 ns after the peak of the drive laser. The development of filament-like structures is characteristic of supersonic turbulence and consistent to those found in the Taurus molecular cloud (d) G.V. Panopoulou et al. MNRAS, 444, 2507 (2014).

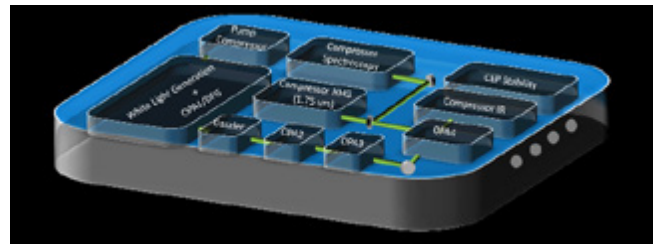
Contact: T.G. White (tgwhite@unr.edu)

Laser Science & Development

Installation of the Mid-IR OPCPA Laser in the RCaH CLF Laboratories

G. Karras, G. Greetham, Y. Zhang, S. Conroy, A.S. Wyatt, A. Cox, P. Rice, S. Spurdle, P. Brummitt, E. Springate, M. Towrie (Central Laser Facility, Research Complex at Harwell, STFC Rutherford Appleton Laboratory, Harwell Campus, Didcot, UK)

The Artemis / ULTRA upgrade continued this year with the relocation of the Artemis laboratory to the Research Complex at Harwell (RCaH). The relocation included the introduction of third generation ultrafast laser technology to these facilities. The installed system has passed the major milestone of factory acceptance, demonstrating its capability, and is now located in the RCaH for installation and site acceptance in January 2020. The system comprises a high average power pump laser, based on an Yb:YAG thin disk regenerative amplifier front end and an OPCPA. In this paper we present results of evaluation measurements regarding the expected efficiency of the laser in producing high harmonic generation photons, and simulations of super continuum generation in the mid-IR region.



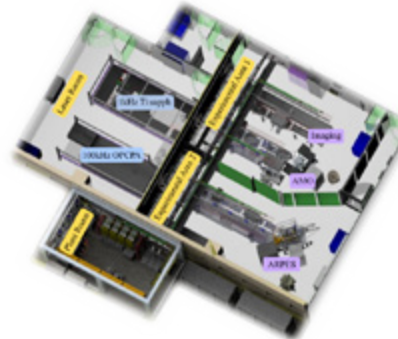
Cartoon layout showing the different sections of the new OPCPA system

Contact: G. Karras (gabriel.karras@stfc.ac.uk)

New laboratories for Artemis in the RCaH

A.S. Wyatt, R.T. Chapman, G. Karras, Y. Zhang, C. Sanders, G. Greetham, A. Cox, P. Rice, S. Spurdle, P. Brummitt, M. Towrie, E. Springate (Central Laser Facility, Research Complex at Harwell, STFC Rutherford Appleton Laboratory, Harwell Campus, Didcot, UK)

The Artemis / ULTRA upgrade continued this year with the relocation of the Artemis laboratory to the Research Complex at Harwell (RCaH). Two adjacent laboratories totalling 120 m² have been fully refurbished for Artemis, doubling the floor space of the facility. In this article we report on the progress made and outline the laboratory configuration and future capabilities.



Schematic of the new Artemis facility in the Research Complex at Harwell

Contact: E. Springate (emma.springate@stfc.ac.uk)

Upgrades to the Artemis Material Science Station

Y. Zhang, C. Toolan, R.T. Chapman, A.S. Wyatt, C. Sanders, E. Springate (Central Laser Facility, Research Complex at Harwell, STFC Rutherford Appleton Laboratory, Didcot UK)

We have upgraded the material science station at Artemis by motorizing the sample manipulator, and installing a new two-dimensional photoelectron detector and high-speed camera. These upgrades will enable new experimental schemes and more efficient data collection.

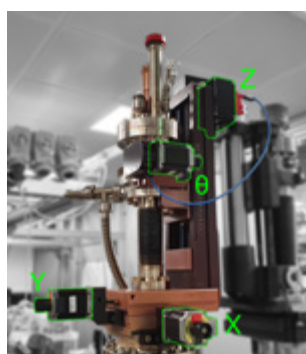


Photo of the manipulator on the motorized translation stage. The corresponding driving motors are highlighted.

Contact: Y. Zhang (yu.zhang@stfc.ac.uk)

Acoustic signature of laser shock peening for a qualitative evaluation of residual stress

S. Banerjee, T.J. Butcher, M. De Vido, K. Ertel, P.D. Mason, P.J. Phillips, J.M. Smith, S. Tomlinson, C.B. Edwards, J.L. Collier (Central Laser Facility, STFC Rutherford Appleton Laboratory, Harwell Campus, Didcot, UK)

Acoustic signals recorded from laser shock peening (LSP) of aluminium, titanium and stainless steel alloys were analysed for different laser pulse widths, energy and confinement conditions. In this paper, we report that different materials and conditions registered unique acoustic signatures. Further, the acoustic signatures in the time domain were transformed to the frequency domain and were fitted to a

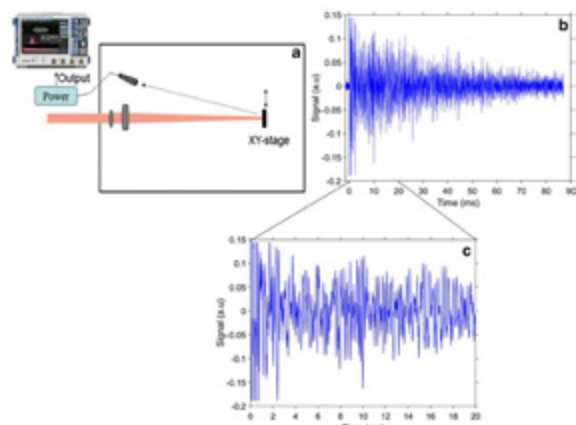


Figure 1: (a) layout of the LSP workstation; (b) typical temporal evolution of the LSP acoustic signal; (c) expanded view of the temporal signal showing convolution of multiple signals

R. Allott (Business and Innovation, STFC Rutherford Appleton Laboratory, Harwell Campus, Didcot, UK)

J. Nygaard (Reaction Engines Ltd, Culham Science Centre, Abingdon, UK)

lognormal distribution, yielding a unique set of parameters for each material and set of conditions. These parameters were benchmarked using the measurements of residual stress by the incremental centre hole-drilling (ICHD) method. Detailed analysis of the acoustic signal reveals that this method once calibrated with few ICHD data, can identify successful peening of materials.

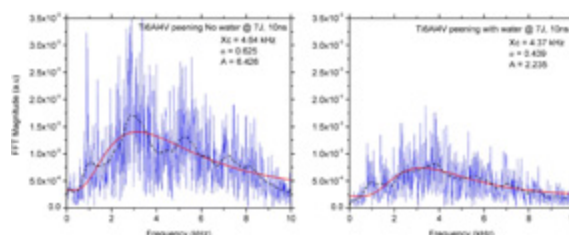


Figure 2: FFT obtained from the temporal acoustic signal for Ti6Al4V with and without a confinement medium (water) at 7 J, 10 ns. The red line shows a lognormal fit to the data. The dashed black line is the adjacent-averaged signal showing multiple peaks. Also given are the set of parameters obtained with the fit.

Reproduced from Banerjee, S., Phillips, P.J., Nygaard, J. et al. Appl. Phys. A 125, 571 (2019). <https://doi.org/10.1007/s00339-019-2869-1>, under the terms of the Creative Commons Attribution 4.0 International License.

Contact: S. Banerjee (saumyabrata.banerjee@stfc.ac.uk)

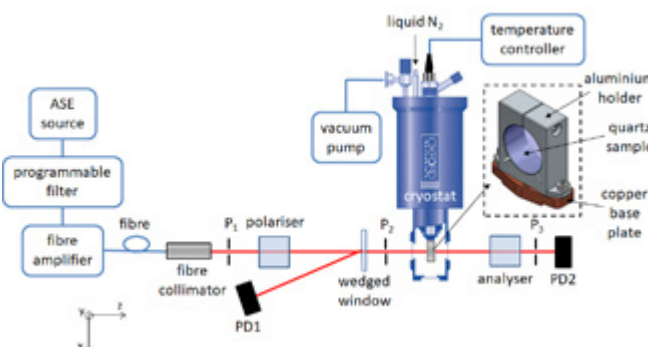
Optical rotatory power of quartz between 77K and 325K for 1030nm wavelength

M. De Vido, K. Ertel, P.D. Mason, P.J. Phillips, S. Banerjee, J.M. Smith, T.J. Butcher, C.B. Edwards (Central Laser Facility, STFC Rutherford Appleton Laboratory, Harwell Campus, Didcot, UK)

A. Wojtusiak (Loughborough University, UK)

We report on the experimental characterisation of the temperature dependence of the optical rotatory power of crystalline α -quartz at 1030 nm wavelength. The temperature range covered in this study is between 77 K and 325 K. For the measurement we propagated light through a 13.11 mm thick quartz plate collinearly with the optic axis. At room temperature, the plate rotates the polarisation plane of 1030 nm light by 89.3 deg, corresponding to a specific rotatory power of 6.8 deg/mm. When placed between parallel polarisers, the transmission through the system was 0.03% at room temperature and increased to 1% at 77 K, showing a measurable change in rotatory power. At 77 K, the angle of rotation imparted by the quartz plate is 85 deg, corresponding to a specific rotatory power of 6.5 deg/mm. To the best of our knowledge, this is the first time that the temperature dependence of optical activity of α -quartz is reported for cryogenic temperatures in the infrared. We expect that these results will assist in the design and characterisation of optical systems operating under cryogenic conditions.

Contact: M. De Vido (mariastefania.de-vido@stfc.ac.uk)



Experimental setup used to characterise the temperature dependence of the rotatory power of quartz

Reproduced from M. De Vido, K. Ertel, A. Wojtusiak, P.D. Mason, P.J. Phillips, S. Banerjee, J.M. Smith, T.J. Butcher, and C. Edwards, "Optical rotatory power of quartz between 77 K and 325 K for 1030 nm wavelength," Opt. Mater. Express 9, 2708-2715 (2019) under the terms of the Creative Commons Attribution 4.0 License. <https://doi.org/10.1364/OME.9.002708>

EPICS-based software for the Vulcan Target Alignment Rig

A. Chipade, T. Zata (Central Laser Facility, STFC Rutherford Appleton Laboratory, Harwell Campus, Didcot, UK)

New EPICS-based software was written to enable the alignment and inspection of targets in Vulcan Target Areas using the existing control hardware, with upgraded cameras.

The Vulcan Target Alignment Rig is used to inspect a component from various angles using three cameras and a rotary target stage, each of which can be controlled in x, y and z axes.

As the custom software written for the original system could not be upgraded to be compatible with Windows 10, it was decided to develop an EPICS-based software control system compatible with the existing motion controllers, while upgrading the cameras.

EPICS input/output controllers implement the required back-end functionality, such as communication with device drivers, inter-device communication and synchronization, parameter settings, etc. An intuitive graphical user interface has been developed with a similar appearance and features to the previous system.

Contact: A. Chipade (apeksha.chipade@stfc.ac.uk)

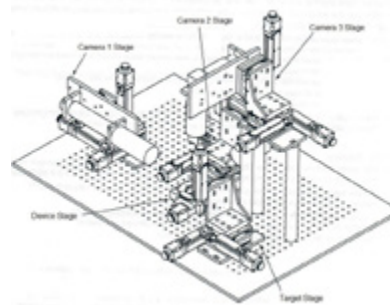


Figure 1: System layout

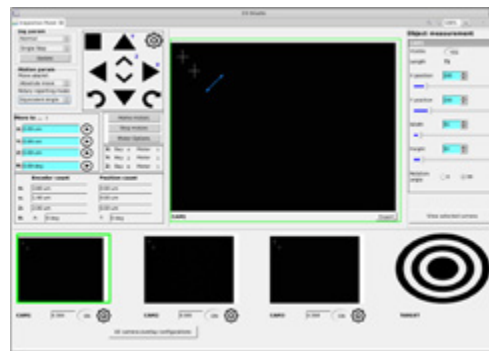


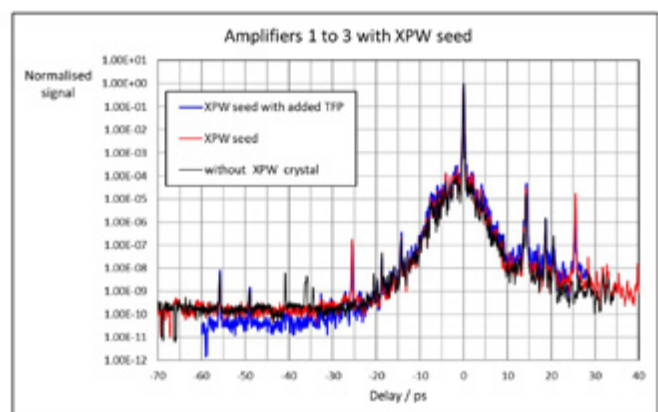
Figure 2: Inspection control panel

Investigation of temporal properties of a cross-polarised wave generation temporal filter at the front-end of the Gemini laser system

O. Chekhlov, S. Hawkes, P.P. Rajeev (Central Laser Facility, STFC Rutherford Appleton Laboratory, Harwell Campus, Didcot, UK)

A temporal control unit (TCU) has been built at the front end of the Gemini system. The core of the TCU is a cross-polarized wave temporal filter (XPWTF). The device also includes a temporal stretcher with a programmable dispersion filter, and a booster amplifier that restores the energy of the pulses to ~ 0.9 mJ, compensating for the energy lost in the non-linear processes. The output of the TCU was recently coupled into the Gemini amplifier chain for the first time, and the energy, spectra and temporal contrast of the pulses were measured. The energy and spectrum were normal. The contrast traces, which are presented in the figure, were measured after the Gemini compressor with a third order cross correlator (Sequoia). Some pre-pulses have been eliminated, and the background level reduced. For a full description of the device and its operation, see the extended online version of this article.

Contact: O. Chekhlov (oleg.chekhlov@stfc.ac.uk)

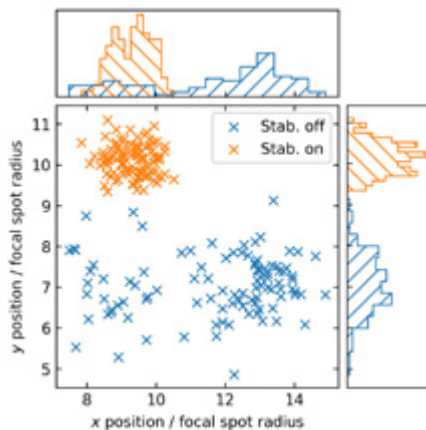


Sequoia traces of the temporal contrast of the cleaned pulse after compression. Black: without XPW crystal in XPWTF; Red: with XPW crystal; Blue: with extra thin film polarizer before XPWTF.

Beam Pointing Stabilisation on the Gemini Laser System

S.J.D. Dann, M. Galimberti, C. Gregory, N. Martin, B. Matthews, B. Parry (Central Laser Facility, STFC Rutherford Appleton Laboratory, Didcot, UK)

We describe a new system in the Gemini facility that uses a back-propagating pilot beam to detect changes in the beam direction. These changes are then corrected using a PID controller and a piezo-actuated mirror. This stabilises the pointing of the forward-propagating full power main beam, halving the observed variation in the target area. This could be used to lock the beam to a small target, or to stabilise one or (in the future) both beams at a collision point. Experiments requiring the best pointing stability, or in which a laser beam needs to interact with an electron beam or a second laser beam, will all benefit from this development.



The beam pointing during full power shots with stabilisation switched on and off, measured in multiples of the focal spot radius.

Contact: S.J.D. Dann (stephen.dann@stfc.ac.uk)

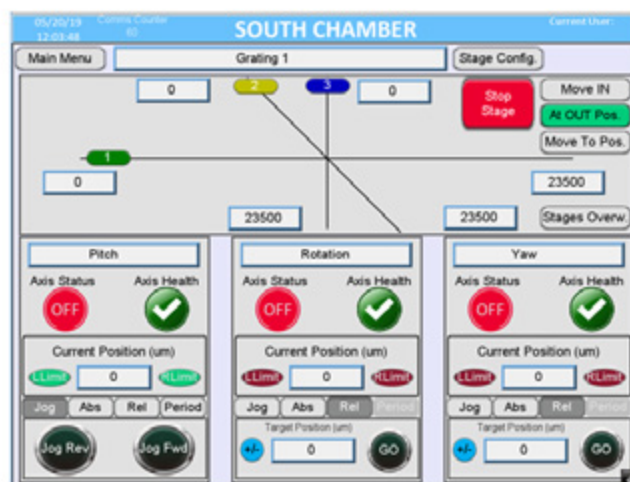
Operational improvements to the Gemini Facility 2018-19

C.J. Hooker, R. Sarasola, K. Rodgers, J. Suarez-Merchan, N. Bourgeois, A. Patel, S. Blake (Central Laser Facility, STFC Rutherford Appleton Laboratory, Harwell Campus, Didcot, UK)

During the year there have been several modest improvements made to the Gemini facility, which individually do not merit separate articles. These include:

- The installation of a new drive system on the south compressor;
- The installation of new beam attenuators that allow the Gemini beams to be attenuated by 100x or 10,000x for setup purposes, without any change in relative timing;
- New lens pairs to enable adjustment of the focal length in the pump beam homogenization optics;
- Improved temperature monitoring in the Gemini laser area.

Each of these developments has led to either an improvement in the usability of the laser or a better understanding of a problem, which will in turn lead to further improvements once the problem has been solved.



Screenshot of the control interface of the new drive system for the Gemini south compressor.

Contact: C.J. Hooker (chris.hooker@stfc.ac.uk)

Software development in Gemini

V.A. Marshall (Central Laser Facility, STFC Rutherford Appleton Laboratory, Harwell Campus, Didcot, UK)

The Gemini laser system software consists of a network of distributed applications which are used to control elements of the laser, and monitor a large number of parameters both on-shot and continuously.

Over the last year, the most significant upgrade to this software has been the introduction of the Experimental Physics and Industrial Control System (EPICS), originally developed at Los Alamos National Laboratory. Software developed for Gemini using this system includes:

- The main control system, which exports around 80 EPICS Process Variables (PVs) detailing the state of the laser and the target areas;
- TA2 control system, the user interface of which has been upgraded and redesigned to display more clearly the state of the system;
- TA3 control system, the user interface of which has also been upgraded and redesigned, with a new in-window timeline facilitating visualisation of the sequence of events in the system (see Figure).

Contact: V.A. Marshall (victoria.marshall@stfc.ac.uk)

In addition, two carefully configured servers have been introduced to act as Gateways between multiple networks (user institute, camera, laser and main site). These allow users to manage their own data acquisition systems, whilst also permitting visibility of Gemini PVs and diagnostic data.



Part of the TA3 Control System main window

Development of thin bond lines for high power laser experiment targets

P. Ariyathilaka (Scitech Precision Ltd, Rutherford Appleton Laboratory, Harwell Science & Innovation Campus, Didcot, UK)

C. Spindloe, A. Hughes (Central Laser Facility, STFC Rutherford Appleton Laboratory, Harwell Campus, Didcot, UK)

This article gives a brief introduction to a micro-assembly project commissioned by the Atomic Weapons Establishment (AWE), to develop targets with $\leq 1 \mu\text{m}$ adhesion layers in between two of the components. Scitech Precision was successful in achieving the specification, with an average adhesion layer thickness of $1.07 \mu\text{m} \pm 0.28 \mu\text{m}$.

The assembled target consisted of a single crystal diamond (SCD) attached to a tungsten washer. Polymethylmethacrylate (PMMA) was spin-coated on to the SCD, to be used as the adhesion layer on which a copper foil was placed in a particular orientation, as instructed in the target specification.



Figure 1: Schematic of the assembled multilayer target

Development work focused in particular on the spin-coated PMMA thin film, which was used as a micron-thick adhesion layer. The average thickness was measured using a touch probe (Tencor Alpha Step IQ). Spin speed and spin time, the main parameters of the spin coater that determine film thickness, were investigated to determine the optimum settings to achieve the required thickness, whilst maintaining a wet film on the SCD that would adhere sufficiently to the copper foil.

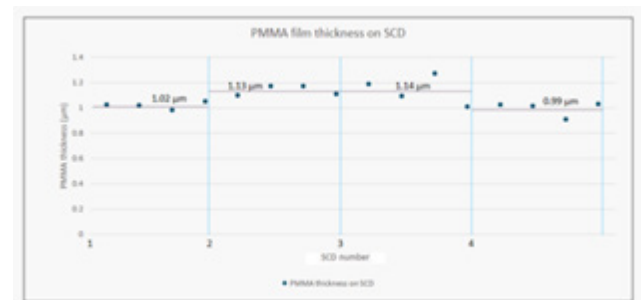


Figure 2: Graph showing the average PMMA film thickness across four different SCDs

Contact: P. Ariyathilaka (pawala.ariyathilaka@scitechprecision.com)

Progression of a tape-drive targetry solution for high rep-rate HPL experiments within the CLF

S. Astbury, C. Spindloe, M. Tolley (Target Fabrication Group, Central Laser Facility, STFC Rutherford Appleton Laboratory, Harwell Campus, Didcot, UK)
L. Harman, P. Sykes (Scitech Precision Ltd, Rutherford Appleton Laboratory, Harwell Science & Innovation Campus, Didcot, UK)

W. Robins (Precision Development Facility, RAL Space, STFC Rutherford Appleton Laboratory, Harwell Campus, Didcot, UK)
R. Sarasola, K. Rodgers (Electrical and Control Group, Central Laser Facility, STFC Rutherford Appleton Laboratory, Harwell Campus, Didcot, UK)

This annual report focuses on the work undertaken by the Target Fabrication Group and the Electrical and Control Group on developing a novel tape-target technology, as well as a system for driving these tapes at a high stability.

The report includes interferometric and chromatic confocal scans of the flatness and stability of the tape, both while stationary and driving at high repetition rate velocities.

The tape drive is shown to have a stability in the laser axis to within $\pm 5 \mu\text{m}$ and supports the use of the system and target technology on future high power laser experiments, without having to refocus between shots.

Future upgrades to the target fabrication methods are discussed, including manufacture of a coating plant compatible tape drive system for coating directly onto long rolls of tape. Improvements to the drive system are also suggested, namely being able to be ran in both directions to allow for even higher shot rates.

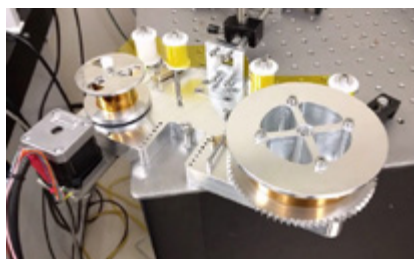


Figure 1. Design of CLF's high-stability tape drive system

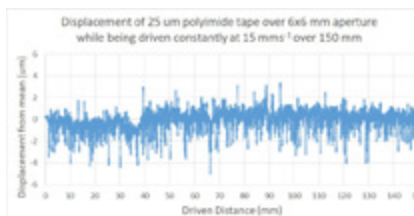


Figure 2. Chromatic confocal displacement scan of tape driving at 15 mms^{-1}

Contact: S. Astbury (sam.astbury@stfc.ac.uk)

Micro computed tomography for characterisation of high-power laser targets

S. Irving, C. Spindloe, A. Hughes (Target Fabrication Group, Central Laser Facility, STFC Rutherford Appleton Laboratory, Harwell Campus, Didcot, UK)

Precise characterisation of targets is a necessity in the field of high power laser experiments, to allow accurate analysis of experimental data, as well as to confirm that the targets produced conform to the agreed specifications.

For targets where features are embedded within other solid regions, standard imaging techniques (e.g. SEM, AFM) are inadequate. Micro-computed X-ray tomography (μCT)

provides a means of imaging the interior of solid targets, thus overcoming this limitation. Using μCT it is possible to detect regions with different densities to the surrounding material within objects.

This report presents two case-studies in the use of μCT for imaging foam targets with embedded components, and the method of characterisation for these samples.

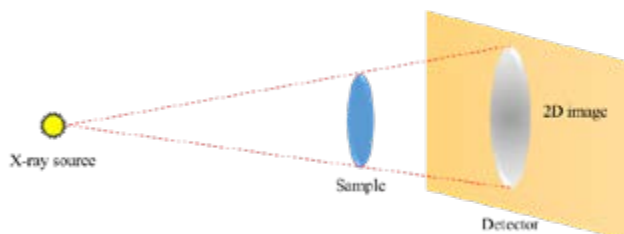


Figure 1: Schematic of the μCT imaging process; X-rays pass through the object, and are rendered on the detector, with denser regions producing darker images

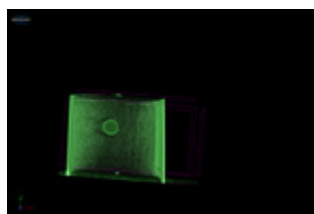


Figure 2: μCT scan of PS bead embedded in a foam target

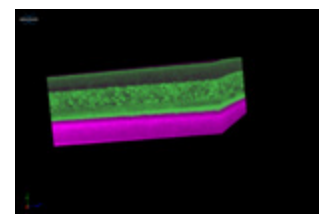


Figure 3: μCT scan of a multilayer target showing four distinctive layers: from bottom to top - Si wafer; 100 mg/cc foam; foam doped with $9 \mu\text{m}$ particles; foam doped with $80 \mu\text{m}$ particles

Contact: S. Irving (samuel.irving@stfc.ac.uk)

Development of Automated Fabrication Processes for High Repetition Rate Micro-target

J. Mills, D. Haddock, S. Astbury, C. Spindloe, M. Tolley (Target Fabrication Group, Central Laser Facility, STFC Rutherford Appleton Laboratory, Harwell Campus, Didcot, UK)
P. Amos (Electrical Engineering Group, Central Laser Facility, STFC Rutherford Appleton Laboratory, Harwell Campus, Didcot, UK)

M. Williams (Diamond Light Source, Diamond House, Harwell Science & Innovation Campus, Didcot, UK)

As laser repetition rates increase, there is more demand for micro-targetry to support experiments.

This paper details a Target Fabrication Group project to enhance automated fabrication processes for micro-targetry. Array targets for use on the Gemini laser system are fabricated using two robots running independently: one to pick and place target foils, and the other to glue lines/dots upon which the target foils are to be placed.

Finding rapid and repeatable ways to fabricate these targets will reduce the strain placed on staff who carry out the fabrication and quality assurance processes. This, in turn, will allow staff more time to develop new capabilities within our laboratories, aiding experiments in the near future through improvements in the quality and rate of micro-targetry fabrication.

Future work is focused on developing more defined processes, with capabilities and reliabilities far beyond what is currently available. Use of data collection equipment, such as a camera and other sensors, will help to define and optimise the automated system, delivering improved manufacturing times, higher repeatability and greater precision without compromising flexibility.

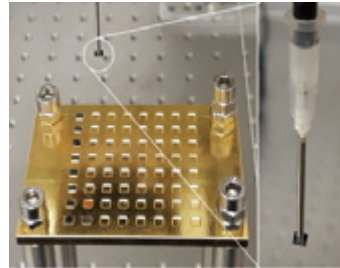


Figure 1: Gold coated, 3D-printed target foil tray. Shown is a pallet of 8x8 indents used to locate targets along with some test targets such as silicon or copper targets. Adjacent to that is a needle tip picking up a silicon target to transport over to a target array.

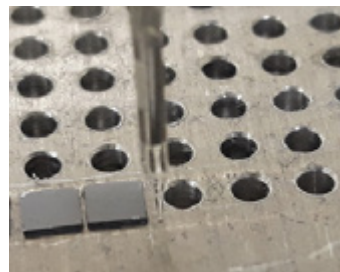


Figure 2: Target array with two targets adhered using glue dispensed from the needle tip shown.

Contact: J. Mills (millsj4@aston.ac.uk)

A compact micro-bolometer array for mid-infrared laser beam alignment, diagnostics and spot-size measurement

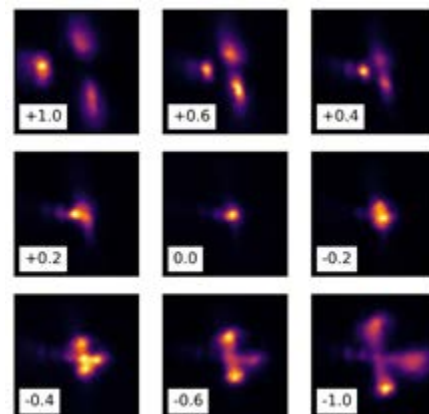
I.P. Clark, M. Towrie (Central Laser Facility, Research Complex at Harwell, STFC Rutherford Appleton Laboratory, Harwell, Didcot, UK)

Knowledge of a laser beam's profile throughout a laser system and experiment can help immensely in diagnosing laser problems, and assisting in beam alignment and focusing at a sample. Obtaining such profiles is a trivial task in the ultraviolet-visible wavelength range, but more challenging with near-infrared to infrared beams. High cost scientific grade bolometer arrays, suitable for such a task, do exist but are relatively big, and have a large pixel size, of the order of 80 μm , which is adequate for profiling larger beams but poses an issue when trying to profile sub 100 μm beams, for example, at a focal point.

We have identified a micro-bolometer array for near- to mid-infrared laser beam profiling, based on an inexpensive Seek Thermal Android camera. The device is very compact, enabling use in confined spaces, and has a small, 12 μm , pixel size permitting the profiling of focused laser beams. This compares to 17 μm for the nearest scientific grade device. This device is a powerful tool for infrared laser spectroscopists, reducing the time required to measure the spot size of beams and to achieve spatial overlap of multiple infrared beams, for example as used in two-dimensional infrared spectroscopy. This has proven to save many hours of setup time. The use of the bolometer array as a spectrographic detector and probe of long-term beam drifts have also been demonstrated.

Contact: I.P. Clark (ian.p.clark@stfc.ac.uk)

Reproduced from Clark, I.; Towrie, M. A, Compact Micro-Bolometer Array for Mid-Infrared Laser Beam Alignment, Diagnostics and Spot-Size Measurement. Preprints 2019, 2019120085 (doi: 10.20944/preprints201912.0085.v1), under the terms of the Creative Commons Attribution License



Images demonstrating the spatial overlapping of three infrared beams at the focal point of an off-axis parabolic mirror, $f = 75 \text{ mm}$, centre image. One of the beams has satellite beams, clearly visible in the last image. Each image shows the bolometer output at a particular point along the experimental optical axis. The bolometer was translated along this axis between images, with the distance, in millimetres from the focal point indicated in each image. Each image, which displays a 50×50 pixel section of the bolometer array, is auto-scaled to use the full colour range for clearer display.

Optimizing the Temperature Recovery Rate in Temperature-Jump IR Spectroscopy

G.M. Greetham, I.P. Clark, E. Gozzard, M. Towrie (Central Laser Facility, Research Complex at Harwell, STFC Rutherford Appleton Laboratory, Harwell, Didcot, UK)

The new temperature-jump facility at ULTRA is briefly described, showing how rapid temperature rise and subsequent cooling can be used to follow temperature-triggered reactions, from nanoseconds to millisecond

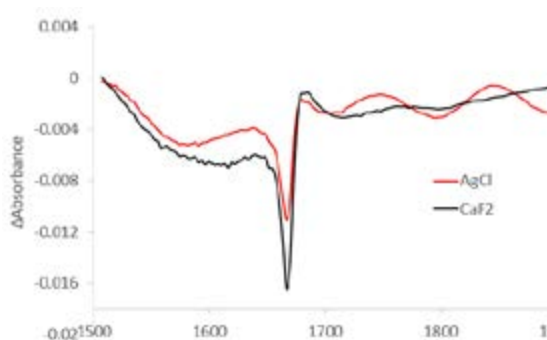


Figure 1: Normalised IR difference spectra of TFA in solution, immediately following the T-jump pulse. Two window materials, AgCl and CaF₂, are shown for comparison.

C.P. Howe, B. Procacci, N.T. Hunt (Department of Chemistry, University of York, UK)

timescales. Control of the temperature-jump kinetics is discussed, showing how one can control the rate of cooling of the sample and so, experiment timescales.

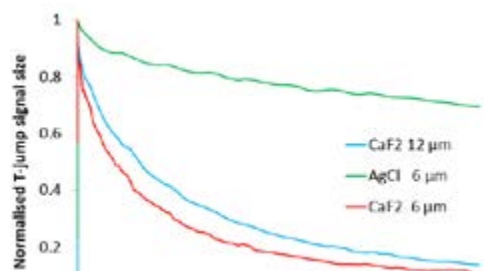


Figure 2: Kinetics of TFA T-jump signal change for different cell windows and sample path-lengths.

Contact: G.M. Greetham (greg.greetham@stfc.ac.uk)

Progress on the Coherent Beam Recombination project

N. Martin, W.H. Fraser, V.C. Lindsay, B. Parry, M. Galimberti (Central Laser Facility, STFC Rutherford Appleton Laboratory, Harwell Campus, Didcot, UK)

The HAPPIE lab project is devoted to investigate coherent beam recombination, a possible solution to overcome the current limitation on the maximum achievable power of the high power laser system. To achieve recombination, all the beams must be spatially and temporally locked to each other, and must also be of the same path length to within a fraction of a micrometre.

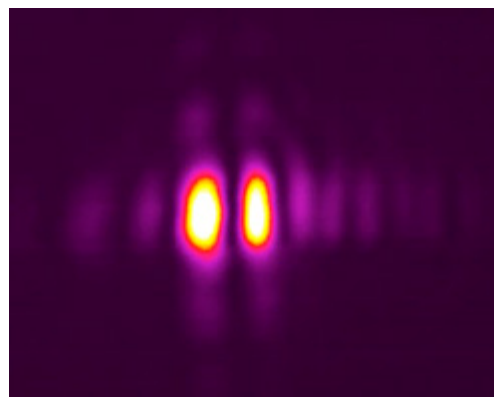
Building on previous work to achieve coherent combination, work this year focused on optimising the system. In particular, three main areas were explored:

- Changing the mounting method of the piezo mirror that stabilises the beam spatially and temporally. The current setup caused aberrations to the far field, most notably astigmatism.
- Developing a low cost PID control system for spatial stabilisation using field-programmable gate arrays, offering an alternative to the expensive analogue SIM modules.

Contact: M. Galimberti (marco.galimberti@stfc.ac.uk)

- Developing an easy method to ensure the difference in path length traversed by the two lasers is within the coherence length so that constructive interference can occur with non-CW lasers

This report details progress of the work to achieve this, along with the preliminary results.



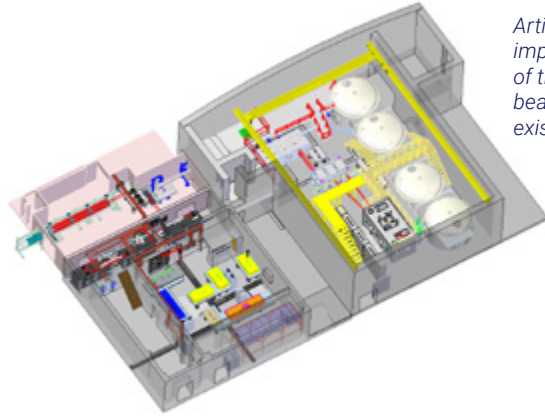
Combined FF of two spatially and temporally overlapping beams

Overview of a new OPCPA beamline in Vulcan TAP

I. Musgrave, G. Archipovaite, S. Blake, N. Booth, D.C. Carroll, R.J. Clarke, R. Heathcote, C. Hernandez-Gomez, M. Galletti, M. Galimberti, P. Johnson, D. Neely, D. Pepler, P. Oliveira, J. Saa, A. Scott, A. Stallwood, T. Winstone, B. Wyborn (Central Laser Facility, STFC Rutherford Appleton Laboratory, Harwell Campus, Didcot, UK)

In this report, we outline our plans for an auxiliary beamline into Vulcan Target Area Petawatt (TAP). The new beamline will be based on Optical Parametric Chirped Pulse Amplification (OPCPA), and it will ultimately deliver 30 J in 30 fs onto target with a centre wavelength of 880 nm. The new beamline will be able to be operated both in conjunction with, and independently of, the existing petawatt beamline.

Artist's impression of the new beamline in the existing facility

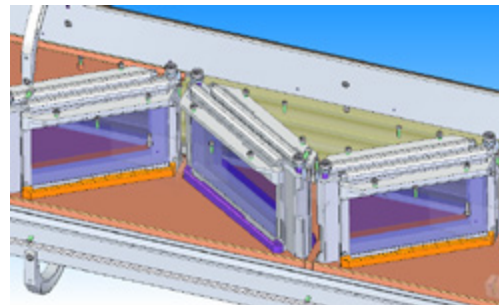


Contact: I.O. Musgrave (ian.musgrave@stfc.ac.uk)

Development of Air-cooled Disc Amplifiers for Vulcan

I. Musgrave, M. Ahmad, S. Chapman, T. Davenne, B. Fischer-Harrison, A. Frackiewicz, M. Harman, C. Hernandez-Gomez, N. O'Donoghue, M. Pitts, D. Robinson, P. Trimble, T. Winstone (Central Laser Facility, STFC Rutherford Appleton Laboratory, Harwell Campus, Didcot, UK)

In this report, we detail the work undertaken at the STFC towards the development of an air-cooled flash-lamp pumped disk amplifier, to increase the repetition rate of high energy flash-lamp pumped lasers. The overall aim is to improve the current repetition rate from one shot every 20 minutes, to one shot every five minutes.



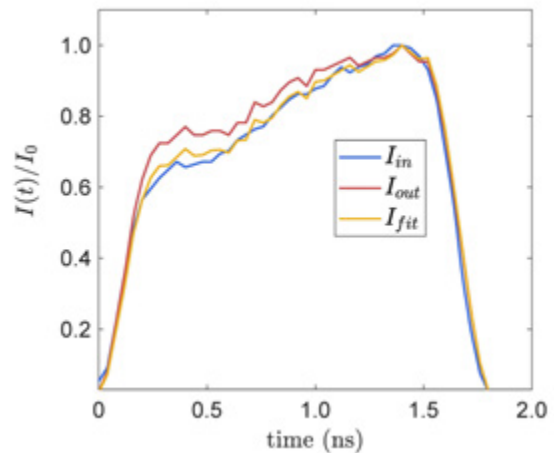
Artist's impression of the prototype air-cooled amplifier

Contact: I.O. Musgrave (ian.musgrave@stfc.ac.uk)

Progress on pulse shaping by compensating for temporal deformation in the Vulcan Nd:glass amplification chain

J.A. Patel, L.E. Bradley, P. Oliveira, A. Kidd, I.O. Musgrave (Central Laser Facility, STFC Rutherford Appleton Laboratory, Harwell Campus, Didcot, UK)

The evolution of the temporal shape of a pulse as it passes through a Nd:glass amplifier chain is difficult to predict and depends on the gain and losses throughout the complete chain. We demonstrate that a time-dependent Frantz-Nodvik model can be employed to get a target output pulse shape. This allows us to calculate the ideal input pulse shape that will compensate for gain saturation from the Vulcan amplifier chain. In the future, we plan on developing this model so that it simulates the deformation from the double-pass and single-pass 108 mm disk amplifiers.



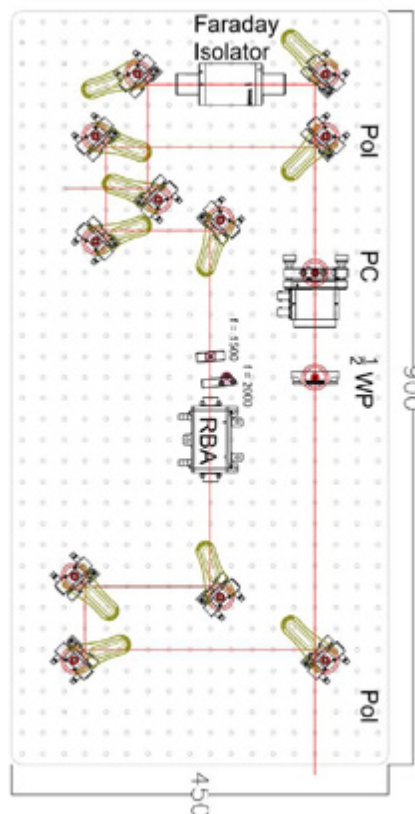
Observation of temporal deformation in the pulse at three stages of the amplifier chain

Contact: P. Oliveira (pedro.oliveira@stfc.ac.uk)

Modification of Regenerative Amplifier Resonating Cavity for New TAP Beam Line OPCPA Pump

C.I. Suci, P. Oliveira, I. Musgrave (Central Laser Facility, STFC Rutherford Appleton Laboratory, Harwell Campus, Didcot, UK)

The new shaped long pulse laser, which is pumping the OPCPA stage of the new Vulcan beam line, features regenerative amplifier, that is currently laid out as a standing wave resonating cavity. It will be moved on the same optical table as the rest of the laser, due to space limitations. This paper discusses improvements that will be made to the cavity to increase its stability and to reduce its size. Ultimately, the cavity will be laid out as a ring cavity, and it will be built on a 450 x 900 mm breadboard.



Arrangement of the ring cavity on a 450 x 900 mm breadboard

Contact: P. Oliveira (pedro.oliveira@stfc.ac.uk)

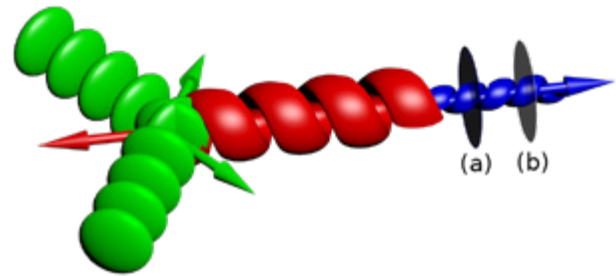
Theory & Computation

Orbital Angular Momentum Coupling in Elastic Photon-Photon Scattering

R. Aboushelbaya, A.F. Savin, M. Mayr, B. Spiers, R. Wang (Clarendon Laboratory, University of Oxford, UK)
K. Glize, J.L. Collier, R.M.G.M. Trines (Central Laser Facility, STFC Rutherford Appleton Laboratory, Harwell Campus, Didcot, UK)
M. Marklund (Department of Physics, University of Gothenburg, Sweden)

R. Bingham (Central Laser Facility, STFC Rutherford Appleton Laboratory, Harwell Campus, Didcot, UK; Department of Physics, University of Strathclyde, UK)
P.A. Norreys (Central Laser Facility, STFC Rutherford Appleton Laboratory, Harwell Campus, Didcot, UK; Clarendon Laboratory, University of Oxford, UK)

In this Letter, we investigate the effect of orbital angular momentum (OAM) on elastic photon-photon scattering in a vacuum for the first time. We define exact solutions to the vacuum electromagnetic wave equation which carry OAM. Using those, the expected coupling between three initial waves is derived in the framework of an effective field theory based on the Euler-Heisenberg Lagrangian and shows that OAM adds a signature to the generated photons thereby greatly improving the signal-to-noise ratio. This forms the basis for a proposed high-power laser experiment utilizing quantum optics techniques to filter the generated photons based on their OAM state.



A sketch of the proposed geometry for the experiment showing the three main initial beams. The $2\omega_0$ (green) beams have a flat phase front whereas the ω_0 (red) beam has a helical front arising from the nonzero OAM. The figure illustrates the generated $3\omega_0$ (blue) spiral photons. (a) and (b) are the frequency and OAM filters, respectively, which will be used to remove background noise.

Reprinted from R. Aboushelbaya, K. Glize, A.F. Savin et al. Orbital Angular Momentum Coupling in Elastic Photo-Photon Scattering. *Phys. Rev. Lett.* 123, 113604 (2019) doi: 10.1103/PhysRevLett.123.113604, published by the American Physical Society, under the Creative Commons Attribution 4.0 International License.

Contact: R. Aboushelbaya
 (ramy.aboushelbaya@physics.ox.ac.uk)

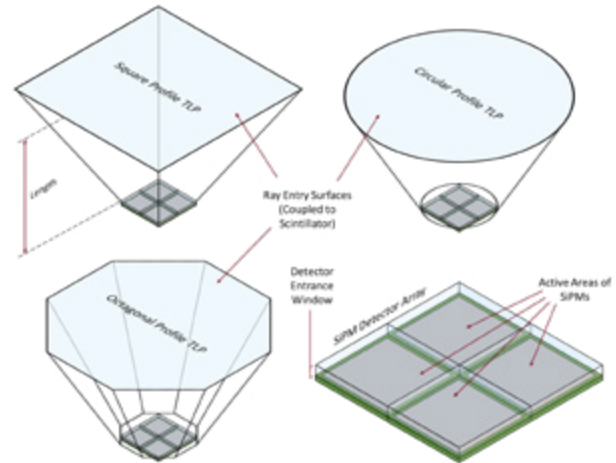
Plasma Diagnostics

Evaluating expected signal loss due to SiPM saturation for short, low flux light pulses in tapered light pipe systems

J. Davies (Department of Physics, Imperial College London, UK)
D. Neely (Central Laser Facility, STFC Rutherford Appleton Laboratory, Harwell Campus, Didcot, UK)

C.D. Armstrong (Department of Plasma Physics, University of Strathclyde, Glasgow, UK;
 Central Laser Facility, STFC Rutherford Appleton Laboratory, Harwell Campus, Didcot, UK)

In many applications, silicon photomultiplier (SiPM) detectors have come to replace photomultiplier tubes (PMTs) due to numerous advantages in scale and operation. There is, however, a concern with SiPMs, which did not affect PMTs, that an illumination from a short light pulse, heavily localised on a detector surface, can lead to the signal response to incoming photons becoming non-linear. This is caused by each detector microcell having a finite recovery time between responses. Raytracing techniques were used to investigate whether tapered light pipe systems produce this type of illumination from input light pulses that are Lambertian and special uniform. Signal losses due to this effect were found to be negligible, making this an unimportant effect to consider when designing light pipe systems. Limited tests were also carried out with Lambertian light sources originating from a single point, which produced similar results; however, non-Lambertian sources may produce different results.



Schematics of the detector and tapered light pipes that were investigated; the detector was modelled as a 2 × 2 array of KETEK PM3325-WB-D0 SiPMs.

Contact: J. Davies (jtd17@ic.ac.uk)

Investigating Contrast, Resolution and Field-of-View of the Questar QM-1 SZ Tele-Microscope

J.A. Hodson (Department of Physics, University of Bath, UK)

M. Notley, D. Carroll, R. Clarke (Central Laser Facility, STFC Rutherford Appleton Laboratory, Harwell Campus, Didcot, UK)

Current imaging diagnostics used in high power laser facilities, such as Vulcan, can be limited by space, resolution, field-of-view or all three. An alternative imaging solution is the tele-microscope, which is able to image at high magnification while being located outside of the target chamber, thereby allowing more space in the chamber for other diagnostics. This paper presents the characterisation of the Questar QM-1 SZ tele-microscope (Figure 1), recently purchased by the CLF.



Figure 1: Image of the QM-1 SZ Tele-microscope.

The resolution of the tele-microscope was tested using a USAF resolution test grid, where the Modulated Transfer Function would then be calculated. The field-of-view was then measured using a ruler. These tests were done at two working distances, with the results for 65 cm distance being shown in Table 1.

Focal Length	Resolution	Field of View
1	39.3 μm	13.5 mm
2	19.6 μm	4 mm
3	13.9 μm	2 mm
4	11.05 μm	1.5 mm
5	6.96 μm	1 mm

Table 1: Table of the results for MTF and field-of-view for a working distance of 65 cm

These tele-microscopes are now ready to be used in real experiments, however two will be re-modified in order to work at a distance over 3 m.

Contact: J.A. Hodson (james.hodson@stfc.ac.uk)

Performance of a Kromek multi-channel analyser for a silicon photomultiplier – scintillator gamma ray detector

J.K. Patel (Loughborough University, UK)

C.D. Armstrong, D. Neely (Central Laser Facility, STFC Rutherford Appleton Laboratory, Harwell Campus, Didcot, UK)

To resolve 511 keV X-rays for a photonuclear activation based gamma ray detector, a multi-channel analyser can be used to easily digitise signals. The lower range of the linear response of a Kromek multi-channel analyser is shown to be improved by using a charge amplifier, which increases pulse widths to 1.2 μ s. Two charge sensitive amplifiers allow a multi-channel

analyser to resolve signals from silicon photomultiplier (SiPM) – scintillator detectors of small and large crystal volumes. A 26.5X gain charge amplifier, CR-112, is ideal for operation with a large scintillator crystal with a 36 mm² SiPM, for the resolution of 50 keV – 2 MeV X-rays.

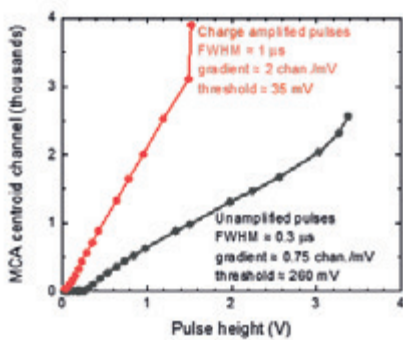


Figure 1: Linearity of multi-channel amplifier response with input pulse heights, for 0.35 μ s FWHM unamplified pulses, and 1.2 μ s charge amplified pulses

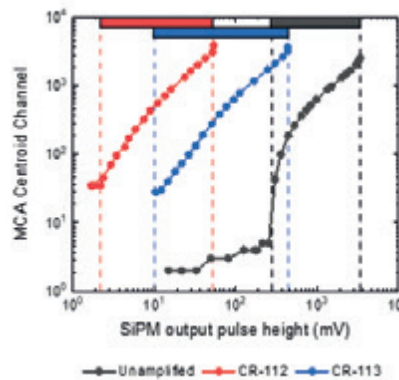


Figure 2: MCA spectrum centroid channels vs. SiPM pulse heights when pulses are unamplified, and amplified with two charge amplifiers with order of magnitude different gain. Coloured rectangles and dashed lines indicate effective dynamic range of detector system with each amplifier. CR-112 amplifier allows resolution of 2-45 mV pulse signals

Contact: C.D. Armstrong (chris.armstrong@stfc.ac.uk)

Gain characterisation of RF amplifiers for silicon photo multiplier – scintillation detector

J.K. Patel (Loughborough University, UK)

C.D. Armstrong, D. Neely (Central Laser Facility, STFC Rutherford Appleton Laboratory, Harwell Campus, Didcot, UK)

This report details and compares the gain character of several different amplifiers, for use with a 36 mm² silicon photomultiplier (SiPM) coupled to a gamma ray counting diagnostic that examines the signals produced from scintillation events. Resolving 511 keV X-rays is essential for counting the 15 MeV – 30 MeV gamma-induced photonuclear reactions in ²⁷₁₃Al. However, such

events typically produce silicon photomultiplier pulses with amplitudes below the 260 mV threshold of a multi-channel analyser. A charge sensitive pre-amplifier is shown to be linear for the required energy range, and its pulse lengthening behaviour lowers the effective detection threshold so that scintillation signals from 0.1 – 2 MeV photons can be resolved by a digitiser.

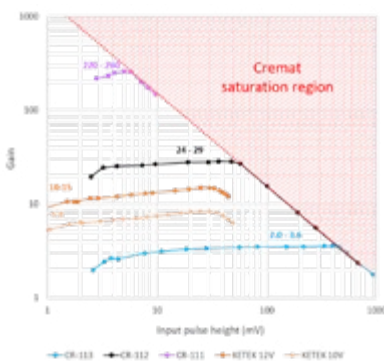


Figure 1: Gain vs. input pulse heights for three charge sensitive amplifiers driven at 13.6 V, and a KETEK SiPM preamplifier driven at 10 V and 12 V. Black dotted lines indicate the dynamic range of the silicon photomultiplier, and the gain of each amplifier is labelled.

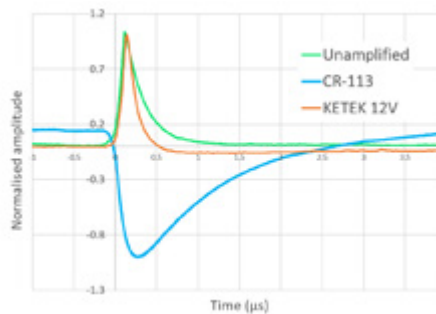


Figure 2: Normalised typical SiPM output traces: unamplified; amplified with a Cremat charge sensitive preamplifier; and amplified with the KETEK SiPM preamplifier. The increase in pulse width with the charge sensitive amplifier is clearly visible.

Contact: C.D. Armstrong (chris.armstrong@stfc.ac.uk)

Design of a Compton Spectrometer with a detection range of 15 keV – 3 MeV for Laser Plasma Experiments

J. Popp (Carl von Ossietzky University of Oldenburg, Germany; Central Laser Facility, STFC Rutherford Appleton Laboratory)

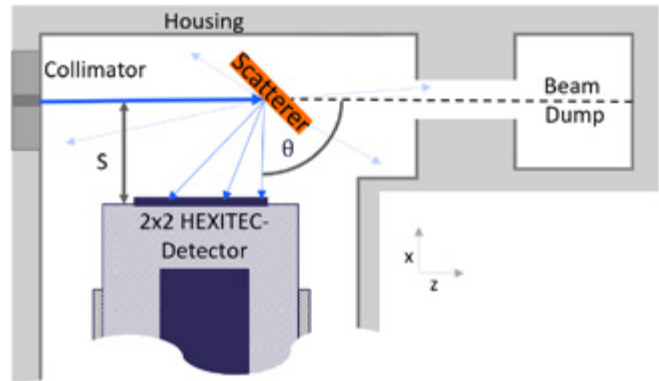
C. Armstrong, D. Neely (Central Laser Facility, STFC Rutherford Appleton Laboratory, Harwell Campus, Didcot, UK)

U. Teubner (Carl von Ossietzky University of Oldenburg, Germany; University of Applied Sciences Emden/Leer, Germany)

Measuring the X- and γ -ray emission spectra from laser-produced plasmas is essential to enable the physical processes at play to be quantified and understood. Operating sensitive detectors capable of energy resolving the incident photons in the primary beam is difficult, due to pulse pile up and possibly γ -ray energies of several MeV. Hence, the energy and flux of the incident radiation have to be adjusted to the specifications of the detector. Using Compton Scattering and placing the detector at an angle can potentially achieve this.

In this report, a design is presented that places a pixelated CdTe detector in a 90° angle towards a 1 mm thin Carbon scattering target. Monte Carlo simulations have been used to evaluate the geometry's performance and it has been computed that the detectors energy range of 10 – 600 keV was extended to 15 keV – 3 MeV with an energy resolution at 511 keV of 5 %.

Contact: J. Popp (jennifer.popp@uni-oldenburg.de)



Geometry of the Compton Spectrometer

Ultrafast & XUV Science

Observation of charge density wave melt down in time resolved ARPES of single layer VSe_2

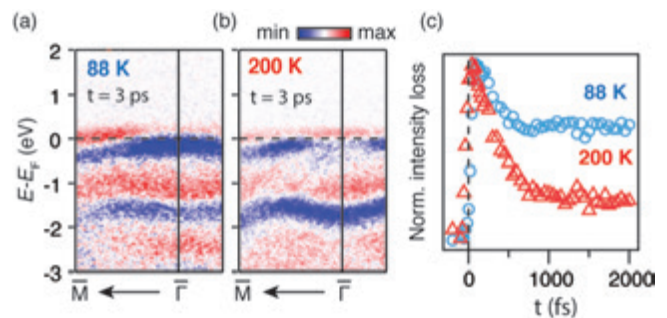
D. Biswas, A. Jones, K. Volckaert, C. Sanders, F. Andreatta, J. Miwa, P. Hofmann, N. Lanata, S. Ulstrup (Department of Physics & Astronomy, Aarhus University, Denmark) P. Majchrzak, Y. Zhang, G. Karras, R.T. Chapman, A. Wyatt, E. Springate (Central Laser Facility, STFC Rutherford Appleton Laboratory, Harwell Campus, Didcot, UK)

B.K. Choi, Y.J. Chang (Department of Physics, University of Seoul, Republic of Korea) T.H. Lee, C.J. Kang (Department of Physics & Astronomy, Rutgers University, Piscataway, New Jersey, USA) I. Marković, P.D.C. King (SUPA, School of Physics & Astronomy, University of St Andrews, UK)

Group V transition metal dichalcogenide (TMD) VSe_2 shows charge density wave (CDW) transition at 110 K with the CDW ordering ($4 \times 4 \times 3$), in its bulk form. Recent experiments have shown that the charge ordering gets enhanced in the monolayer (ML) VSe_2 with an increased transition temperature ~ 140 K. Moreover, in CDW phase almost the whole Fermi surface vanishes, forming CDW gap.

Multiple charge order structures are reported in literature – (4×4), ($\sqrt{3} \times 2$), ($\sqrt{3} \times \sqrt{7}$). It is very clear that the nature and the mechanism of CDW in bulk and ML VSe_2 are very different. Here we use time and angle resolved photoelectron spectroscopy (trARPES) to study the electron dynamics in both CDW and normal phase, and hence to shed light on the CDW mechanism in ML VSe_2 . We have also simulated the ARPES intensity to extract different many-body and transient parameters.

Our measurements showed the melt down of the charge order on pumping, but there was no recovery even after 3 ps. This unusually long-time dependence points towards the possibility of a bottleneck in the hot carrier relaxation and the crucial role of the substrate in ML VSe_2 .



(a), (b) The difference spectra at 3 ps time delay for 88 K and 200 K sample temperature respectively – different hot carrier dynamics

(c) Intensity variation close to $\bar{\Gamma}$ point showing the loss of back folded intensity for sample at 88 K after pumping – melting of charge order

Contact: D. Biswas (deepnarayan7@phys.au.dk)

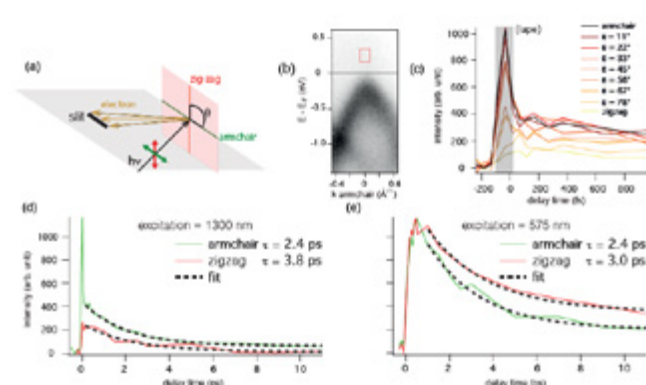
Assessing the anisotropic response in the out-of-equilibrium electron dynamics of black phosphorus

A. Crepaldi, S. Roth, G. Gatti, S. Polishuck, M. Puppini, M. Chergui, M. Grillo (École Polytechnique Fédérale de Lausanne (EPFL), Switzerland) A.S. Wyatt, R.T. Chapman, G. Karras, Y. Zhang (Central Laser Facility, STFC Rutherford Appleton Laboratory, Harwell Campus, Didcot, UK)

F. Grillo (EaStCHEM and School of Chemistry, University of St. Andrews, UK)

One of the most striking aspects of the physics of black phosphorus (BP) is the large anisotropy in its transport and optical properties. We have investigated the electron dynamics in the conduction band of BP, which is transiently populated by an ultrafast optical excitation. We resolve a change in the characteristic relaxation (τ) time when the

light polarization is varied in the surface plane, from the armchair to the zig-zag direction. Our results suggest that the orbital polarization, which is responsible for the dichroism in the optical absorption, might also influence the electronic scattering mechanisms.



a) Experimental geometry. (b) Band dispersion of BP measured along the armchair direction at the G point of the 2nd Brillouin Zone. (c) Electron dynamics at the bottom of conduction band, in the region indicated in panel (b) by a red rectangle. The colour of the curves encodes the evolution of the pump polarization direction from armchair to zig-zag. (d) Comparison between the dynamics for an optical excitation centred at 1300 nm. The characteristic decay times are indicated. (e) The same comparison, but for an optical excitation centred at 575 nm.

Contact: A. Crepaldi (alberto.crepaldi@epfl.ch)

A new three-dimensional probe of molecular structure and dynamics on the ultrafast timescale

J.W.L. Lee, H. Köckert, D. Heathcote, D. Popat, C. Vallance (Department of Chemistry, University of Oxford)

Ultrafast laser pump-probe methods allow chemical reactions to be followed in real time, and have provided unprecedented insight into some of the most fundamental aspects of chemical reactivity. While evolution of the electronic structure of the system under study is immediately evident from changes in the observed spectral signatures, information on rearrangement of the nuclear framework is generally obtained indirectly. Disentangling the contributions to the signal from competing photochemical pathways can also be challenging in many cases.

Here, we introduce the new technique of three-dimensional covariance-map Coulomb explosion imaging, which has the potential to provide complete three-dimensional information on molecular structure and dynamics as they evolve in real time during a gas-phase chemical reaction. We describe our experimental approach and present first proof-of-concept data from recent measurements on CF_3I , performed at the Artemis ultrafast laser facility. Covariance analysis of the data allows the contributions from competing fragmentation pathways to be isolated and characterised. With further development, we envisage that the method will allow 'molecular movies' to be recorded for a wide variety of gas-phase chemical processes.

Reprinted from Lee, J.W.L., Köckert, H., Heathcote, D. et al. Three-dimensional covariance-map imaging of molecular structure and dynamics on the ultrafast timescale. *Commun Chem* 3, 72 (2020), under the terms of the Creative Commons CC BY license. doi: 10.1038/s42004-020-0320-3

Contact: C. Vallance (claire.vallance@chem.ox.ac.uk)

R. Chapman, P. Majchrzak, E. Springate (Central Laser Facility, STFC Rutherford Appleton Laboratory, Harwell Campus, Didcot, UK)

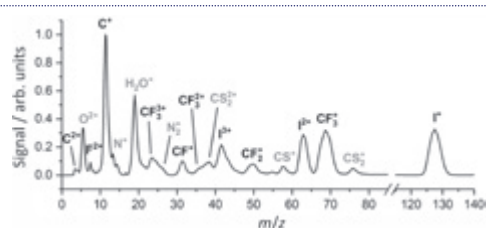


Figure 1: Time-of-flight spectrum for the charged fragments formed in the laser-induced Coulomb explosion of CF_3I

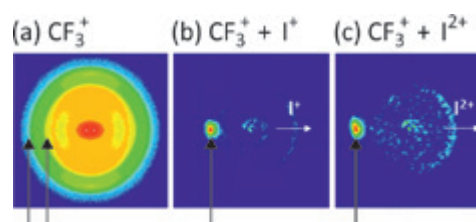


Figure 2: (a) 2D projection of the 3D velocity distribution recorded for CF_3^+ fragments; (b) covariance-map image of CF_3^+ formed with an I^+ partner ion; (c) covariance-map image of CF_3^+ formed with an I_2^+ partner ion

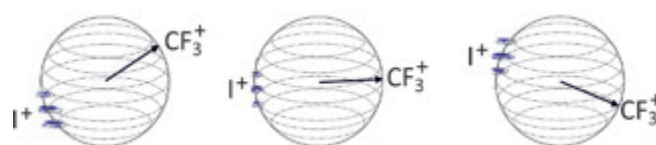


Figure 3: 3D covariance-map images for the $\text{CF}_3^+ + \text{I}^+$ fragmentation channel

Femtosecond UV and XUV Photoelectron Spectroscopy of Dissociating Methyl Iodide

B. Downes-Ward, E.M. Warne, J. Woodhouse, R.S. Minns (Chemistry, University of Southampton, UK)

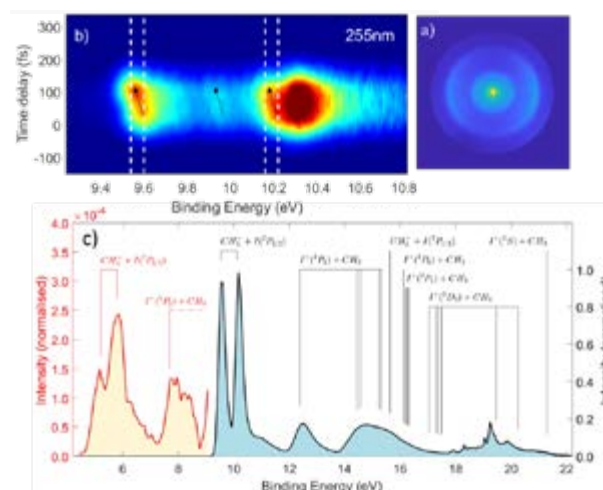
A.S. Wyatt, P. Majchrzak, G. Karras, Y. Zhang, E. Springate, R.T. Chapman (Central Laser Facility, STFC Rutherford Appleton Laboratory, Harwell Campus, Didcot, UK)

M.A. Parkes (Department of Chemistry, University College London, UK)

Pump probe photoelectron spectroscopy using UV and XUV probe photon energies has been used to monitor the ultrafast photodissociation of methyl iodide. The UV photoelectron imaging measurements provide a detailed view of the changing structure that is limited to very early times close to the initial geometry. By contrast the XUV photoelectron spectroscopy dynamics show the changes occurring over the full reaction. The two measurement provide complementary information on the dissociating molecule, allowing us to uncover complexities in the dynamics that have previously been missed.

Summary of the photoelectron spectroscopy data showing a photoelectron image (a) and time dependent photoelectron spectrum (b) obtained following excitation at 255 nm and ionisation with 400 nm light, and the photoelectron spectrum obtained following XUV ionisation (c) of the ground (blue) and excited state (red) population

Contact: R.S. Minns (r.s.minns@soton.ac.uk)



Imaging & Dynamics for Physical & Life Sciences

The development of a high throughput drug-responsive model of white adipose tissue comprising adipogenic 3T3-L1 cells in a 3D matrix

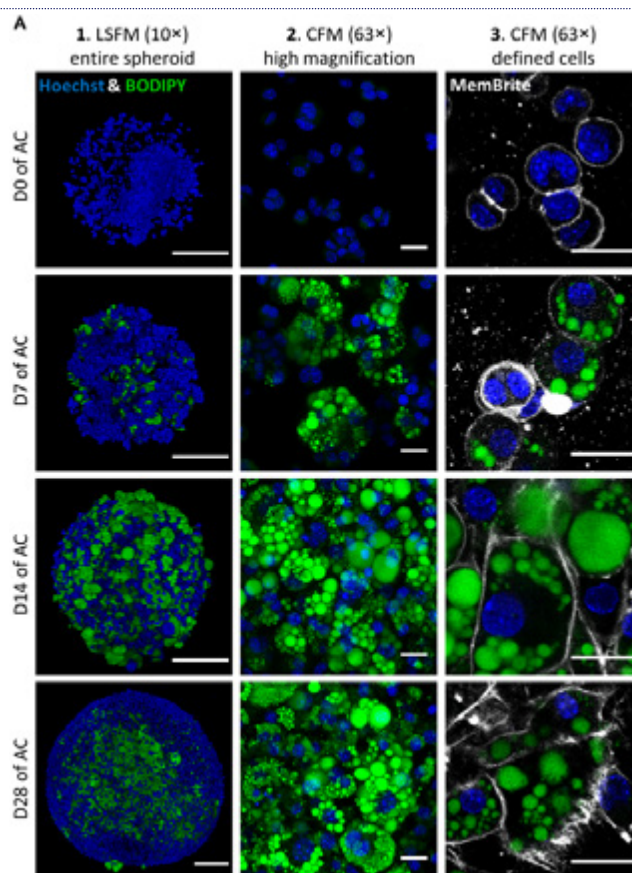
A.D. Graham, V.S. Tsancheva, T.S. Babra, X. Xue, J. Gannon, S.N. Olof (OxSyBio Ltd, Building B27, Rutherford Appleton Laboratory, Harwell Campus, Didcot, UK)
R. Pandey, L.A.K. Zolkiewski, L. Bentley, R.D. Cox (Medical Research Council Harwell Institute, Mammalian Genetics Unit, Harwell Campus, Oxfordshire, UK)
A. Candeo, S.W. Botchway (Central Laser Facility, Research Complex at Harwell, STFC Rutherford Appleton Laboratory, Harwell Campus, Didcot, UK)

A.J. Allan, L. Teboul (Medical Research Council Harwell Institute, Mary Lyon Centre, Harwell Campus, Oxfordshire, UK)
K. Madi (3Dmagination, Building B27, Rutherford Appleton Laboratory, Harwell Campus, Didcot, UK)

Adipose models have been applied to mechanistic studies of metabolic diseases (such as diabetes) and the subsequent discovery of new therapeutics. However, typical models are either insufficiently complex (2D cell cultures) or expensive and labour intensive (mice/*in vivo*). To bridge the gap between these models and to better inform pre-clinical studies, we have developed a drug-responsive 3D model of white adipose tissue (WAT). Here, spheroids ($680 \pm 60 \mu\text{m}$) comprising adipogenic 3T3-L1 cells encapsulated in 3D matrix were fabricated manually on a 96 well scale. Spheroids were highly characterised for lipid morphology, selected metabolite and adipokine secretion, and gene expression; displaying significant upregulation of certain adipogenic-specific genes compared with a 2D model. Furthermore, induction of lipolysis and promotion of lipogenesis in spheroids could be triggered by exposure to 8-br-cAMP and oleic acid respectively. Metabolic and high content imaging data of spheroids exposed to an adipose-targeting drug, rosiglitazone, resulted in dose-responsive behaviour. Thus, our 3D WAT model has potential as a powerful scalable tool for compound screening and for investigating adipose biology.

Reproduced from Alexander D Graham et al. 2020 *Biofabrication* 12 015018, under the terms of the Creative Commons Attribution 3.0 licence. doi:10.1088/1758-5090/ab56fe

Contact: S.N. Olof (sam.nicholas.olofof@gmail.com)
 R.D. Cox (r.cox@har.mrc.ac.uk)



Lipid morphology of 3T3-L1 spheroids exposed to adipogenic cocktail. (A) A matrix of image projections depicting the change of lipid morphology within singlet spheroids over 28 days of adipogenic cocktail (AC) exposure. Spheroids were stained for nuclei (Hoechst 33342, blue), lipid droplets (BODIPY 493/503, green) and the cell membrane (MemBrite, white). Fluorescence z-stack micrographs were acquired by either light sheet fluorescence microscopy (LSFM, (A1), $200 \mu\text{m}$ scale bar) or confocal fluorescence microscopy (CFM, (A2) and (A3), $25 \mu\text{m}$ scale bars).

The Rho family GEF FARP2 is activated by aPKC ζ to control tight junction formation and polarity

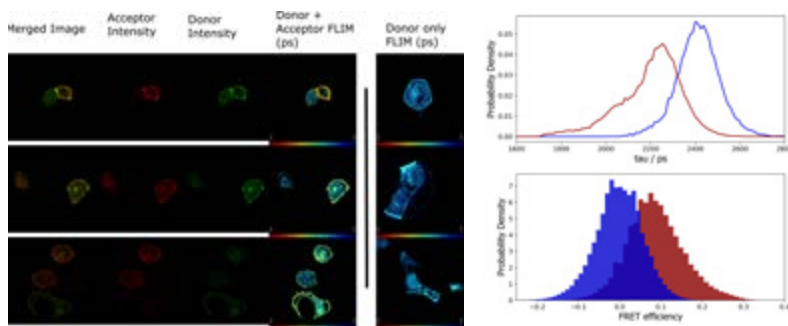
A. Elbediwy, B.J. Thompson (Epithelial Biology Laboratory, Francis Crick Institute, London, UK)
Y. Zhang, M. Cobbaut, P. Riou, R.S. Tan (Protein Phosphorylation Laboratory, Francis Crick Institute, London, UK)
S.K. Roberts, C. Tynan, M.L. Martin-Fernandez (Central Laser Facility, STFC Rutherford Appleton Laboratory, Harwell Campus, Didcot, UK)

R. George, S. Kjaer (Structural Biology Team, Francis Crick Institute, London, UK)
N.Q. McDonald (Signalling and Structural Biology Laboratory, Francis Crick Institute, London, UK)
P.J. Parker (Protein Phosphorylation Laboratory, Francis Crick Institute, London, UK; School of Cancer and Pharmaceutical Sciences, King's College London, UK)

The elaboration of polarity is central to organismal development and to the maintenance of functional epithelia. Among the controls determining polarity are the PAR proteins, PAR6, aPKC ζ and PAR3, regulating both known and unknown effectors. Here, we identify FARP2 as a 'RIPR' motif-dependent partner and substrate of aPKC ζ that is required for efficient polarisation and junction formation. Binding is conferred by a FERM/FA domain–kinase domain interaction and detachment promoted by aPKC ζ -dependent phosphorylation. FARP2 is shown

to promote GTP loading of Cdc42, which is consistent with it being involved in upstream regulation of the polarising PAR6–aPKC ζ complex. However, we show that aPKC ζ acts to promote the localised activity of FARP2 through phosphorylation. We conclude that this aPKC ζ –FARP2 complex formation acts as a positive feedback control to drive polarisation through aPKC ζ and other Cdc42 effectors.

Reproduced from Elbediwy A, Zhang Y, Cobbaut M, et al. *J Cell Sci*. 2019;132(8):jcs223743, published by The Company of Biologists Ltd, under the terms of the Creative Commons Attribution License 4.0. doi: 10.1242/jcs.223743



GFP-PKC ζ and FLAG-FARP2 were coexpressed in HCT116 cells. GFP lifetime was monitored at 488nm in the absence (indicated Donor only) or presence of Anti-HA Alexa 647 as exemplified in the upper panels. Lifetime values of doubly transfected cells were captured and quantified. Lifetimes (τ) in picoseconds (ps) and the derived FRET efficiencies are shown for the donor only (blue) and donor-acceptor (red) analyses

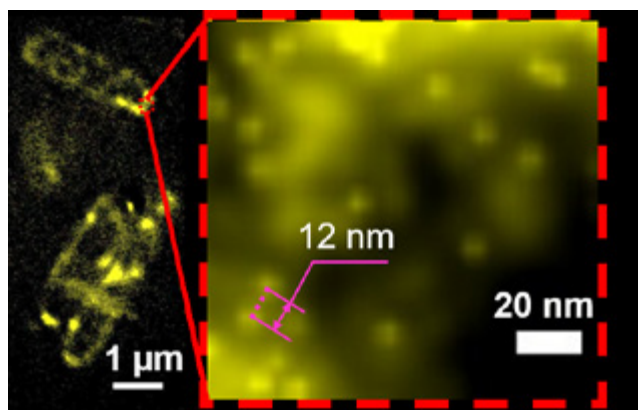
Contact: S.K. Roberts (selene.roberts@stfc.ac.uk) P.J. Parker (peter.parker@crick.ac.uk)

Solid immersion microscopy images cells under cryogenic conditions with 12 nm resolution

L. Wang, B. Bateman, L.C. Zanetti-Domingues, A.N. Moores, S. Astbury, C. Spindloe, S.R. Needham, D.J. Rolfe, D.T. Clarke, M.L. Martin-Fernandez (Central Laser Facility, Research Complex at Harwell, STFC Rutherford Appleton Laboratory, Harwell Campus, Didcot, UK)

M.C. Darrow (Diamond Light Source, Harwell Science & Innovation Campus, Didcot, UK)
M. Romano, K. Beis (Department of Life Sciences, Imperial College London, UK; Research Complex at Harwell, STFC Rutherford Appleton Laboratory, Harwell Campus, Didcot, UK)

Super-resolution fluorescence microscopy plays a crucial role in our understanding of cell structure and function by reporting cellular ultrastructure with 20–30 nm resolution. However, this resolution is insufficient to image macromolecular machinery at work. A path to improve resolution is to image under cryogenic conditions. This substantially increases the brightness of most fluorophores and preserves native ultrastructure much better than chemical fixation. Cryogenic conditions are, however, underutilised because of the lack of compatible high numerical aperture objectives. Here, using a low-cost super-hemispherical solid immersion lens (superSIL) and a basic set-up we achieve 12 nm resolution under cryogenic conditions, to our knowledge the best yet attained in cells using simple set-ups and/or commercial systems. By also allowing multicolour imaging, and by paving the way to total-internal-reflection fluorescence imaging of mammalian cells under cryogenic conditions, superSIL microscopy opens a straightforward route to achieve unmatched resolution on bacterial and mammalian cell samples.



Cryogenic solid immersion localisation microscopy imaging of *E. coli* cells. On the left hand side, it is shown the image of a field of *E. coli* cells in which ATP-binding cassette (ABC) transporter protein PH1735 were fused with EGFP. On the right hand side, it is shown the enlarged image of the region of the cell indicated by the red dashed border box. Two 12 nm apart PH1735 proteins can be clearly resolved.

Reproduced from Wang, L., Bateman, B., Zanetti-Domingues, L.C. et al. *Commun Biol* 2, 74 (2019) under the terms of the Creative Commons CC BY License. doi: org/10.1038/s42003-019-0317-6 © Springer Nature 2019

Contact: M.L. Martin-Fernandez (marisa.martin-fernandez@stfc.ac.uk)

A signal motif retains Arabidopsis ER- α -mannosidase I in the cis-Golgi and prevents enhanced glycoprotein ERAD

J. Schoberer, J. König, C. Veit, U. Vavra, E. Liebminger, R. Strasser (Department of Applied Genetics and Cell Biology, University of Natural Resources and Life Sciences, Vienna, Austria)
 S.W. Botchway (Central Laser Facility, Research Complex at Harwell, STFC Rutherford Appleton Laboratory, Harwell Campus, Didcot, UK)

F. Altmann (Department of Chemistry, University of Natural Resources and Life Sciences, Vienna, Austria)

V. Kriechbaumer, C. Hawes (Department of Biological and Medical Sciences, Faculty of Health and Life Sciences, Oxford Brookes University, UK)

The Arabidopsis ER- α -mannosidase I (MNS3) generates an oligomannosidic N-glycan structure that is characteristically found on ER-resident glycoproteins. The enzyme itself has so far not been detected in the ER. Here, evidence is provided indicating plants MNS3 exclusively resides in the Golgi apparatus. Notably, MNS3 remains on dispersed punctate structures when subjected to different approaches that commonly result in the relocation of Golgi enzymes to the ER. Responsible for this rare behaviour is an amino acid

signal motif (LPYS) within the cytoplasmic tail of MNS3 that acts as a specific Golgi retention signal. The physiological importance of the very specific MNS3 localization is demonstrated.

Reproduced from Schoberer, J., König, J., Veit, L. et al. *Nat Commun* 10, 3701 (2019), under the terms of the Creative Commons Attribution 4.0 International License. doi: 10.1038/s41467-019-11686-9

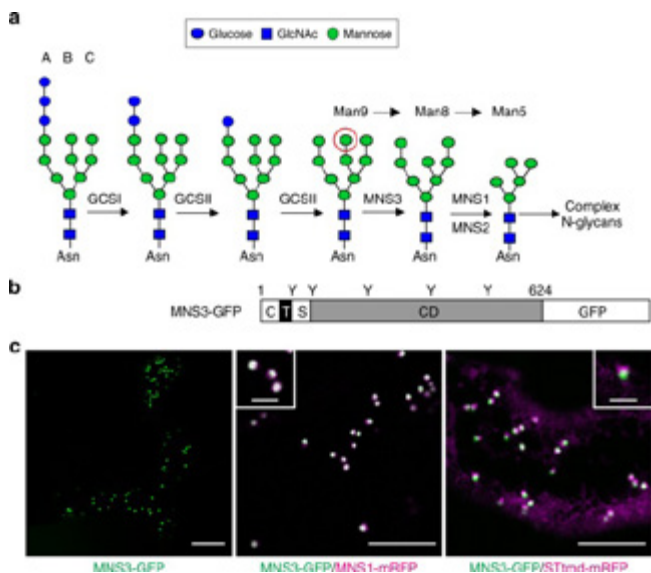


Figure 1: Arabidopsis MNS3 is a Golgi-resident protein. (a) Early steps of N-glycan processing in *A. thaliana* are shown. Confocal images show *N. benthamiana* leaf epidermal cells transiently expressing MNS3-GFP (green) alone (scale bar = 20 μ m) and in combination with the cis/medial-Golgi protein MNS1-mRFP (magenta, scale bar = 5 μ m) or the medial/trans-Golgi marker STmd-mRFP (magenta, scale bar = 5 μ m). The insets show a higher magnification of individual dual-colored Golgi stacks (scale bar = 2 μ m). Images were acquired two days post infiltration (dpi).

Contact: S. Botchway (stan.botchway@stfc.ac.uk)

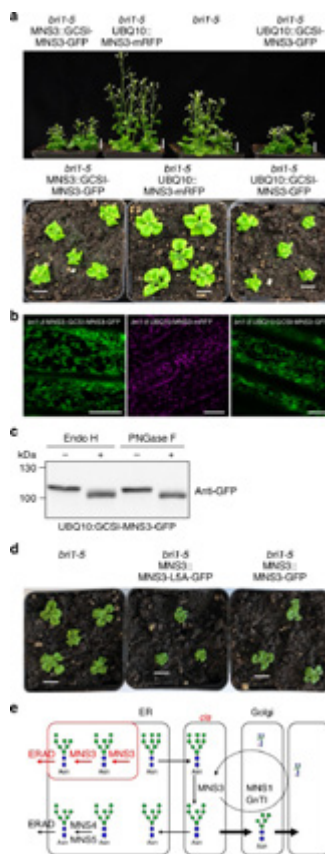


Figure 2: ER retention of MNS3 enhances the *bri1-5* phenotype. (a) Phenotype of Arabidopsis *bri1-5* and transgenic *bri1-5* plants. Images of 5-week-old (upper panel) or 26-day-old (lower panel) soil-grown plants are shown. Scale bars = 1 cm. (b) Confocal images of transgenic *bri1-5* plants expressing either MNS3::GCSI-MNS3-GFP (green), UBQ10::MNS3-mRFP (magenta), or UBQ10::GCSI-MNS3-GFP (green). Scale bar = 15 μ m. (c) Crude protein extracts from leaves of *N. benthamiana* wild-type plants transiently expressing UBQ10::GCSI-MNS3-GFP (d) Phenotype of *bri1-5* and transgenic *bri1-5* plants expressing either MNS3::MNS3-L5A-GFP or MNS3::MNS3-GFP. Images of 22-day-old soil-grown plants are shown. Scale bars = 1 cm. (e) Proposed model for MNS3-catalyzed mannose trimming. See doi: 10.1038/s41467-019-11686-9 for full details of figures

Candidalysin activates innate epithelial immune responses via epidermal growth factor receptor

J. Ho, X. Yang, S.-A. Nikou, A. Donkin, N.O. Ponde, J.P. Richardson, C. Murciano, D.L. Moyes, J.R. Naglik (Centre for Host-Microbiome Interactions, Faculty of Dental, Oral and Craniofacial Sciences, King's College London, UK)

N. Kichik (Centre for Host-Microbiome Interactions, Faculty of Dental, Oral and Craniofacial Sciences, King's College London, UK; Department of Life Sciences, Imperial College London, UK)

R.L. Gratacap, L.S. Archambault, C.P. Zwirner (Department of Molecular & Biomedical Science, University of Maine, Orono, USA)

R.T. Wheeler (Department of Molecular & Biomedical Science, University of Maine, Orono, USA; Graduate School of Biomedical Sciences and Engineering, University of Maine, Orono, USA)

R. Henley-Smith, S. Thavaraj (Centre for Oral, Clinical & Translational Science, Faculty of Dental, Oral and Craniofacial Sciences, King's College London, UK)

C. Tynan (Central Laser Facility, Research Complex at Harwell, STFC Rutherford Appleton Laboratory, Harwell Campus, Didcot, UK)

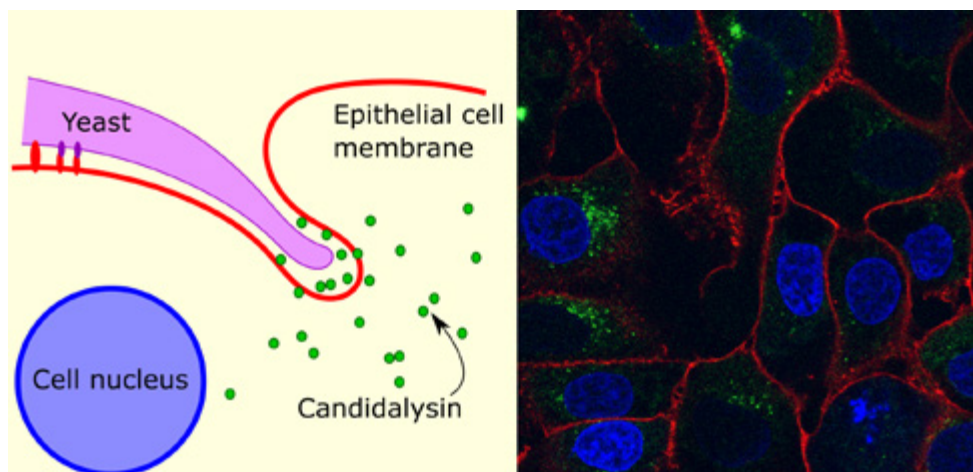
S.L. Gaffen (Division of Rheumatology and Clinical Immunology, University of Pittsburgh, USA)

B. Hube (Department of Microbial Pathogenicity Mechanisms, Leibniz Institute for Natural Product Research and Infection Biology, Hans Knöll Institute, Jena, Germany; Friedrich Schiller University, Jena, Germany)

Candida albicans is a fungal pathobiont, able to cause epithelial cell damage and immune activation. These functions have been attributed to its secreted toxin, candidalysin, though the molecular mechanisms are poorly understood. Here, we identify epidermal growth factor receptor (EGFR) as a critical component of candidalysin-triggered immune responses. We find that both *C. albicans* and candidalysin activate human epithelial EGFR receptors and candidalysin-deficient fungal mutants poorly induce EGFR phosphorylation during murine oropharyngeal candidiasis. Furthermore, inhibition of EGFR impairs candidalysin-triggered MAPK signalling and release of neutrophil activating chemokines in vitro, and diminishes

neutrophil recruitment, causing significant mortality in an EGFR-inhibited zebrafish swimbladder model of infection. Investigation into the mechanism of EGFR activation revealed the requirement of matrix metalloproteinases (MMPs), EGFR ligands and calcium. We thus identify a PAMP-independent mechanism of immune stimulation and highlight candidalysin and EGFR signalling components as potential targets for prophylactic and therapeutic intervention of mucosal candidiasis.

Reproduced from Ho, J., Yang, X., Nikou, S. et al. *Nat Commun* 10, 2297 (2019), under the terms of the Creative Commons Attribution License 4.0. doi:10.1038/s41467-019-09915-2



Candidalysin is a recently discovered toxin secreted by *Candida albicans* during yeast infection of human epithelial cells. The confocal microscope image on the right demonstrates how the OCTOPUS facility was used to image purified, fluorescently labelled candidalysin (coloured green) entering cultured cells (cell membranes are red, cell nuclei are blue) in order to study the mechanism of candidalysin triggered immune responses.

Contact: J. Ho (jemima.ho@kcl.ac.uk)
J.R. Naglik (Julian.naglik@kcl.ac.uk)

The cell wall regulates dynamics and size of plasma-membrane nanodomains in *Arabidopsis*

J.F. McKenna, A.F. Tolmie, C. Hawes, J. Runions (Department of Biological and Medical Sciences, Oxford Brookes University, UK)

D.J. Rolfe, S.E.D. Webb, S.W. Botchway, M.L. Martin-Fernandez (Central Laser Facility, Research Complex at Harwell, STFC Rutherford Appleton Laboratory, Didcot, UK)

Plant plasma-membrane (PM) proteins are involved in several vital processes, such as detection of pathogens, solute transport, and cellular signalling. For these proteins to function effectively there needs to be structure within the PM allowing, for example, proteins in the same signalling cascade to be spatially organized. Here we demonstrate that several proteins with divergent functions are located in clusters of differing size in the membrane using subdiffraction-limited Airyscan and Total Internal Reflection Fluorescence (TIRF) imaging. Single particle tracking (SPT) microscopy and analysis conducted at the OCTOPUS facility reveals that these proteins move at different rates within the

membrane. Actin and microtubule cytoskeletons appear to significantly regulate the mobility of one of these proteins (the pathogen receptor FLS2) and we further demonstrate that the cell wall is critical for the regulation of cluster size by quantifying single particle dynamics of proteins with key roles in morphogenesis (PIN3) and pathogen perception (FLS2). We propose a model in which the cell wall and cytoskeleton are pivotal for regulation of protein cluster size and dynamics, thereby contributing to the formation and functionality of membrane nanodomains.

Reproduced from McKenna JF, Rolfe DJ, Webb SED, et al. *Proc Natl Acad Sci U S A*. 2019;116(26):12857-12862, under the terms of the Creative Commons Attribution License 4.0 (CC BY). doi:10.1073/pnas.1819077116

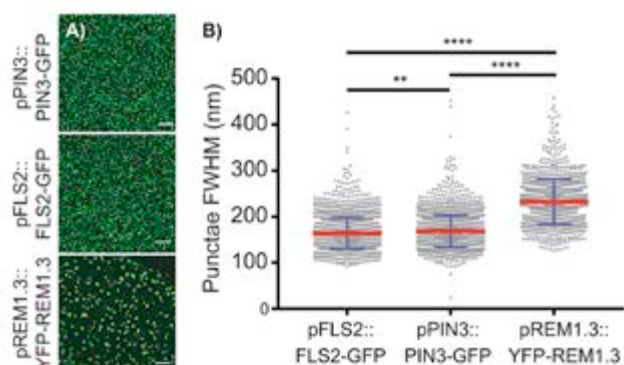


Figure 1: Zeiss Airyscan and TIRF imaging approaches were used to visualise single proteins labelled with GFP (green dots) in the plasma membrane of plant cells (A). Different membrane proteins exist in membrane microdomains of different sizes (B). The smallest of these microdomains, that of the protein PIN3-GFP, a hormone receptor, were approximately 160 nm in diameter. This is well below the theoretical limit for imaging by light microscopy and demonstrates the utility of these new super-resolution techniques.

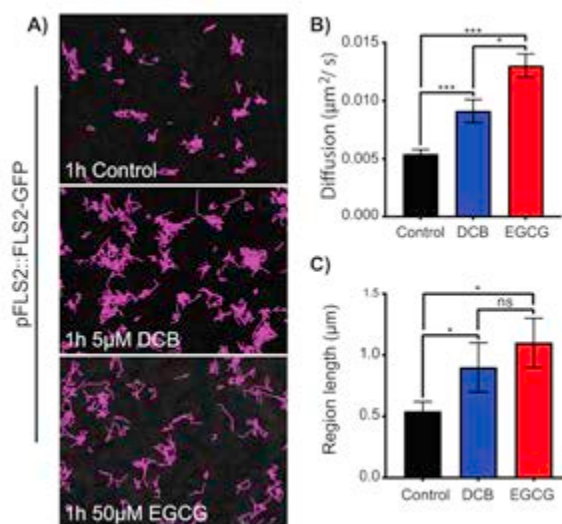


Figure 2: Timelapse imaging of the membrane protein microdomains described in Figure 1. The FLS2-GFP protein, a plant receptor that acts in the defense against pathogen attack pathway, moves laterally within the plane of the plasma membrane (pink tracks in (A)). The rate of diffusive movement of this protein and the size of the region in which it moves were calculated using SPT analysis techniques (B). Treatment of cells with chemicals that alter properties of the cell wall (DCB and EGCG) caused FLS2-GFP to move faster and increased the size of the membrane region within which it diffuses. This demonstrates the role of the cell wall in spatially regulating the distribution of defensive proteins. They are not distributed randomly but, rather, occur as discretely separated units to maximise membrane coverage.

Contact: J. Runions (jrunions@brookes.ac.uk)

Determination of the refractive index of insoluble organic extracts from atmospheric aerosol over the visible wavelength range using optical tweezers

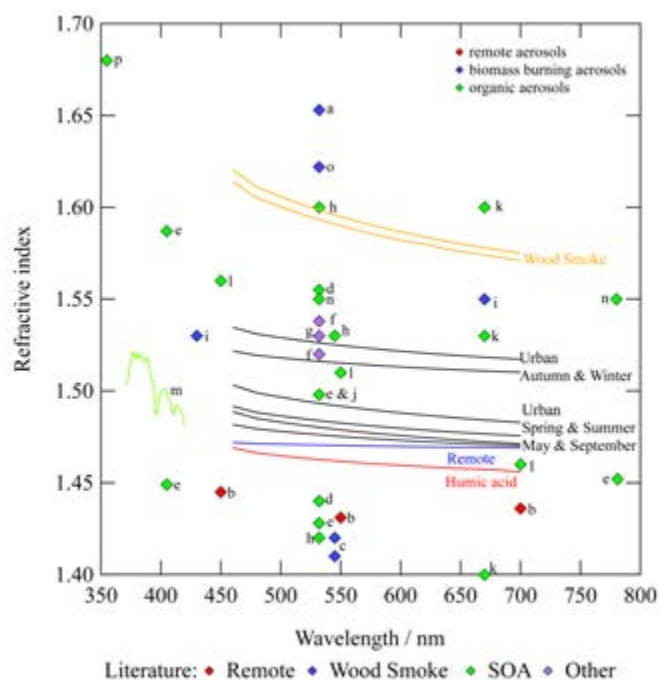
R.H. Shepherd (Department of Earth Sciences, Royal Holloway University of London, Egham, UK; Central Laser Facility, Research Complex at Harwell, STFC Rutherford Appleton Laboratory, Harwell Campus, Didcot, UK)
M.D. King (Department of Earth Sciences, Royal Holloway University of London, Egham, UK)

A.A. Marks, N. Brough (British Antarctic Survey, High Cross, Cambridge, UK)
A.D. Ward (Central Laser Facility, Research Complex at Harwell, STFC Rutherford Appleton Laboratory, Harwell Campus, Didcot, UK)

Atmospheric aerosol can contain a complex mixture of chemical compounds with a wide variety of physiochemical properties. The presence of organic material may alter the physical, chemical, and optical properties of cloud droplets or aerosol particles. Laser levitation of micro-droplets in air when combined with Mie spectroscopy provides a new technique to determine the refractive index of insoluble organic material extracted from atmospheric aerosol samples. The refractive index of the insoluble organic extracts was shown to follow a Cauchy equation between 460 nm and 700 nm for organic aerosol extracts collected from urban (London) and remote (Antarctica) locations. In general, the refractive index of aerosol material was found to increase from remote Antarctic summer ($n_D = 1.470$) to an urban summer ($n_D = 1.478$) to an urban autumn ($n_D = 1.522$) to woodsmoke ($n_D = 1.584$). The measured values of refractive

index compare well with previous monochromatic or small wavelength range measurements of refractive index.

Aerosol optical absorption is characterised by an Ångström exponent which defines the optical thickness of an aerosol with respect to wavelength. Mie spectra were used to determine the Ångström exponent of woodsmoke and humic acid aerosol as the spectral intensity decreases as absorption increases. Finally, a radiative-transfer calculation of the top-of-the-atmosphere albedo was applied to model an atmosphere containing a 3 km thick layer of aerosol comprising pure water, pure insoluble organic aerosol, or an aerosol consisting of an aqueous core with an insoluble organic shell. The calculation demonstrated that the top-of-the-atmosphere albedo increases by 0.01 to 0.03 for core-shell organic particles relative to water particles of the same size.



Refractive index dispersions for urban, remote, and woodsmoke atmospheric aerosol extracts and humic acid aerosol, compared to refractive index values from the literature. A sample from literature studies that investigated aerosols from remote locations (red), biomass burning (blue) and organic aerosols (green and purple)

Reproduced from R.H. Shepherd, M.D. King, A.A. Marks, N. Brough, A.D. Ward, *Atmos. Chem. Phys.*, 18, 5235–5252, 2018, under the terms of the Creative Commons Attribution 4.0 License. doi.org/10.5194/acp-18-5235-2018

Contact: M.D. King (m.king@rhul.ac.uk)
 A.D. Ward (andy.ward@stfc.ac.uk)

The architecture of EGFR's basal complexes reveals autoinhibition mechanisms in dimers and oligomers

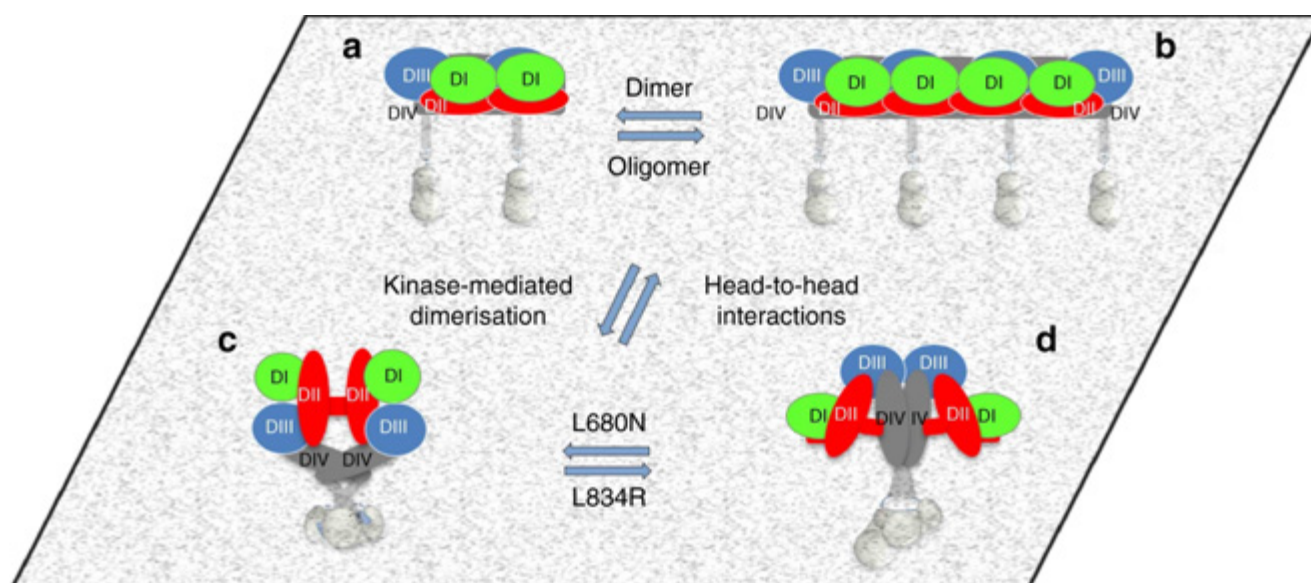
L.C. Zanetti-Domingues, D. Korovesis, S.R. Needham, C.J. Tynan, S.K. Roberts, D.T. Clarke, D.J. Rolfe, M.L. Martin-Fernandez (Central Laser Facility, Research Complex at Harwell, STFC Rutherford Appleton Laboratory, Harwell Oxford, Didcot, UK)
S. Sagawa, Y. Shan (D.E. Shaw Research, New York, USA)
D.E. Shaw (D.E. Shaw Research, New York, USA; Department of Biochemistry & Molecular Biophysics, Columbia University, New York, USA)
A. Kuzmanic, F.L. Gervasio (Department of Chemistry, Faculty of Maths & Physical Sciences, University College London, UK)
E. Ortiz-Zapater, G. Santis (Peter Gore Department of Immunobiology, School of Immunology & Microbial Sciences, Kings College London, UK)

P. Jain, P.M.P. van Bergen en Henegouwen (Division of Cell Biology, Science faculty, Department of Biology, Utrecht University, The Netherlands)
R.C. Roovers (Merus, LSI, Utrecht, The Netherlands)
A. Lajevardipour, A.H.A. Clayton (Centre for Micro-Photonics, Faculty of Science, Engineering & Technology, Swinburne University of Technology, Hawthorn, Australia)
P.J. Parker (Protein Phosphorylation Laboratory, The Francis Crick Institute, London, UK; School of Cancer & Pharmaceutical Sciences, King's College London, UK)

Our current understanding of epidermal growth factor receptor (EGFR) autoinhibition is based on X-ray structural data of monomer and dimer receptor fragments, and does not explain how mutations achieve ligand-independent phosphorylation. Using a repertoire of imaging technologies and simulations, we reveal an extracellular head-to-head interaction through which ligand-free receptor polymer chains of various lengths assemble. The architecture of the head-to-head interaction prevents kinase-mediated dimerisation. The latter, afforded by mutation or intracellular treatments, splits the autoinhibited head-to-head polymers to form stalk-to-stalk flexible non-extended dimers structurally coupled across the plasma membrane to active asymmetric tyrosine kinase

dimers, and extended dimers coupled to inactive symmetric kinase dimers. Contrary to the previously proposed main autoinhibitory function of the inactive symmetric kinase dimer, our data suggest that only dysregulated species bear populations of symmetric and asymmetric kinase dimers that coexist in equilibrium at the plasma membrane under the modulation of the C-terminal domain.

Reproduced from Zanetti-Domingues, L.C., Korovesis, D., Needham, S.R. et al, *Nat Commun* 9, 4325 (2018), under the terms of the Creative Commons Attribution 4.0 License. <https://doi.org/10.1038/s41467-018-06632-0>



Cartoon models of ligand-free EGFR species on the cell surface. *a, b* Autoinhibited ligand-free receptors form *a* dimers and *b* larger oligomers via extracellular head-to-head interactions. Within head-to-head dimers and oligomers the ICMs remain as non-interacting units. *c, d* Kinase-mediated receptor dimerisation outcompetes head-to-head interactions to form two types of receptor dimers that typically coexist in equilibrium (bearing aTKD and sTKD dimer configurations). Head-to-head dimers and oligomers are disrupted by kinase-mediated dimerisation independently of whether the driver mutation and/or

treatment is activating or not. The ECM architecture of one dimer type is consistent with a back-to-back dimer and structurally coupled to an sTKD dimer_{6,22} (*c*). The ECM architecture of the other is consistent with a stalk-to-stalk dimer and structurally coupled via an N-terminal TM crossing to the aTKD dimer₄₀ (*d*). The L680N kinase domain mutation shifts the equilibrium toward the dimer population bearing sTKD dimers while L834R shifts the equilibrium towards the dimer population bearing the aTKD dimer. For all panels, DI is in green, DII in red, DIII in blue, DIV, TMD and JMD in grey, TKD in silver

Contact: M.L. Martin-Fernandez
 (marisa.martin-fernandez@stfc.ac.uk)

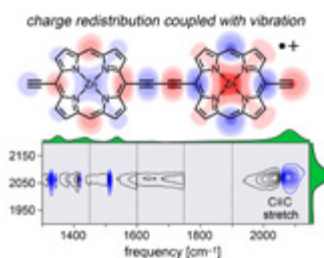
Mechanisms of IR Amplification in Radical Cation Polarons

G.M. Greetham, I.V. Sazanovich, P.M. Donaldson, M. Towrie, A.W. Parker (Central Laser Facility, Research Complex at Harwell, STFC Rutherford Appleton Laboratory, Harwell Campus, Didcot, UK)

Break down of the Born-Oppenheimer approximation is caused by mixing of electronic and vibrational transitions in the radical cations of some conjugated polymers, resulting in intense vibrational bands known as *infrared active vibrations* (IRAVs). We have investigated the mechanism of this amplification. Spectroelectrochemical time-resolved infrared (TRIR) and two-dimensional infrared (2D-IR) spectroscopies were used to investigate the radical cations of two butadiyne-linked porphyrin oligomers: a linear dimer and a cyclic hexamer. The 2D-IR spectra reveal strong coupling between all the IRAVs and the electronic π - π^* polaron band. Intramolecular vibrational energy redistribution (IVR) and vibrational relaxation occur within ~ 0.1 – 7 ps. TRIR spectra show that the transient ground state bleach (GSB) and excited state absorption (ESA) signals have anisotropies of 0.31 ± 0.07 and 0.08 ± 0.04 for the linear dimer and cyclic hexamer cations, respectively. The small TRIR anisotropy for the cyclic hexamer radical cation indicates that the vibrationally excited polaron migrates round the nanoring on a time scale faster than the measurement, i.e. within 0.5 ps, at 298 K. Density functional

W.J. Kendrick, M. Jirásek, M.D. Peeks, H.L. Anderson (Department of Chemistry, University of Oxford, UK)

theory (DFT) calculations qualitatively reproduce the IRAVs, and show how specific vibrational modes cause redistribution of the singly occupied molecular orbital (SOMO), amplifying the oscillator strength. These results show that IRAVs originate from the strong coupling of charge redistribution to nuclear motion, and from the similar energies of electronic and vibrational transitions.



Calculated distribution of the SOMO of the porphyrin dimer radical cation distorted by the triple bond stretch vibration. (below) 2D-IR spectra of this radical cation at 400 fs delay, with pump (FWHM ~ 80 cm^{-1}) centred at 2080 cm^{-1} . Black solid and blue dashed contour lines correspond to positive (ESA) and negative (GSB) signals, respectively.

Contact: H.L. Anderson (harry.anderson@chem.ox.ac.uk)

Influence of zeolite topology in Catalytic Fast Pyrolysis of Biomass: a Kerr-gated Raman study using model compounds

E. Campbell, I. Lezcano-Gonzalez, A.M. Beale (Department of Chemistry, University College London, UK; Research Complex at Harwell, STFC Rutherford Appleton Laboratory, Harwell Campus, Didcot, UK)

Biomass offers a route to obtain chemical products normally derived from crude oil, from a more sustainable and carbon neutral source (since biomass absorbs CO_2 for photosynthesis). The oxygen content of biomass, however, poses some problems, causing bio-oils to be more acidic and unstable than their crude oil derived counterparts. One method for the removal of oxygenates is through Catalytic Fast Pyrolysis of biomass (CFP), where biomass is pyrolyzed using fast heating rates and the resulting vapours are upgraded over zeolite catalysts.

Mechanistic studies are few in this area but some point towards the idea of a hydrocarbon pool mechanism, where hydrocarbons build up in zeolite pores to react with further pyrolysis vapours, undergoing decarbonylation, decarboxylation and dehydrogenation to produce aromatic species, olefins, CO and CO_2 , as well as undesirable coke which builds up. During this upgrading process, zeolites deactivate rapidly through coking, making frequent regeneration necessary and affecting process efficiency. Through understanding these chemical transformations, we can gain insight as to how reaction efficiency can be improved.

Raman Spectroscopy is a useful tool for mechanistic studies, but in many cases catalyst defects or emissive hydrocarbon species present can cause intense

Contact: A.M. Beale (andrew.beale@ucl.ac.uk)

I. Sazanovich, M. Towrie (Central Laser Facility, Research Complex at Harwell, STFC Rutherford Appleton Laboratory, Harwell Campus, Didcot, UK)

M.J. Watson (Johnson Matthey PLC, Billingham, UK)

fluorescence, preventing Raman signals from being detected. To avoid fluorescence, UV or near-IR probe wavelengths can be used but these often result in sample damage and low signal intensity respectively. This work uses a visible wavelength source (400 nm) with a Kerr-gated spectrometer that allows Raman signals to be separated from fluorescence due to their different lifetimes.

In this work, we study the interaction of oxygenated hydrocarbons with zeolites by operando Kerr-gated Raman Spectroscopy and identify reaction intermediates whilst measuring catalytic activity through mass spectrometry (MS).

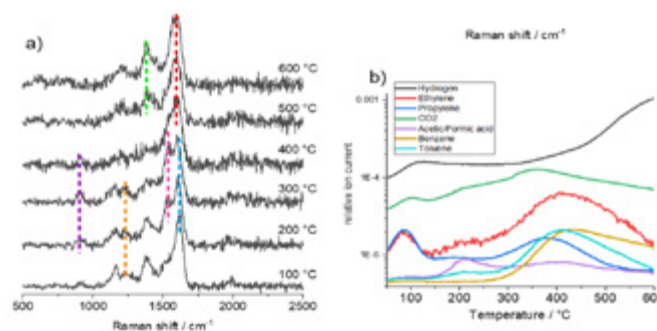


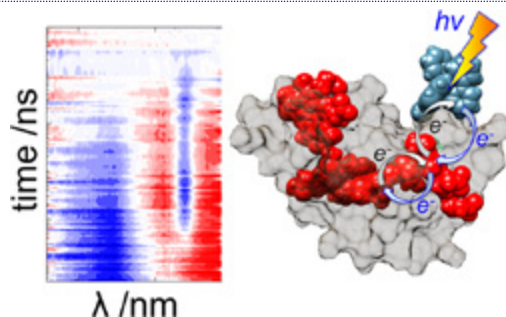
Figure a) Raman spectra collected during temperature ramp experiment of furan on H-ZSM-5 Si/Al 40 b) MS data simultaneously measured

Ultrafast Light-Driven Electron Transfer in a Ru(II)tris(bipyridine)-Labeled Multiheme Cytochrome

J.H. van Wonderen, C.R. Hall, K. Adamczyk, I. Heisler, S.E. Piper, T.A. Clarke, N.J. Watmough, S.R. Meech, J.N. Butt (School of Chemistry and School of Biological Sciences, University of East Anglia, Norwich, UK)
X. Jiang, A. Carof (Department of Physics and Astronomy and Thomas-Young Centre, University College London, UK)

I.V. Sazanovich, M. Towrie (Central Laser Facility, Research Complex at Harwell, STFC Rutherford Appleton Laboratory, Harwell Campus, Didcot, UK)
J. Blumberger (Department of Physics and Astronomy and Thomas-Young Centre, University College London, UK; Institute for Advance Study, Technische Universität München, Garching, Germany)

Multiheme cytochromes attract much attention for their electron transport properties. These proteins conduct electrons across bacterial cell walls and along extracellular filaments and when purified can serve as bionanoelectronic junctions. Thus, it is important and necessary to identify and understand the factors governing electron transfer in this family of proteins. To this end we have used ultrafast transient absorbance spectroscopy, to define heme–heme electron transfer dynamics in the representative multiheme cytochrome STC from *Shewanella oneidensis* in aqueous solution. STC was photosensitized by site-selective labelling with a tris(bipyridine) Ru(II) dye and the dynamics of light-driven electron transfer described by a kinetic model corroborated by molecular dynamics simulation and density functional theory calculations. The results are significant in demonstrating the opportunities for pump–probe spectroscopies to resolve interheme electron transfer in Ru-labelled multiheme cytochromes.



Differential transient absorbance (left) for visible wavelengths (blue = positive features, red = negative features) following excitation of tris(bipyridine) Ru(II) attached to the STC protein (right).

Reproduced from J.H. van Wonderen et al. *J. Am. Chem. Soc.* 2019, 141, 38, 15190–15200, doi: 10.1021/jacs.9b06858, © 2019 American Chemical Society, under the terms of the Creative Commons Attribution 4.0 International License

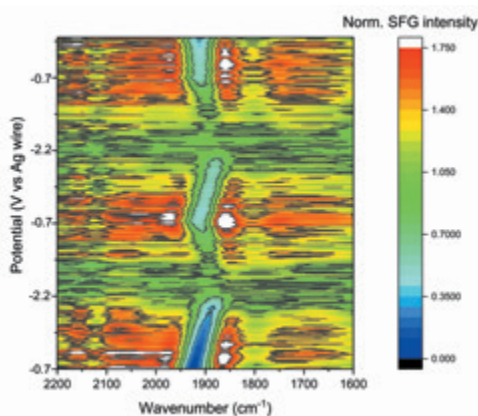
Contact: J.N. Butt (J.Butt@uea.ac.uk)

Assessing the Viability of Heterodyne VSFG Spectroscopic Studies of Electrode Interfaces

A.M. Gardner, K.H. Saeed, A.J. Cowan (Stephenson Institute for Renewable Energy, University of Liverpool, UK)

P.M. Donaldson (Central Laser Facility, STFC Rutherford Appleton Laboratory, Harwell Campus, Didcot, UK)

Heterodyne vibrational sum frequency generation (HD-VSFG) spectroscopy allows for detection of molecules at surfaces, even at very low coverages, and yields both the phase and amplitude of SFG signal. Past application of HD-VSFG to the chemistry occurring at electrode surfaces is, however, limited. Here we report our efforts towards a broad-band HD-VSFG experiment for the study of CO₂ reduction electrocatalysis.



HD-VSFG spectra recorded as the potential of the Au working electrode is modulated between -0.7 and -2.2 V in the presence of [Mo(bpy)(CO)₄] at 10 mV s⁻¹.

Contact: A.J. Cowan (acowan@liverpool.ac.uk)

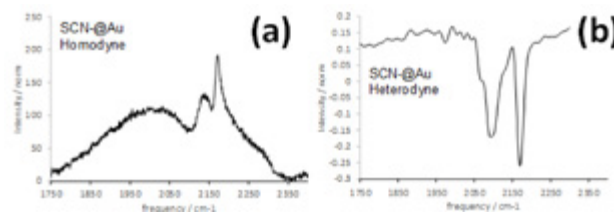
Towards heterodyne detected IR-Visible Sum Frequency Generation at CLF-Ultra

G. Karras, C. Kirkbride, P.M. Donaldson (Central Laser Facility, STFC Rutherford Appleton Laboratory, Harwell Campus, Didcot, UK)

O. Al Bahri, J.M. Cole (Molecular Engineering Group, University of Cambridge, UK)
K. Saeed, A.M. Gardner, A.C. Cowan (School of Physical Sciences, University of Liverpool, UK)

Surface specific IR-Visible Sum Frequency Generation (SFG) has the ability to measure vibrational spectra of monolayer level buried interfaces. The provision of IR-Visible SFG spectroscopy at CLF-Ultra has been driven by successful studies of catalysis at electrochemical interfaces. In this article we demonstrate progress towards measuring SFG spectra with heterodyne detection, which has the advantage of being background free and free from the artefacts associated with in-quadrature detection.

Contact: P.M. Donaldson (paul.donaldson@stfc.ac.uk)



A comparison of SCN- ions on a gold substrate measured with homodyne (a) and heterodyne (b) detected IR-Visible SFG spectroscopy. (a) was recorded with a 2 second accumulation of signal; (b) was recorded with a 20 second accumulation of signal. Heterodyne signal fringes were recovered from a spectrum recorded with a 4 ps delay between the local oscillator and the SFG signal.

2D-IR spectroscopy reveals multiple hydrogen bonded ensembles of the thiocyanate ion in the protic ionic liquid ethyl ammonium nitrate

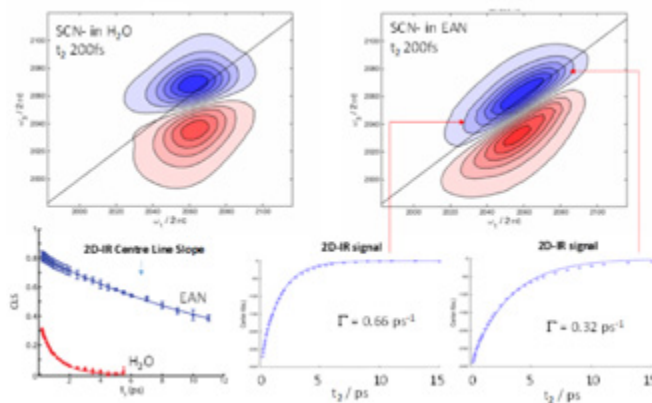
A.W. Parker, P.M. Donaldson (Central Laser Facility, STFC Rutherford Appleton Laboratory, Harwell Campus, Didcot, UK)

C. Johnson, S.G. Roe (Department of Chemistry, University of Pittsburgh, USA)

2D-IR spectroscopy can measure the ultrafast structural dynamics of solvated molecules in equilibrium. Here we are interested in the hydrogen bonding dynamics of the simplest protic ionic liquid – ethyl ammonium nitrate (EAN), which we study via the 2D-IR spectrum of a guest solute ion thiocyanate (SCN^-). We bring together advances in both experiment and in data modelling/fitting to provide a most concise and quantitative measure of the hydrogen bond dynamics of SCN^- in EAN.

We have applied polarization and temperature-dependent 2D-IR spectroscopy to quantify the ultrafast (<10 ps) hydrogen bond dynamics of a guest ion SCN^- in the protic ionic liquid EAN. Not only did we learn quantitatively about the energetics and rates of hydrogen bonding in the two different ensembles observed, this type of measurement (a first for the Ultra facility) and the data analysis techniques used represent a powerful protocol for future studies of other electrolytes.

Contact: S.G. Roe (sgr@pitt.edu)
P.M. Donaldson (paul.donaldson@stfc.ac.uk)



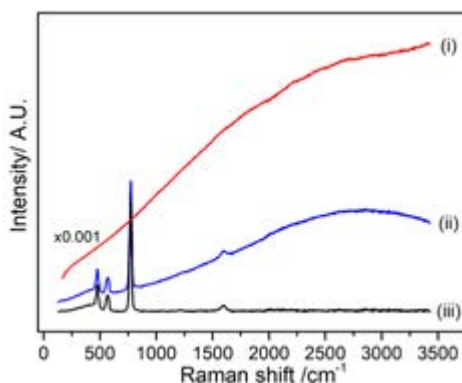
2D-IR spectroscopy reveals that the structural and vibrational dynamics of SCN^- in protic ionic liquid EAN is significantly different from that of water

Kerr gated Raman spectroscopy of LiPF_6 salt and LiPF_6 -based organic carbonate electrolyte for Li-ion batteries

L. Cabo-Fernandez, A.R. Neale, F. Braga, L.J. Hardwick (Stephenson Institute for Renewable Energy, Department of Chemistry, University of Liverpool, Peach Street, UK)
I.V. Sazanovich (Central Laser Facility, Research Complex at Harwell, STFC Rutherford Appleton Laboratory, Harwell Campus, Didcot, UK)

R. Kosteckí (Energy Storage and Distributed Resources Division, Lawrence Berkeley National Laboratory, California, USA)

Fluorescent species are formed during cycling of lithium ion batteries as a result of electrolyte decomposition due to the instability of the non-aqueous electrolytes and side reactions that occur at the electrode surface. The increase in the background fluorescence due to the presence of these components makes it harder to analyse data due to the spectroscopic overlap of Raman scattering and fluorescence. Herein, Kerr gated Raman spectroscopy was shown to be an effective technique for the isolation of the scattering effect from the fluorescence enabling the collection of the Raman spectra of LiPF_6 salt and LiPF_6 -based organic carbonate electrolyte, without the interference of the fluorescence component. Kerr gated Raman was able to identify POF_3 on the LiPF_6 particle surface, after the addition of trace water.



Raman spectra of anhydrous LiPF_6 measured with a 400 nm laser excitation in (i) CW mode and (ii) Kerr gated mode and (iii) the baseline corrected Kerr gated spectra. Intensity of (i) scaled by $\times 0.001$ to view data on same axis.

Reproduced from *Phys. Chem. Chem. Phys.*, 2019, 21, 23833-23842, with permission from the Royal Society of Chemistry under the Creative Commons Attribution 3.0 Unported Licence.

Contact: L.J. Hardwick (hardwick@liverpool.ac.uk)

2D-IR spectroelectrochemistry of singly oxidized $\text{cis-}[\text{Ru}(4,4'-(\text{MeO})_2\text{-bpy})_2(\text{NCS})_2]^+$ and reduced $\text{cis-}[\text{Ru}(4,4'-(\text{COOEt})_2\text{-bpy})_2(\text{NCS})_2]$ (bpy = 2,2'-bipyridine) complexes

M. Piží, A. Viček (Queen Mary University of London, School of Biological and Chemical Sciences, London, UK)
J.O. Taylor, F. Hartl (Department of Chemistry, University of Reading, UK)

P.M. Donaldson (Central Laser Facility, Research Complex at Harwell, STFC Rutherford Appleton Laboratory, Harwell Campus, Didcot, UK)

Infra-red transmittance spectroelectrochemistry is now well-established as a go-to technique for investigating a host of different redox reactions. The enormous potential of this technique has yet to be fully realised. Proof-of-concept measurements supported by anharmonic-frequency quantum-chemical calculations have revealed the exciting potential of this technique in combination with pump-probe 2D-IR laser spectroscopy. Vibrational relaxation of the IR-active thiocyanate stretching modes in the two title reference complexes was investigated in their ground states as well as $1e^-$ Ru-oxidized (for Ru-bis(dimethoxy)bpy) and $1e^-$ bpy-reduced (for Ru-bis(ester)bpy) states. Dramatic shortening of the NCS-stretching vibrational relaxation was observed for the Ru-oxidized complex, comparable to the triplet Ru-to-bpy excited state of the same complex. On the other hand, the bis(ester)bpy-localized reduction has a negligible effect on the dynamics of the NCS-stretching vibration. An accurate analysis of the experimental data and understanding of the dynamic behaviour requires high-level DFT calculations of anharmonic vibrational energies and diagonal/off-diagonal anharmonicity. The results will have an important impact on the description of relaxation processes in photoinduced electron-transfer reactions and their role in photo-redox catalysis.

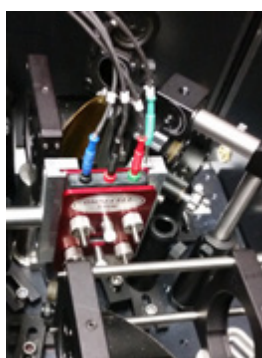


Figure 1: LIFETIME-OTTLE cell setup used for the 2D-IR spectroelectrochemical experiments

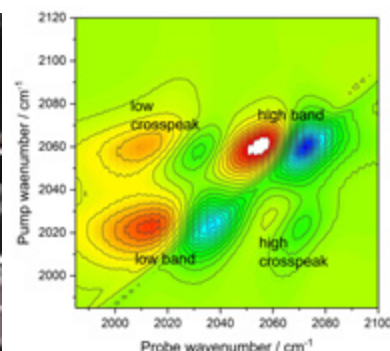


Figure 2: Representative 2D-IR spectrum of in situ generated $\text{cis-}[\text{Ru}(4,4'-(\text{MeO})_2\text{-bpy})_2(\text{NCS})_2]^+$ in DMF

Contact: F. Hartl (f.hartl@reading.ac.uk)

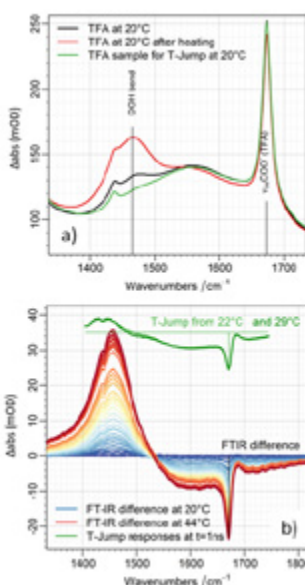
Temperature-Jump Time Resolved Infrared Spectroscopy of Trifluoroacetic Acid Solutions – Characterising the T-Jump

R. Fritsch, L. Minnes (Department of Physics, University of Strathclyde, Glasgow, UK)
 G.M. Greetham, I.P. Clark, M. Towrie, A.W. Parker (Central Laser Facility, STFC Rutherford
 Appleton Laboratory, Harwell Campus, Didcot, UK)

D. J. Shaw, N.T. Hunt (Department of Chemistry, University of York, York, UK)

There is an increasing appreciation of the involvement of dynamic structural changes in biological function, from the unwinding of double stranded DNA to structural changes of proteins during their biological mechanisms. The molecular details of these transitions are of significant interest, and the ability to measure them in real time would provide valuable experimental insight. Temperature jump time-resolved spectroscopy, in which a nanosecond duration infrared laser pulse tuned to solvent absorptions induces a rapid rise in temperature, has become a powerful method for studying biomolecular transitions. It is, however, important to carefully calibrate the temperature jump achieved in order to separate biomolecular dynamics from those of the solvent bath. In this report, we describe the use of trifluoroacetic acid solutions to characterise the magnitude and dynamics of a temperature jump initiated using a high repetition rate pumping and time resolved multiple probe infrared detection methodology.

Contact: N.T. Hunt (neil.hunt@york.ac.uk)



a) IR absorption spectra of TFA in D_2O solution (black and red). NB the increase in absorbance of the HOD bending vibrational mode after heating due to further exchange with the environment. Green shows the absorption spectrum of the sample used to acquire the data in b).

b) Temperature-dependent IR absorption difference spectra of TFA (lower). Colour scale runs from 20°C (blue) to 44°C (red). The difference spectra are relative to the spectrum at 20°C. Green traces show T-jump-IR spectra of the same sample obtained at a T-jump-probe delay time of 1 ns.

Evaluation of Ultra A for the detection and analysis of drug-target structural changes using EVV 2DIR spectroscopy

D.R. Klug (Department of Chemistry, Imperial College London, UK)

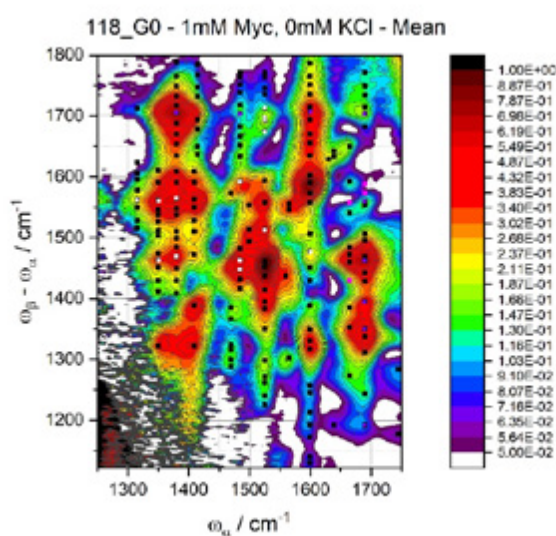
When two molecules come together to form a complex, part of the interaction is the coupling of molecular vibrations that originated on the unbound molecular species. Previous research has shown that the new couplings can be detected by EVV 2DIR spectroscopy[1]. However, despite the power of existing structural biology methods, many limitations remain such that structural data is not available in sufficient quantity or quality to drive particular drug-discovery/development strategies.

The limiting factor in our studies of drug-target binding has been the signal to noise and reproducibility achievable by the spectroscopic apparatus. In collaboration with the CLF, we ported our EVV experiment onto CLF apparatus. This was successfully completed and showed that EVV 2DIR experiments could be successfully performed on both Ultra A and LifeTIME.

Following this knowledge transfer activity, we explored the utility of the new apparatus against drug-kinase binding, and the ability of EVV 2DIR spectroscopy to be used to assign structural features to G-quadruplex DNA.

Modifications to the Ultra A-EVV 2DIR setup have been identified which have the potential to improve the signal to noise and reproducibility of the data, and make the system comparable or superior to the performance of the obsolete Imperial College system.

[1] Guo, R. et al., *Phys. Chem. Chem. Phys.* 11(38): 8417-8421, 2009



EVV 2DIR spectrum of Myc2345 in the absence of potassium ions taken using Ultra A. Over 170 individual peaks are identifiable.

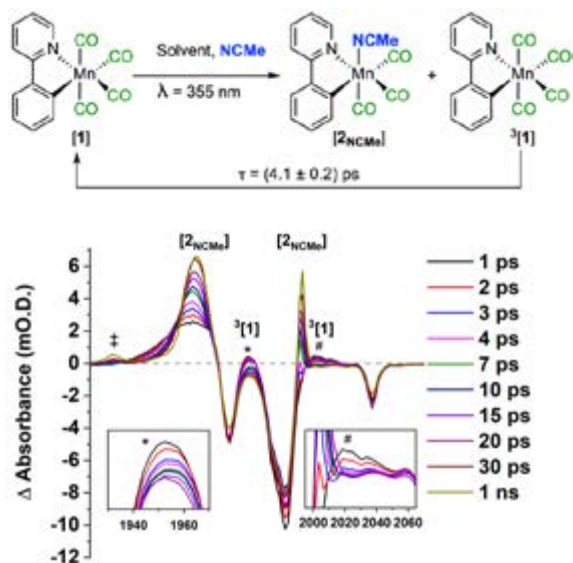
Contact: D. Klug (d.klug@imperial.ac.uk)

Time-resolved Infra-red Spectroscopy Provides Insight into the Solvation of Unsaturated Transition Metal Complexes

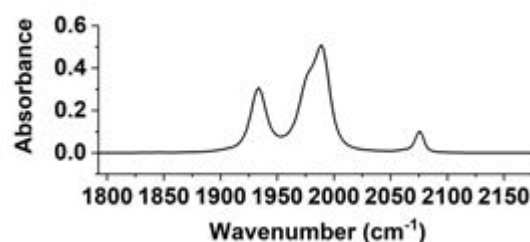
B.J. Aucott, L.A. Hammarback, B.E. Moulton, A.K. Duhme-Klair, I.J.S. Fairlamb, J.M. Lynam
(Department of Chemistry, University of York, UK)

I.P. Clark, I.V. Sazanovich, M. Towrie (Central Laser Facility, STFC Rutherford Appleton Laboratory, Harwell Campus, Didcot, UK)

Photolysis of $[\text{Mn}(\text{ppy})(\text{CO})_4][1]$ (ppy = 2-phenylpyridine) results in ultrafast (< 1 ps) dissociation of a carbonyl ligand and formation of complexes $\text{fac-}[\text{Mn}(\text{ppy})(\text{CO})_3(\text{S})]$ where S is the solvent medium employed. The nature of the complexes, and in particular the binding mode of the solvent, was probed by time-resolved multiple-probe spectroscopy (TR^MPS). It was found that the solvation process is kinetically controlled, for



example, when ether solvents such as THF are employed, initial binding to the metal occurs through a C-H bond in a σ -type interaction. Subsequent isomerisation to the more thermodynamically stable oxygen-bound isomer then occurs over the course of ca. 20 ps. These data provide insight into solvation processes which are relevant to a number of reaction steps that underpin catalysis.



Top left: Scheme showing the reaction pathway.

Bottom left: TRIR spectra showing the formation of $[2_{\text{NCMe}}]$ and $^3[\text{Mn}(\text{ppy})(\text{CO})_4]$.

Right: Ground state spectrum of $[1]$ in NCMe.

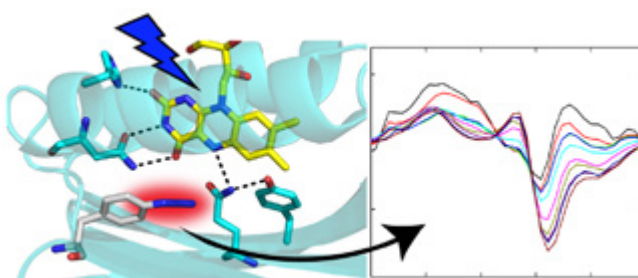
Contact: I.P. Clark (ian.p.clark@stfc.ac.uk)

Site-Specific Protein Dynamics Probed by Ultrafast Infrared Spectroscopy of a Noncanonical Amino Acid

C.R. Hall, K. Adamczyk, S.R. Meech (School of Chemistry, University of East Anglia, Norwich, UK)
J. Tolentino Collado, J.N. Iuliano, A.A. Gil, P.J. Tonge (Department of Chemistry, Stony Brook University, New York, USA)

A. Lukacs (Department of Biophysics, Medical School, University of Pecs, Hungary)
G.M. Greetham, I.V. Sazanovich (Central Laser Facility, STFC Rutherford Appleton Laboratory, Harwell Campus, Didcot, UK)

Real-time observation of structure changes associated with protein function remains a major challenge. Ultrafast pump-probe methods record dynamics in light activated proteins, but the assignment of spectroscopic observables to specific structure changes can be difficult. The BLUF (blue light using flavin) domain proteins are an important class of light sensing flavoprotein. Here, we incorporate the unnatural amino acid (UAA) azidophenylalanine (AzPhe) at key positions in the H-bonding environment of the isoalloxazine chromophore of two BLUF domains, namely, PixD and AppABLUF; both proteins retain the red-shift on irradiation characteristic of photoactivity. Steady state and ultrafast time resolved infrared difference measurements of the azido mode reveal site-specific information on the nature and dynamics of light driven structure change. AzPhe dynamics are thus shown to be an effective probe of BLUF domain photoactivation, revealing significant differences between the two proteins and a differential response of the two sites to chromophore excitation.



Reprinted with permission from Hall CR, Tolentino Collado J, Iuliano JN, et al. Site-Specific Protein Dynamics Probed by Ultrafast Infrared Spectroscopy of a Noncanonical Amino Acid. *J Phys Chem B*. 2019;123(45):9592-9597. doi:10.1021/acs.jpccb.9b09425. Copyright 2019 American Chemical Society.

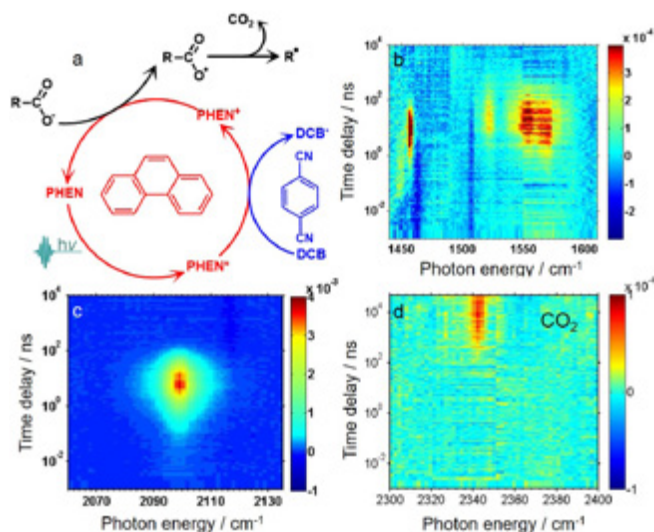
Contact: S.R. Meech (s.meech@uea.ac.uk)

Picosecond to millisecond tracking of a photocatalytic decarboxylation reaction provides direct mechanistic insights

A. Bhattacharjee (School of Chemistry, University of Bristol, UK; AMOLF, Amsterdam, The Netherlands)

M. Sneha, L. Lewis-Borrell, O. Tau, A. Orr-Ewing (School of Chemistry, University of Bristol, UK)
I.P. Clark (Central Laser Facility, STFC Rutherford Appleton Laboratory, Harwell Campus, Didcot, UK)

The photochemical decarboxylation of carboxylic acids is a versatile route to free radical intermediates for chemical synthesis. However, the sequential nature of this multi-step reaction renders the mechanism challenging to probe. Here, we employ a 100 kHz mid-infrared probe in a transient absorption spectroscopy experiment to track the decarboxylation of cyclohexanecarboxylic acid in acetonitrile- d_3 over picosecond to millisecond timescales using a photooxidant pair (phenanthrene and 1,4-dicyanobenzene). Selective excitation of phenanthrene at 256 nm enables a diffusion-limited photoinduced electron transfer to 1,4-dicyanobenzene. A measured time offset in the rise of the CO_2 byproduct reports on the lifetime (520 ± 120 ns) of a reactive carboxyl radical in solution, and spectroscopic observation of the carboxyl radical confirm its formation as a reaction intermediate. Precise clocking of the lifetimes of radicals generated in situ by an activated C-C bond fission will pave the way for improving the photocatalytic selectivity and turnover.



Photoredox cycle converting deprotonated carboxylic acids to reactive radicals (a), and the time-dependence of IR bands of (b) $PHEN^+$, (c) DCB^+ , and (d) CO_2 products

Reproduced from Bhattacharjee, A., Sneha, M., Lewis-Borrell, L. et al. *Nat Commun* 10, 5152 (2019), under the terms of the Creative Commons Attribution 4.0 International License. doi: 10.1038/s41467-019-13154-w

Contact: A. Orr-Ewing (a.orr-ewing@bristol.ac.uk)

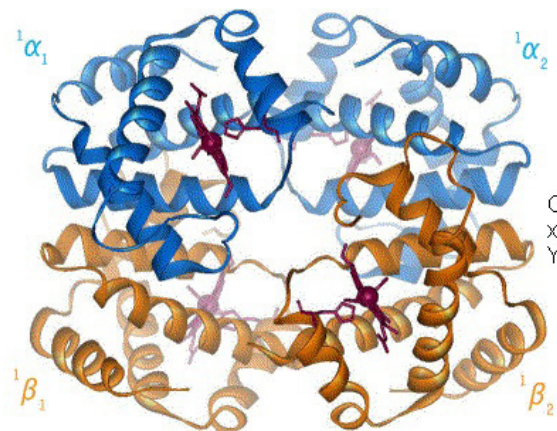
Time-Resolved Multiple-Probe Infrared Spectroscopy Studies of Carbon Monoxide Migration through Internal Cavities in Haemoglobin

M.V. Parkhats, B.M. Dzhangarov, S.V. Lepeshkevich (B.I. Stepanov Institute of Physics, National Academy of Sciences of Belarus, Minsk, Belarus)

I.V. Sazanovich (Central Laser Facility, STFC Rutherford Appleton Laboratory, Harwell Campus, Didcot, UK)

S. N. Gilevich (Institute of Bioorganic Chemistry, National Academy of Sciences of Belarus, Minsk, Belarus)

Human haemoglobin reactivity towards ligands such as O_2 and CO as well as ligand migration via the protein matrix is modulated by internal cavities. In the present work, a time-resolved multiple-probe picosecond to millisecond infrared technique developed at Ultra Facility was applied to determine the dynamics of the ligand migration via the internal cavities of haemoglobin. We studied both native haemoglobin (see figure) and its isolated α and β chains. We succeeded in following the evolution of photodissociated CO ligand inside the protein matrix during geminate recombination. Moreover, we managed to detect the photodissociated CO molecules escaped from the protein into external media.



The schematic structure of human haemoglobin in Oxy state with α and β subunits colour-coded.

Contact: I.V. Sazanovich (igor.sazanovich@stfc.ac.uk)

Artemis operational statistics

R.T. Chapman (Central Laser Facility, STFC Rutherford Appleton Laboratory, Harwell Campus, Didcot, UK)

This year was a shortened year of user access in Artemis, as the decommissioning phase of the Artemis upgrade project began in November 2018. The team delivered six user experiments over seven slots, totalling 15 weeks of access with five setup weeks. As well as the user experiments, the team delivered two weeks of development with external collaborators and three weeks of preparatory work for design of the 100 kHz beamline as part of the upgrade. Figure 2 shows the schedule for the year.

Experiments

Three of the experiments used the atomic and molecular physics (AMO) chamber. All three used the velocity map imaging (VMI) detector, but for different experimental techniques: photoelectron circular dichroism, coulomb explosion imaging and ultrafast photoelectron spectroscopy. The VMI was swapped for a time of flight spectrometer during the ultrafast photoelectron spectroscopy experiment, to collect data at a different energy range. The three remaining experiments were carried out using the angle resolved photoemission chamber for studying condensed matter samples. Typically, a week of setup is dedicated to each experiment before users arrive. Similar experiments are grouped together to minimise setup time.

Facility performance and reliability

Figure 1 shows the availability and reliability calculations for the 2018-19 year. We run the laser continuously from Mondays through to Fridays during experiments, and regularly carry on data-taking over weekends. In this calculation, the availability for unsupported data-taking overnight and at weekends is weighted equally with supported hours. Laser reliability through the half year of user experiments was very good and we were able to recover the two experiments we lost due to problems in the previous year.

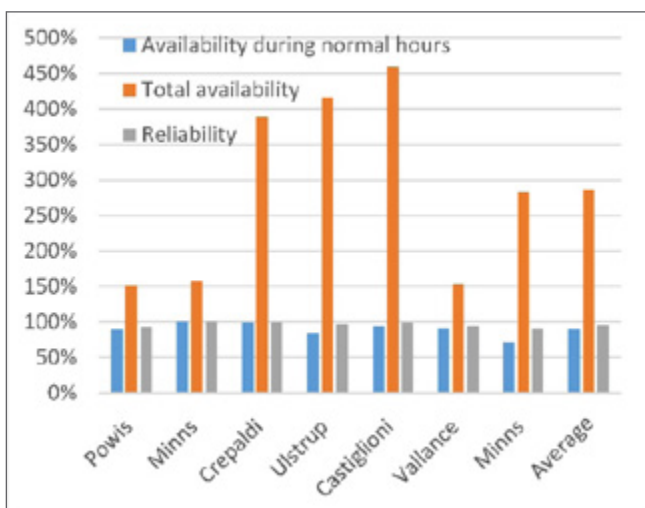


Figure 1: Artemis availability and reliability for user experiments in 2018-19

Contact: R. Chapman (richard.chapman@stfc.ac.uk)

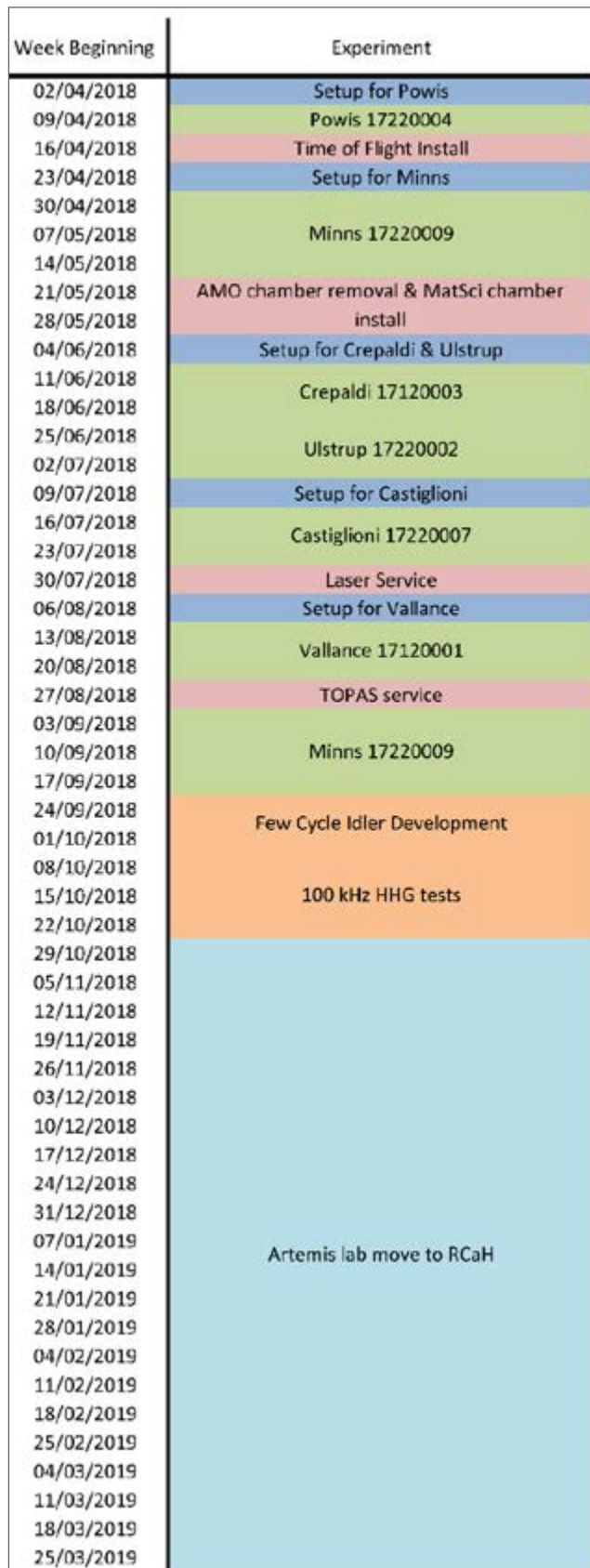


Figure 2: Artemis Schedule for 2018-19

Gemini operational statistics

S. Hawkes (Central Laser Facility, STFC Rutherford Appleton Laboratory, Harwell Campus, Didcot, UK)

During the reporting year, April 2018 – April 2019, a total of seven complete experiments were delivered in the Gemini Target Area and two experiments in TA2. In total 33 high power laser experimental weeks were delivered in the Gemini Target Area and 20 weeks in TA2. The delivered schedule is presented in Figure 2.

The availability of the Gemini laser system (delivery to the Gemini Target Area) was 86% during normal working hours, rising to 143% with time made up from running out of normal working hours. The reliability of the Gemini laser was 91%. TA2 availability was 88% during normal working hours, rising to 142% with time made up from running out of normal working hours. An individual breakdown of the availability and reliability for the experiments conducted is presented in Figure 1.

The high levels of total availability were made possible by the continued unique operational model employed on Gemini, which involves running the laser late into the evening. In addition, frequent weekend operational days were made available.

As well as the delivered experimental schedule, a system access slot was scheduled to demonstrate the Active beam stabilization on the Gemini South beam (see Annual Report article by Dann *et al.* for further details).

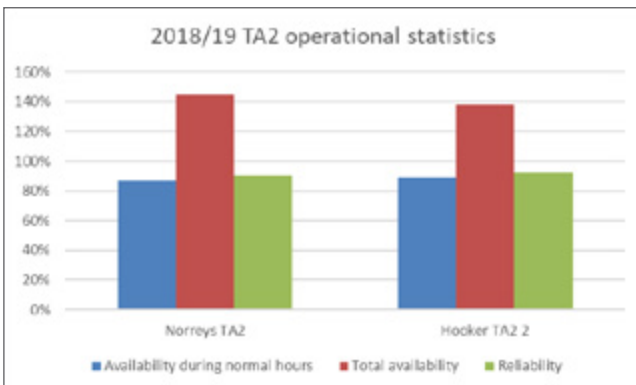
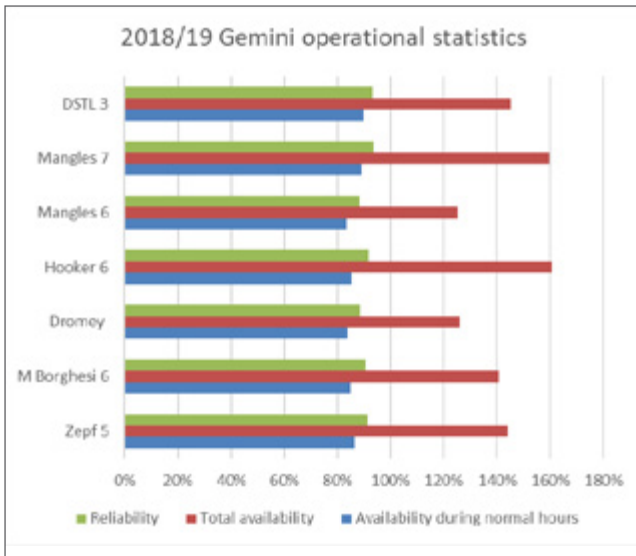


Figure 1: 2018/19 Gemini/TA2 operational statistic

Week beginning	Gemini	TA2
02/04/2018		
09/04/2018	Beamline switchover	
16/04/2018	Zepf 17210015	Hooker (part 2) 17210008
23/04/2018		
30/04/2018		
07/05/2018		
14/05/2018		
21/05/2018	XPW	
28/05/2018	Grating change	
04/06/2018	Plasma mirror setup	
11/06/2018		
18/06/2018		
25/06/2018		Hooker (part 3)
02/07/2018	Borghesi 17210027	17210008
09/07/2018		
16/07/2018		
23/07/2018		
30/07/2018	Beamline setup	
06/08/2018	Dromey 18110012	Norreys (part 1) 18110024
13/08/2018		
20/08/2018		
27/08/2018		
03/09/2018		
10/09/2018		
17/09/2018	Pulse train setup	
24/09/2018	Hooker 18110004	Norreys (part 2) 18110024
01/10/2018		
08/10/2018		
15/10/2018		
22/10/2018		
29/10/2018		
05/11/2018	Quantel service	
12/11/2018	Hooker ctd.	
19/11/2018	System access Beam stabilisation	System access
26/11/2018		
03/12/2018		
10/12/2018		
17/12/2018		
24/12/2018	Christmas 2018	
31/12/2018		
07/01/2019	Mangles 17210011	
14/01/2019		
21/01/2019	Mangles 18110023	
28/01/2019		
04/02/2019		
11/02/2019	Maintenance	
18/02/2019	Commercial access 18220000	
25/02/2019		
04/03/2019		
11/03/2019		
18/03/2019		
25/03/2019		

Figure 2: 2018/19 Gemini/TA2 operational schedule

Contact: S. Hawkes (steve.hawkes@stfc.ac.uk)

Octopus and Ultra Operational Statistics

B.C. Bateman, M. Szynkiewicz, E. Gozzard, D.T. Clarke (Central Laser Facility, STFC Rutherford Appleton Laboratory, Harwell Campus, Didcot, UK)

Octopus facility

In the reporting period (April 2018 to March 2019), 54 unique User groups submitted a total of 76 proposals bidding for time at the Octopus facility. 42 experiments comprising 104 weeks access time were awarded and delivered to the UK User community throughout the year. A full breakdown of number of weeks applied for versus number of weeks scheduled is shown in Figure 1, indicating an oversubscription ratio of 1.97:1. Figure 3 shows that Biology and Bio-materials formed the majority of applications.

There were a total of 22 formal reviewed publications recorded throughout the year.

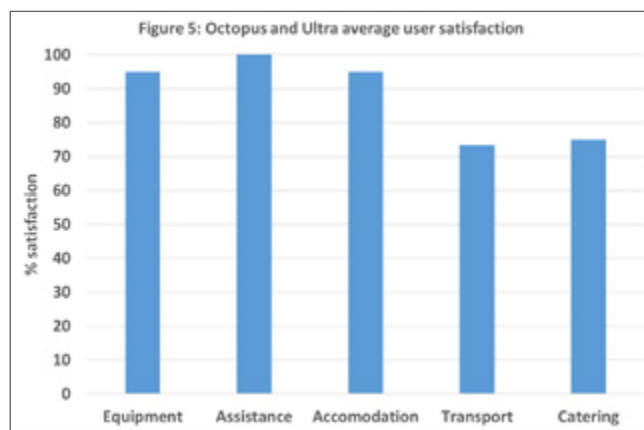
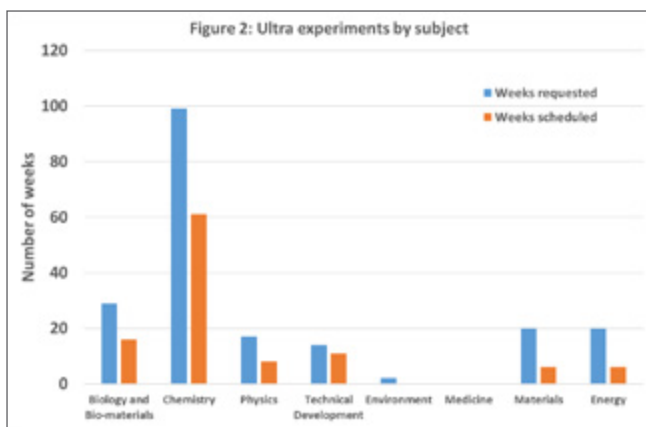
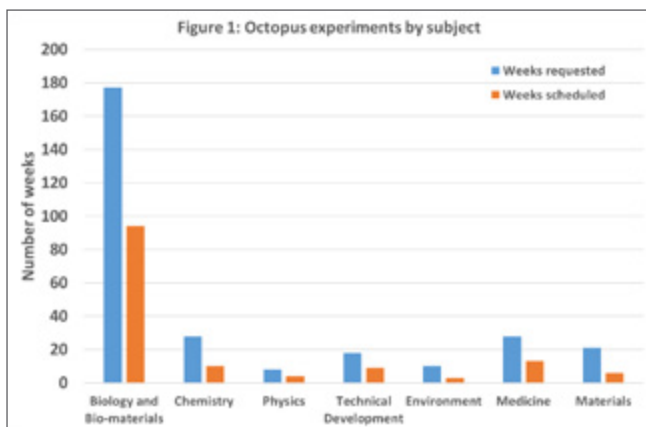
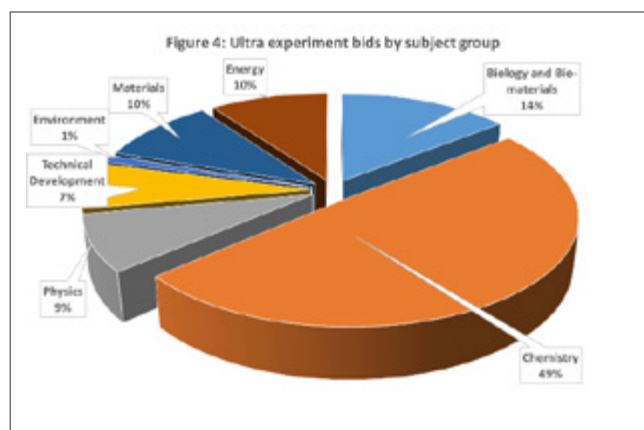
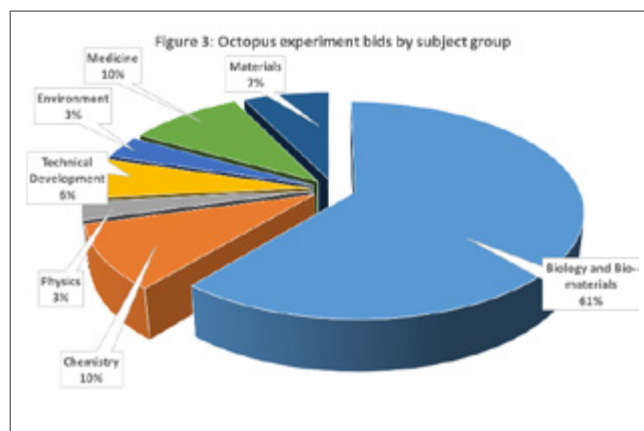
Ultra facility

In the reporting period (April 2018 to March 2019), 30 unique User groups submitted a total of 46 proposals bidding for time at the Ultra facility. 26 experiments comprising 60 weeks access time were awarded and delivered to the UK User community. A full breakdown of number of weeks applied for versus number of weeks scheduled is shown in Figure 2, indicating an oversubscription ratio of 1.8:1. Figure 4 shows that Chemistry formed the majority of applications.

There were a total of 19 formal reviewed publications recorded throughout the year.

User satisfaction

The average User satisfaction marks obtained from the scheduled Octopus and Ultra Users are shown in Figure 5, with an average satisfaction of 88% across the categories. There was a total of 53 hours downtime reported over the combined 164 weeks of access.



Contact: D.T. Clarke (dave.clarke@stfc.ac.uk)

Target Fabrication Operational Statistics

D. Haddock, C. Spindloe & M.K. Tolley (Target Fabrication Group, Central Laser Facility, STFC Rutherford Appleton Laboratory, Harwell Campus, Didcot, UK)

Experimental Support

This paper details Target Fabrication support given to experimental groups in the Vulcan target areas TAW and TAP, along with those in the Gemini Target Area, between April 2018 and April 2019. Target Fabrication supported seven solid target Vulcan experiments and three solid target Gemini experiments, totalling 40 weeks of Vulcan access (plus training weeks) and 20 weeks of Gemini access. Additional experiments were also supported for filters and other diagnostic elements, which are non-trivial but not reported on in these statistics. At 60, the total number of weeks supported is less than the previous year (71 in 2017-2018), but more than 2016-2017 (56) and 2015-2016 (57)

The Target Fabrication Group also supported academic access experiments at AWE and internal experiments.

From this reporting year onwards, Gemini and Vulcan targets will be separated out for tables and graphics. This is due to Gemini targets being produced in arrays or tapes: with multiple shots available per object delivered, each position on the array or tape will now be referred to as an individual target. Quantifying these together with Vulcan single-shot targets disproportionately skews analysis. When it comes to target types, Gemini almost exclusively requires ultra-thin films which, although they are processed similarly to Vulcan targets, end up being used very differently in the experiment.

This report does not include support for other areas of the CLF, including Artemis and the LSF.

1) Supported experiments

For the reporting year, the total number of targets produced for each experiment is shown in Table 1. This year, to better understand the amount of resources required for each experiment, a classification of complexity has been introduced: Class 1 targets require no R&D and have been fabricated before; Class 2 targets require some short-term R&D and/or complex manufacture processes; Class 3 targets require long-term R&D using multiple technologies, with detailed characterisation to verify, and are also referred to as “high-specification targets”.

The total number of targets supplied to target areas at RAL by the Group this reporting year is 2088, 972 for Vulcan and 1116 for Gemini. This reporting year saw greater complexity of requirements, with fewer low-complexity thick-foil targets produced and multiple experiments requiring low-quantity, high-complexity targets. The number of high specification targets increased to 323 from 119 last reporting year and 98 in 2016-2017.

Experiment		Total Targets Produced	Class 1	Class 2	Class 3
VULCAN	0418 TAW	44	8		36
	0718 TAW	21	10		11
	0818 TAP	141	57	84	
	1118 TAW	93	93		
	1118 TAP	123	67	56	
	0119 TAW	321	231		86
	0319 TAW	229	39		190
	Total	972	505	140	323
GEMINI	0818 GTA	1116	1116		
	Total	1116			

Table 1: Targets produced by experiment and their relative complexity, with Class 1 being ‘standard’ targets and Class 3 requiring the most resources

2) Experimental Response

It is seen as a significant strength of Target Fabrication to be rapidly responsive to experimental results and conditions by working collaboratively with user groups. The Group responds to experimental changes during a campaign, and often implements a number of modifications or redesigns to the original requests. The number of modifications and variations on each experiment differs and is dependent on the type of experiment and also on external conditions, such as diagnostic and laser performance.

Target Fabrication’s Quality Management System (QMS) ensures that there is tracking of all targets that are modified in some way from the initial design. These are targets that were delivered, but were not initially defined on the approved target list: this includes modifications to approved designs or completely new requests during the campaign. It is important to note this capability to change designs can often ensure experimental success. For the reporting year the data on modified targets is shown in Chart 1.

Chart 1 shows that this reporting year had far fewer modified requests compared to previous years; good evidence that the experiments in this reporting year ran more-or-less to plan. As mentioned in the operational statistics for last year, there were four experiments that involved drastic changes early in the period and required >60% modifications. The reduction in modifications compared to previous years can be explained by the number of experiments that had high levels of complexity and therefore flexibility was impractical.

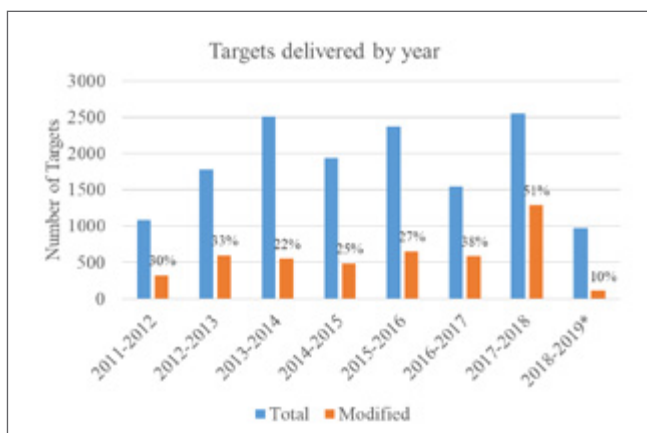


Chart 1: Total targets delivered by year, with the percentage of those that were modified from initial agreed deliverables. This reporting year only Vulcan targets are included. For Gemini, no modifications were required to the 1116 targets delivered. Modified targets include any target that did not appear on the agreed target list.

3) Target Categories

Targets can be separated into seven main categories as shown in Table 2 and Chart 2.

Ultra-thin foil targets are specified as having a thickness <500 nm, and require a coating capability and a skilled fabricator to process; thick foils make up the rest of single component foils. Multilayer foils are stacks or layers of foils that require thin film coating capability to deposit multiple layers onto an existing foil; they are often different composition layers with different thicknesses. Alignment targets are specified as wires or pinholes that are used for set-up purposes. 3D micro-structures are complex 3D geometries that combine multiple fabrication techniques with skilled assembly.

In contrast to last year, this year had more high-complexity experiments. Demand for targets requiring coating capability has remained consistently high throughout the previous five years.

It should be noted that Chart 2 is not a reflection of staff effort, because assembly time for a single thick foil target is relatively short, whereas for a batch of 3D targets, trials, manufacture and characterisation activities can amount to weeks of effort.

Target Category	2018-2019	2017-2018	2016-2017	2015-2016	2014-2015
Ultra-thin Foil	104	485	449	197	530
Thick Foils	438	1208	743	1349	708
Multi-layered Foils	38	577	237	605	500
Alignment	66	159	78	110	85
3D Micro-structures	229	73	38	99	82
Foam/Mass-limited	10	47	0	11	0
TOTAL (Vulcan)	972*	2551	1546	2371	1937

Table 2: Target type by year. *Only Vulcan targets are recorded in this total. Gemini targets totalled 1116, all of which were ultra-thin foils.

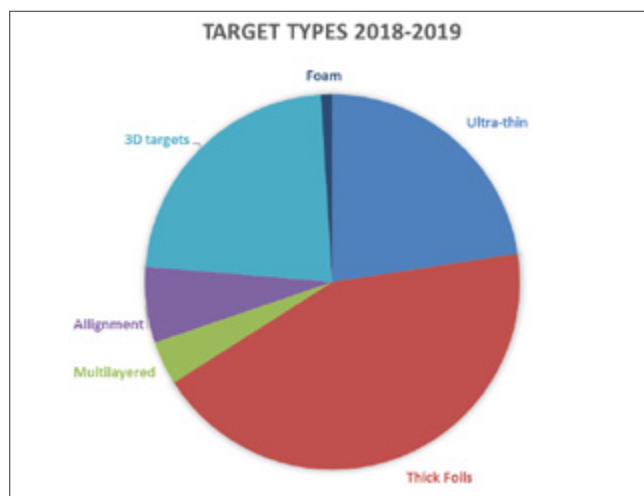


Chart 2: Target types for 2018-2019 delivered to Vulcan

4) Adapting to Demand

Experiments usually require similar targets with varying thickness, composition or geometry; for example, a thin foil experiment typically requests a thickness scan of a particular material. In such experiments, each thickness or composition change requires a separate thin-film coating run. Experiments using 3D targets are such that each geometry change requires a new assembly set up. Each new target thickness or geometry is designated a unique target variation.

This reporting period, within the total of 972 targets for Vulcan, there were 220 unique target variations, which averages around five targets per variation. Last reporting year the average number of targets per variation was around 7; a similar average to the two previous years. The number of target variations is a good measure of how complex an experiment is: for example, the 0119 TAW Neely experiment had one target variation accounting for over 60 targets and was therefore a relatively low complexity experiment; the 0418 TAW Read experiment had only 44 targets delivered and averaged two targets per variation, a good example of a low total number of targets but high effort experiment. The flexibility provided by the Group to provide such variability is a key capability of the CLF and enables the user community to fully utilize the limited time that is available during each experiment.

5) Waste Reduction

Unexpected delays or changes during an experiment often result in a number of targets that have been fabricated but that are not used by the end of experimental campaign. Un-shot targets in this reporting period totalled 114, accounting for 10% of the total targets made. The comparison with previous years can be seen in Chart 3 below. A value of 10% is considered an acceptable amount of surplus manufacture: the nature of experiments means that complications are hard to anticipate and the number of targets requested is based on a best-case scenario.

Any un-issued or returned targets are carefully sorted, and high specification targets are stored under closely controlled conditions for potential use on future experiments. Where possible, all spare target components and mounts are also stored for future use. The variety of mounts and components held in stock contributes to the Group's ability to adapt target

designs quickly in response to experimental changes. Target Fabrication also continued to use its new 3D printing capability to manufacture the majority of target posts, both reducing costs and improving adaptability and responsiveness.

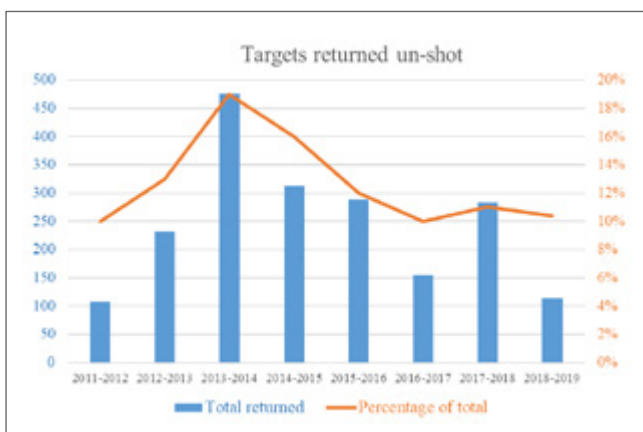


Chart 3: Total number of targets returned un-shot in blue. The orange line shows the returned targets as a percentage of total targets delivered in that reporting year.

There has been a noticeable reduction in waste since the implementation of the ISO9001 QMS, which has allowed the Target Fabrication Group to plan experimental delivery of targets in a more structured way. The improved planning processes enable long-term delivery projects to be managed effectively. It should be noted that this has not led to less flexibility, as the percentage of modified and re-designed targets is in line with the figures for before QMS implementation (2009-2010, 2010-2011).

Only 0.6% of targets were returned as non-conforming under the QMS, compared to 1% last reporting period, and 3% the preceding year. It should be noted that accurate reporting is difficult, because these are often just captured as “returned un-shot”. Work is ongoing to ensure user groups record targets that do not meet their requirements as “non-conforming”, rather than simply requesting additional targets. Over the last year, Target Fabrication has made a concerted effort to ask user groups to record non-conformities, but this did not translate into any more being recorded. Based on these results, it is possible that the non-conformity and returned un-shot numbers are truly representative, and that users are simply overestimating the number of shots and requesting too many targets. Targets that do not meet specifications are vetted as part of the manufacturing process and are simply not delivered.

Orion Academic Access

The Target Fabrication Group has continued to support and supply targets to the Orion Academic Access campaign. In the reporting year, targets were delivered to an experiment led by Queen’s University Belfast investigating ion and neutron beam production. This experiment used a combination of ultra-thin foils and complex coil targets that required a large amount of fabrication time and effort. A final total of 64 complex targets were delivered and a number of targets were made during the experimental run, which added resource demand on the programme. The targets required the integration of a range of complex assembly and characterisation capabilities across

STFC, including collaboration with the Technology Department for the manufacture of precision coils and Scitech Precision Ltd for the laser machining of target components.

External Contracts

Scitech Precision Ltd (a spinout company from the Central Laser Facility) provides high power laser targets and micro engineering solutions to the high power laser community and supplies targets, specialist coatings, laser machining services and consultancy across the world. In the year 2018-2019, a total of 35 unique customers were supplied with 126 contracts. Of these contracts, 58% were for high power laser targets, 34% for laser micromachining, 7% for phase plates, and 1% for MEMS based contracts (not target related). The spread of contracts is similar to the previous year, with approximately one-third of the business being laser machining support for the Harwell Campus, including Diamond Light Source, and a number of spin out and spin in companies. Target contracts were delivered to large scales facilities including experiments carried out on the Orion laser at AWE, LMJ in France, SG-II in China and LLE in the US.

Summary

Target Fabrication has supported eight experiments in the CLF and 12 in other international facilities in the last year, as well as providing an increasing amount of characterisation services and acting as a knowledge base for target fabrication activities throughout Europe.

The total number of targets delivered was fewer than the previous three reporting years, largely due to this year containing multiple high-complexity experiments. This year has seen three-times the number of high-specification targets delivered compared to last year. The average number of target iterations further showed how complex this year’s delivery was, with around five targets per variation.

The number of modifications to target requests was at an encouraging level; 5% compared to 50% last year.

Demand for thin-films requiring coating plant capability was slightly lower than last reporting year, but has remained relatively high showing that coatings are a key capability for the facility.

References

1. D. Haddock, C. Spindloe & M. Tolley, Target Fabrication Operational Statistics, CLF Annual Report 2017-2018, p45-48
2. D. Haddock, C. Spindloe & M. Tolley, Target Fabrication Operational Statistics, CLF Annual Report 2016-2017, p48-50
3. D. Haddock, C. Spindloe & M. Tolley, Target Fabrication Operational Statistics, CLF Annual Report 2015-2016, p49-51
4. D. Haddock, C. Spindloe & M. Tolley, Target Fabrication Operational Statistics, CLF Annual Report 2014-2015, p58-60
5. D. Haddock, C. Spindloe & M. Tolley, Target Fabrication Operational Statistics, CLF Annual Report 2013-2014, p68-70
6. D. Haddock, C. Spindloe & M. Tolley, Target Fabrication Operational Statistics, CLF Annual Report 2012-2013, p74-75
7. D. Haddock, C. Spindloe & M. Tolley, Target Fabrication Operational Statistics, CLF Annual Report 2011-2012, p71-72
8. H.F. Lowe, C. Spindloe & M. Tolley, Target Fabrication Operational Statistics, CLF Annual Report 2010-2011, p76-77
9. H.F. Lowe, C. Spindloe & M. Tolley, Target Fabrication Operational Statistics, CLF Annual Report 2009-2010, p55-56

Contact: D. Haddock (david.haddock@stfc.ac.uk)

Vulcan Operational Statistics

AK Kidd and P Oliveira (Central Laser Facility, STFC Rutherford Appleton Laboratory, Harwell Campus, Didcot, UK)

Introduction

Vulcan has completed an active experimental year, with 35 full experimental weeks allocated to target areas TAW and TAP between April 2018 and March 2019.

Table 1 shows the operational schedule for the year, and reports the shot rate statistics for each experiment.

Numbers in parentheses indicate the total number of full energy laser shots delivered to target, followed by the number of these that failed and the percentage of successful shots. The second set of numbers shows the availability of the laser to target areas during normal operating hours and including outside hours operations.

PERIOD	TAW	TAP
2018		
16 Apr – 20 May	<p>M Read</p> <p><i>An all-optical platform for magnetized high energy density physics research</i></p> <p>(37, 11, 70.3%)</p> <p>(86.5%, 99.3%)</p> <p>(5 weeks)</p>	
23 Jul – 30 Sep	<p>Z Najmudin</p> <p><i>Development of a bright betatron backlighter for Vulcan Target Area West</i></p> <p>(87, 14, 83.9%)</p> <p>65.4%, 105.6%)</p> <p>(6 weeks + 2 weeks, 2 days overrun)</p>	
03 Sep – 21 Oct		<p>D Margarone</p> <p><i>Brilliant, fast neutron source employing cryogenic ribbons of solid deuterium</i></p> <p>(86, 10, 88.4%)</p> <p>(91.0%, 139.7%)</p> <p>(5 weeks + 1 week overrun)</p>
12/05 Nov – 09 Dec	<p>L Gizzi</p> <p>Role of laser plasma interactions in the shock ignition regime</p> <p>(48, 18, 62.5%)</p> <p>(86.5%, 114.6%)</p> <p>(4 weeks + 3 day overrun (Sat,Sun,Mon))</p>	<p>G Hicks (McKenna)</p> <p><i>Laser-solid interaction physics at intensities up to 1022W/cm2 and tight focusing conditions</i></p> <p>(73, 13, 82.2%)</p> <p>(85.2%, 96.5%)</p> <p>(5 weeks)</p>
2019		
14 Jan – 17 Feb	<p>D Neely</p> <p><i>Intense THz field-driven lattice dynamics probed with ultrafast X-ray diffraction</i></p> <p>(125, 28, 77.6%)</p> <p>(86.3%, 109.9%)</p> <p>(5 weeks + Saturday overrun)</p>	
04 Mar – 07 Apr	<p>S Kar</p> <p><i>All-optical staged acceleration of proton beams using helical coils</i></p> <p>(151, 19, 80.8%)</p> <p>(85.7%, 109.3%)</p> <p>(5 weeks)</p>	

Table 1: Experimental schedule for the period April 2018 – March 2019

(Total shots fired, failed shots, reliability)
(Availability normal, additional hours)

The total number of full disc amplifier shots that have been fired to target this year is 607. Table 2 shows that this figure is less than in the four previous years. 113 shots failed to meet user requirements. The overall shot success rate to target for the year is 81%, compared to 88%, 91%, 90% and 86% in the previous four years. Figure 1 shows the reliability of the Vulcan laser to all target areas over the past five years.

	No of shots	Failed shots	Reliability
14-15	1087	133	88%
15-16	1143	108	91%
16-17	948	93	90%
17-18	934	132	86%
18-19	607	113	81%

Table 2: Shot totals and proportion of failed shots for the past five years

The shot reliability to TAW is 80%, down 3% from the previous year. The shot reliability to TAP is 86% - down from 92% in 2017-18.

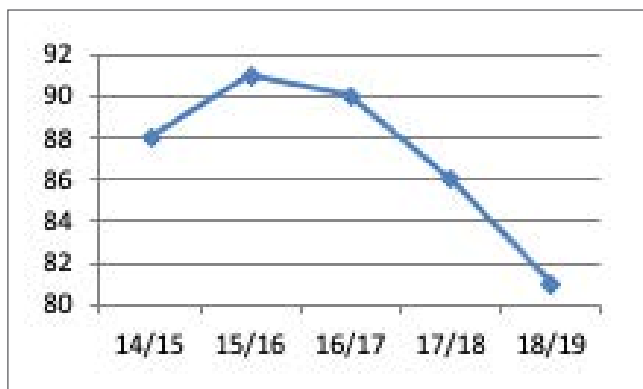


Figure 1: All areas shot reliability for each year 2014-15 to 2018-19.

Analysis of the failure modes reveals that, as in recent years, the two overriding causes of failed shots are beam alignment and front end related issues. These two causes are manifested in low or high energy output of the rod amplifier chain (outside of +/-20% of the requested energy). Approximately three-quarters of failed shots are due to this cause. Investigation into the reasons for this instability have revealed the following :

1. Instability in the pulse energy is introduced during propagation from the front end room to the laser area
2. There is a discrepancy in the pulse energy measured at the end of the rod chain during a test (rod chain) shot and a full energy (disc amplifier) shot.

Instability is particularly evident in the short pulse beamlines to TAW (seeded by the Insight laser). Additional measures are being taken to improve stability including installing diagnostics to monitor stability - specifically additional near- and far-field cameras - securing of optics and testing a fast beam stabilization scheme.

There is a requirement which was originally instigated for the EPSRC FAA that the laser system be available, during the five week periods of experimental data collection, from 09:00 to 17:00 hours, Monday to Thursday, and from 09:00 to 16:00 hours on Fridays (a total of 195 hours over the five week experimental period). The laser has not always met the startup target of 9:00 am but it has been common practice to operate the laser well beyond the standard contracted finish time on several days during the week. In addition, the introduction of early start times on some experiments continues to lead to improvements in availability.

On average, Vulcan has been available for each experiment to target areas for 85.1% of the time during contracted hours, compared with 77.2% for the previous year. Although this figure is a considerable improvement, the overall availability to all target areas has only slightly increased from 111.5% in 2017-18 to 112.9%. The time that the laser is unavailable to users is primarily the time taken for beam alignment at the start of the day.

Publications

Journal Papers

ARTEMIS

AD Smith, EM Warne, D Bellshaw, DA Horke, M Tudorovskya, E Springate, AJ Jones, C Cacho, RT Chapman, A Kirrander, RS Minns

Mapping the Complete Reaction Path of a Complex Photochemical Reaction

PHYSICAL REVIEW LETTERS, 120, 183003 (2018)

M Battiato, J Minar, W Wang, W Ndiaye, M Richter, O Heckmann, J Mariot, F Parmigiani, K Hricovini, C Cacho
Distinctive Picosecond Spin Polarization Dynamics in Bulk Half Metals

PHYSICAL REVIEW LETTERS, 121, 77205 (2018)

CALTA

P Mason, S Banerjee, J Smith, T Butcher, J Phillips, H Höppner, D Möller, K Ertel, M De Vido, I Hollingham, A Norton, S Tomlinson, T Zata, J Suarez Merchan, C Hooker, M Tyldesley, T Toncian, C Hernandez-Gomez, C Edwards, J Collier

Development of a 100 J, 10 Hz laser for compression experiments at the High Energy Density instrument at the European XFEL

HIGH POWER LASER SCIENCE AND ENGINEERING, 6, e65 (2018)

GEMINI

J Warwick, A Alejo, T Dzelzainis, W Schumaker, D Doria, L Romagnani, K Poder, J Cole, M Yeung, K Krushelnick, S Mangles, Z Najmudin, G Samarin, D Symes, A Thomas, M Borghesi, G Sarri

General features of experiments on the dynamics of laser-driven electron-positron beams

NUCLEAR INSTRUMENTS AND METHODS IN PHYSICS RESEARCH SECTION A ACCELERATORS SPECTROMETERS DETECTORS AND ASSOCIATED EQUIPMENT, 909, 95-101 (2018)

M Streeter, S Kneip, M Bloom, R Bendoyro, O Chekhlov, A Dangor, A Döpp, C Hooker, J Holloway, J Jiang, N Lopes, H Nakamura, P Norreys, C Palmer, P Rajeev, J Schreiber, D Symes, M Wing, S Mangles, Z Najmudin
Observation of Laser Power Amplification in a Self-Injecting Laser Wakefield Accelerator

PHYSICAL REVIEW LETTERS, 120, 254801 (2018)

K Poder, M Tamburini, G Sarri, A Di Piazza, S Kuschel, C Baird, K Behm, S Bohlen, J Cole, D Corvan, M Duff, E Gerstmayr, C Keitel, K Krushelnick, S Mangles, P McKenna, C Murphy, Z Najmudin, C Ridgers, G Samarin, D Symes, A Thomas, J Warwick, M Zepf

Experimental Signatures of the Quantum Nature of Radiation Reaction in the Field of an Ultraintense Laser

PHYSICAL REVIEW X, 8, 31004 (2018)

JM Cole, DR Symes, NC Lopes, JC Wood, K Poder, S Alatabi, SW Botchway, PS Foster, S Gratton, S Johnson, C Kamperidis, O Kononenko, M De Lazzari, CAJ Palmer, D Rusby, J Sanderson, M Sandholzer, G Sarri, Z Szoke-Kovacs, L Teboul, JM Thompson, JR Warwick, H Westerberg, MA Hill, DP Norris, SPD Mangles, Z Najmudin

High-resolution mu CT of a mouse embryo using a compact laser-driven X-ray betatron source

PROCEEDINGS OF THE NATIONAL ACADEMY OF SCIENCES USA, 115, 6335-6340 (2018)

KT Behm, JM Cole, AS Joglekar, E Gerstmayr, JC Wood, CD Baird, TG Blackburn, M Duff, C Harvey, A Ilderton, S Kuschel, SPD Mangles, M Marklund, P McKenna, CD Murphy, Z Najmudin, K Poder, CP Ridgers, G Sarri, GM Samarin, D Symes, J Warwick, M Zepf, K Krushelnick, AGR Thomas

A spectrometer for ultrashort gamma-ray pulses with photon energies greater than 10 MeV

REVIEW OF SCIENTIFIC INSTRUMENTS, 89, 113303 (2018)

JC Wood, DJ Chapman, K Poder, NC Lopes, ME Rutherford, TG White, F Albert, KT Behm, N Booth, JSJ Bryant, PS Foster, S Glenzer, E Hill, K Krushelnick, Z Najmudin, BB Pollock, S Rose, W Schumaker, RHH Scott, M Sherlock, AGR Thomas, Z Zhao, DE Eakins, SPD Mangles
Ultrafast Imaging of Laser Driven Shock Waves using Betatron X-rays from a Laser Wakefield Accelerator

SCIENTIFIC REPORTS, 8, 11010 (2018)

AE Hussein, N Senabulya, Y Ma, MJV Streeter, B Kettle, SJD Dann, F Albert, N Bourgeois, S Cipiccia, JM Cole, O Finlay, E Gerstmayr, IG González, A Higginbotham, DA Jaroszynski, K Falk, K Krushelnick, N Lemos, NC Lopes, C Lumsdon, O Lundh, SPD Mangles, Z Najmudin, PP Rajeev, CM Schlepütz, M Shahzad, M Smid, R Spesyvtsev, DR Symes, G Vieux, L Willingale, JC Wood, AJ Shahani, AGR Thomas

Laser-wakefield accelerators for high-resolution X-ray imaging of complex microstructures

SCIENTIFIC REPORTS, 9, 3249 (2019)

F Hanton, P Chaudhary, D Doria, D Gwynne, C Maiorino, C Scullion, H Ahmed, T Marshall, K Naughton, L Romagnani, S Kar, G Schettino, P McKenna, S Botchway, DR Symes, PP Rajeev, KM Prise, M Borghesi

DNA DSB Repair Dynamics following Irradiation with Laser-Driven Protons at Ultra-High Dose Rates

SCIENTIFIC REPORTS, 9, 4471 (2019)

N Booth, S Astbury, E Bryce, RJ Clarke, CD Gregory, J Green, D Haddock, RI Heathcote, C Spindloe

Debris studies for high-repetition rate and high-power laser experiments at the Central Laser Facility

PROCEEDINGS OF SPIE, 10763, 107630S (2018)

LASER DEVELOPMENTS

M Galletti, H Pires, V Hariton, CP João, S Künzel, M Galimberti, G Figueira
High efficiency second harmonic generation of nanojoule-level femtosecond pulses in the visible based on BiBO
 HIGH POWER LASER SCIENCE AND ENGINEERING, 7, e11 (2019)

M Galletti, C Coyle, P Oliveira, M Galimberti, F Bisesto, D Giulietti
VULCAN and FLAME ultra-short pulses characterization by GROG algorithm
 JOURNAL OF INSTRUMENTATION, 14, C02005 (2019)

AB Sharba, O Chekhlov, AS Wyatt, R Pattathil, M Borghesi, G Sarri
Characterization of ultrashort laser pulses employing self-phase modulation dispersion-scan technique
 JOURNAL OF OPTICS, 20, 35502 (2018)

G Figueira, L Braga, S Ahmed, A Boyle, M Galimberti, M Galletti, P Oliveira
Simultaneous measurement of pulse front tilt and pulse duration with a double trace autocorrelator
 JOURNAL OF THE OPTICAL SOCIETY OF AMERICA B, 36, 366-373 (2019)

P Oliveira, S Addis, J Gay, K Ertel, M Galimberti, I Musgrave
Control of temporal shape of nanosecond long lasers using feedback loops
 OPTICS EXPRESS, 27, 6607-6617 (2019)

M Galimberti, A Boyle, IO Musgrave, P Oliveira, D Pepler, W Shaikh, TB Winstone, A Wyatt, C Hernandez-Gomez
Spectral gain investigation of large size OPCPA based on partially deuterated KDP
 EPJ WEB OF CONFERENCES, 167, 1006 (2018)

PLASMA PHYSICS

JD Sadler, LO Silva, RA Fonseca, K Glize, MF Kasim, A Savin, R Aboushelbaya, MW Mayr, B Spiers, RHW Wang, R Bingham, RMGM Trines, PA Norreys
Advantages to a diverging Raman amplifier
 COMMUNICATIONS PHYSICS, 1, 19 (2018)

DC Speirs, K Ronald, ADR Phelps, ME Koepke, RA Cairns, A Rigby, F Cruz, RMGM Trines, R Bamford, BJ Kellett, B Albertazzi, JE Cross, F Frascchetti, P Graham, P Kozlowski, Y Kuramitsu, F Miniati, T Morita, M Oliver, B Reville, Y Sakawa, S Sarkar, C Spindloe, M Koenig, L Silva, D Lamb, P Tzeferacos, S Lebedev, G Gregori, R Bingham
Maser radiation from collisionless shocks: application to astrophysical jets
 HIGH POWER LASER SCIENCE AND ENGINEERING, 7, e17 (2019)

D Del Sorbo, DR Blackman, R Capdessus, K Small, C Slade-Lowther, W Luo, MJ Duff, APL Robinson, P McKenna, Z Sheng, J Pasley, CP Ridgers
Efficient ion acceleration and dense electron-positron plasma creation in ultra-high intensity laser-solid interactions
 NEW JOURNAL OF PHYSICS, 20, 33014 (2018)

T Davenne, P Loveridge, R Bingham, J Wark, J Back, O Caretta, C Densham, J O'Dell, D Wilcox, M Fitton
Observed proton beam induced disruption of a tungsten powder sample at CERN
 PHYSICAL REVIEW ACCELERATORS AND BEAMS, 21, 73002 (2018)

L Ceurvorst, A Savin, N Ratan, MF Kasim, J Sadler, PA Norreys, H Habara, KA Tanaka, S Zhang, MS Wei, S Ivancic, DH Froula, W Theobald
Channel optimization of high-intensity laser beams in millimeter-scale plasmas
 PHYSICAL REVIEW E, 97, 43208 (2018)

Y Shi, J Vieira, R Trines, R Bingham, B Shen, R Kingham
Magnetic field generation in plasma waves driven by co-propagating intense twisted lasers
 PHYSICAL REVIEW LETTERS, 121, 145002 (2018)

APL Robinson, J Pasley
Potential for the Vishniac instability in ionizing shock waves propagating into cold gases
 PHYSICS OF PLASMAS, 25, 52701 (2018)

APL Robinson, AV Arefiev
Interaction of an electron with coherent dipole radiation: Role of convergence and anti-dephasing
 PHYSICS OF PLASMAS, 25, 53107 (2018)

M Shaikh, K Jana, AD Lad, I Dey, SL Roy, D Sarkar, YM Ved, APL Robinson, J Pasley, G Ravindra Kumar
Tracking ultrafast dynamics of intense shock generation and breakout at target rear
 PHYSICS OF PLASMAS, 25, 113106 (2018)

Z Gong, APL Robinson, XQ Yan, AV Arefiev
Highly collimated electron acceleration by longitudinal laser fields in a hollow-core target
 PLASMA PHYSICS AND CONTROLLED FUSION, 61, 35012 (2019)

TARGET FABRICATION

F Seiboth, LB Fletcher, D McGonegle, S Anzellini, LE Dresselhaus-Cooper, M Frost, E Galtier, S Goede, M Harmand, HJ Lee, AL Levitan, K Miyanishi, B Nagler, I Nam, N Ozaki, M Rödel, A Schropp, C Spindloe, P Sun, JS Wark, J Hastings, SH Glenzer, EE McBride
Simultaneous 8.2 keV phase-contrast imaging and 24.6 keV X-ray diffraction from shock-compressed matter at the LCLS
APPLIED PHYSICS LETTERS, 112, 221907 (2018)

C Spindloe, Y Fukuda, P Fitzsimmons, K Du, C Danson
Review of HPLSE special issue on target fabrication
HIGH POWER LASER SCIENCE AND ENGINEERING, 6, e13 (2018)

EE McBride, A Krygier, A Ehn, E Galtier, M Harmand, Z Konôpková, HJ Lee, H Liermann, B Nagler, A Pelka, M Rödel, A Schropp, RF Smith, C Spindloe, D Swift, F Tavella, S Toleikis, T Tschentscher, JS Wark, A Higginbotham
Phase transition lowering in dynamically compressed silicon
NATURE PHYSICS, 15, 89-94 (2018)

S Karim, S Piano, R Leach, M Tolley
Error modelling and validation of a high-precision five degree of freedom hybrid mechanism for high-power high-repetition rate laser operations
PRECISION ENGINEERING, 54, 182-197 (2018)

C Atkins, C Feldman, D Brooks, S Watson, W Cochrane, M Roulet, E Hugot, M Beardsley, C Spindloe, S Alcock, I Nistea, C Morawe, F Perrin, M Harris, R Geyl, R Navarro
Topological design of lightweight additively manufactured mirrors for space
PROCEEDINGS OF SPIE, 10706, 107060I (2018)

VULCAN

P Bradford, NC Woolsey, GG Scott, G Liao, H Liu, Y Zhang, B Zhu, C Armstrong, S Astbury, C Brenner, P Brummitt, F Consoli, I East, R Gray, D Haddock, P Huggard, PJR Jones, E Montgomery, I Musgrave, P Oliveira, DR Rusby, C Spindloe, B Summers, E Zemaityte, Z Zhang, Y Li, P McKenna, D Neely
EMP control and characterization on high-power laser systems
HIGH POWER LASER SCIENCE AND ENGINEERING, 6, e21 (2018)

H Liu, G Liao, Y Zhang, B Zhu, Z Zhang, Y Li, GG Scott, D Rusby, C Armstrong, E Zemaityte, P Bradford, N Woolsey, P Huggard, P McKenna, D Neely
Study of backward terahertz radiation from intense picosecond laser-solid interactions using a multichannel calorimeter system
HIGH POWER LASER SCIENCE AND ENGINEERING, 7, e6 (2019)

M King, NMH Butler, R Wilson, R Capdessus, RJ Gray, HW Powell, RJ Dance, H Padda, B Gonzalez-Izquierdo, DR Rusby, NP Dover, GS Hicks, OC Ettlinger, C Scullion, DC Carroll, Z Najmudin, M Borghesi, D Neely, P McKenna
Role of magnetic field evolution on filamentary structure formation in intense laser-foil interactions
HIGH POWER LASER SCIENCE AND ENGINEERING, 7, e14 (2019)

M Manuel, J Strehlow, J Green, D Parker, E Alfonso, J Jaquez, L Carlson, D Neely, F Beg, T Ma
Intrinsic resolution limits of monolithic organic scintillators for use in rep-rated proton imaging
NUCLEAR INSTRUMENTS AND METHODS IN PHYSICS RESEARCH SECTION A ACCELERATORS SPECTROMETERS DETECTORS AND ASSOCIATED EQUIPMENT, 913, 103-106 (2019)

ZE Davidson, B Gonzalez-Izquierdo, A Higginson, KL Lancaster, SDR Williamson, M King, D Farley, D Neely, P McKenna, RJ Gray
An optically multiplexed single-shot time-resolved probe of laser-plasma dynamics
OPTICS EXPRESS, 27, 4416-4423 (2019)

IY Skobelev, SN Ryazantsev, DD Arich, PS Bratchenko, AY Faenov, TA Pikuz, P Durey, L Doehl, D Farley, CD Baird, KL Lancaster, CD Murphy, N Booth, C Spindloe, P McKenna, SB Hansen, J Colgan, R Kodama, N Woolsey, SA Pikuz
X-ray absorption spectroscopy study of energy transport in foil targets heated by petawatt laser pulses
PHOTONICS RESEARCH, 6, 234-237 (2018)

G Scott, D Carroll, S Astbury, R Clarke, C Hernandez-Gomez, M King, A Alejo, I Arteaga, R Dance, A Higginson, S Hook, G Liao, H Liu, S Mirfayzi, D Rusby, M Selwood, C Spindloe, M Tolley, F Wagner, E Zemaityte, M Borghesi, S Kar, Y Li, M Roth, P McKenna, D Neely
Dual ion species plasma expansion from isotopically layered cryogenic targets
PHYSICAL REVIEW LETTERS, 120, 204801 (2018)

L Romagnani, A Robinson, R Clarke, D Doria, L Lancia, W Nazarov, M Notley, A Pipahl, K Quinn, B Ramakrishna, P Wilson, J Fuchs, O Willi, M Borghesi
Dynamics of the Electromagnetic Fields Induced by Fast Electron Propagation in Near-Solid-Density Media
PHYSICAL REVIEW LETTERS, 122, 25001 (2019)

C Armstrong, CM Brenner, E Zemaityte, GG Scott, D Rusby, G Liao, H Liu, Y Li, Z Zhang, Y Zhang, B Zhu, P Bradford, N Woolsey, P Oliveira, C Spindloe, W Wang, P McKenna, D Neely
Bremsstrahlung emission profile from intense laser-solid interactions as a function of laser focal spot size
PLASMA PHYSICS AND CONTROLLED FUSION, 61, 34001 (2018)

G Liao, Y Li, H Liu, GG Scott, D Neely, Y Zhang, B Zhu, Z Zhang, C Armstrong, E Zemaityte, P Bradford, PG Huggard, DR Rusby, P McKenna, CM Brenner, NC Woolsey, W Wang, Z Sheng, J Zhang
Multimillijoule coherent terahertz bursts from picosecond laser-irradiated metal foils
 PROCEEDINGS OF THE NATIONAL ACADEMY OF SCIENCES USA, **116**, 201815256 (2019)

DR Rusby, CD Armstrong, CM Brenner, RJ Clarke, P McKenna, D Neely
Novel scintillator-based x-ray spectrometer for use on high repetition laser plasma interaction experiments
 REVIEW OF SCIENTIFIC INSTRUMENTS, **89**, 73502 (2018)

H Liu, G Liao, Y Zhang, B Zhu, Z Zhang, Y Li, GG Scott, DR Rusby, C Armstrong, E Zemaityte, DC Carroll, S Astbury, P Bradford, NC Woolsey, P McKenna, D Neely
Cherenkov radiation-based optical fibre diagnostics of fast electrons generated in intense laser-plasma interactions
 REVIEW OF SCIENTIFIC INSTRUMENTS, **89**, 83302 (2018)

R Aboushelbaya, AF Savin, L Ceurvorst, J Sadler, PA Norreys, AS Davies, DH Froula, A Boyle, M Galimberti, P Oliveira, B Parry, Y Katzir, K Glize
Single-shot frequency-resolved optical gating for retrieving the pulse shape of high energy picosecond pulses
 REVIEW OF SCIENTIFIC INSTRUMENTS, **89**, 103509 (2018)

RI Heathcote, N Booth, RJ Clarke, A Anderson-Asubonteng, MP Selwood, C Spindloe
Coded aperture x-ray imaging of high power laser-plasma interactions on the Vulcan Laser System
 PROCEEDINGS OF SPIE, **10763**, 107630U (2018)

AY Faenov, J Colgan, SA Pikuz, A Zhidkov, TA Pikuz, J Abdallah, E Tubman, NMH Butler, RJ Dance, IY Skobelev, MZ Alkhimova, N Booth, J Green, C Gregory, A Andreev, M Nishiuchi, H Sakaki, A Sagisaka, AS Pirozhkov, K Ogura, Y Fukuda, M Kanasaki, N Hasegawa, M Nishikino, M Kando, T Kawachi, K Kondo, P McKenna, GJ Tallents, N Woolsey, R Kodama
Ultra-intense X-Ray Radiation Photopumping of Exotic States of Matter by Relativistic Laser-Plasma in the Radiation-Dominated Kinetic Regime
 X-RAY LASERS 2016, 149-158 (2018)

T Robinson, S Giltrap, S Eardley, F Consoli, R De Angelis, F Ingenito, N Stuart, C Verona, RA Smith
Electro-optic analysis of the influence of target geometry on electromagnetic pulses generated by petawatt laser-matter interactions
 EPJ WEB OF CONFERENCES, **167**, 3007 (2018)

ULTRA

K Takematsu, HR Williamson, P Nikolovski, JT Kaiser, Y Sheng, P Pospíšil, M Towrie, J Heyda, D Hollas, S Záliš, HB Gray, A Vlček, JR Winkler
Two Tryptophans Are Better Than One in Accelerating Electron Flow through a Protein
 ACS CENTRAL SCIENCE, **5**, 192-200 (2019)

CLA Leung, S Marussi, M Towrie, RC Atwood, PJ Withers, PD Lee
The effect of powder oxidation on defect formation in laser additive manufacturing
 ACTA MATERIALIA, **166**, 294-305 (2019)

CLA Leung, S Marussi, M Towrie, J del Val Garcia, RC Atwood, AJ Bodey, JR Jones, PJ Withers, PD Lee
Laser-matter interactions in additive manufacturing of stainless steel SS316L and 13-93 bioactive glass revealed by in situ X-ray imaging
 ADDITIVE MANUFACTURING, **24**, 647-657 (2018)

N Scrutton, U Choudry, D Heyes, S Hardman, M Sakuma, I Sazanovich, J Woodhouse, E De La Mora, M Pederson, M Wulff, M Weik, G Schiro
Photochemical mechanism of an atypical algal phytochrome
 CHEMBIOCHEM, **9**, 1036-1043 (2018)

MW Hanson-Heine, JA Calladine, J Yang, M Towrie, R Horvath, NA Besley, MW George
A Combined Time-Resolved Infrared and Density Functional Theory Study of the Lowest Excited States of 9-Fluorenone and 2-Naphthaldehyde
 CHEMICAL PHYSICS, **512**, 44-52 (2018)

Y Xiong, AV Jentsch, JWM Osterrieth, E Sezgin, IV Sazanovich, K Reglinski, S Galiani, AW Parker, C Eggeling, HL Anderson
Correction: Spironaphthoxazine switchable dyes for biological imaging
 CHEMICAL SCIENCE, **9**, 3892- (2018)

FA Black, A Jacquart, G Toupalas, S Alves, A Proust, IP Clark, EA Gibson, G Izzet
Rapid photoinduced charge injection into covalent polyoxometalate-bodipy conjugates
 CHEMICAL SCIENCE, **9**, 5578-5584 (2018)

N Pöldme, L O'Reilly, I Fletcher, J Portoles, IV Sazanovich, M Towrie, C Long, JG Vos, MT Pryce, EA Gibson
Photoelectrocatalytic H₂ evolution from integrated photocatalysts adsorbed on NiO
 CHEMICAL SCIENCE, **10**, 99-112 (2019)

PM Keane, J Tory, M Towrie, IV Sazanovich, CJ Cardin, SJ Quinn, F Hartl, JM Kelly, C Long
Spectro-electrochemical Studies on [Ru(TAP)₂(dppz)]²⁺— Insights into the Mechanism of its Photosensitized Oxidation of Oligonucleotides
 INORGANIC CHEMISTRY, **58**, 663-671 (2018)

AM Brown, CE McCusker, MC Carey, AM Blanco-Rodríguez, M Towrie, IP Clark, A Vlček, JK McCusker
Vibrational Relaxation and Redistribution Dynamics in Ruthenium(II) Polypyridyl-Based Charge-Transfer Excited States: A Combined Ultrafast Electronic and Infrared Absorption Study
 JOURNAL OF PHYSICAL CHEMISTRY A, **122**, 7941-7953 (2018)

K Takematsu, P Pospíšil, M Pižl, M Towrie, J Heyda, S Záliš, JT Kaiser, JR Winkler, HB Gray, A Vlček
Hole Hopping Across a Protein-Protein Interface
 JOURNAL OF PHYSICAL CHEMISTRY B, **123**, 1578-1591 (2019)

K Sowoidnich, M Towrie, P Matousek
Lock-in detection in Raman spectroscopy with charge-shifting CCD for suppression of fast varying backgrounds
 JOURNAL OF RAMAN SPECTROSCOPY, **50**, jrs.5597 (2019)

LA Hammarback, IP Clark, IV Sazanovich, M Towrie, A Robinson, F Clarke, S Meyer, IJS Fairlamb, JM Lynam
Mapping out the key carbon-carbon bond-forming steps in Mn-catalysed C-H functionalization
 NATURE CATALYSIS, **1**, 830-840 (2018)

G Neri, JJ Walsh, G Teobaldi, PM Donaldson, AJ Cowan
Detection of catalytic intermediates at an electrode surface during carbon dioxide reduction by an earth-abundant catalyst
 NATURE CATALYSIS, **1**, 952-959 (2018)

SP Laptinok, AA Gil, CR Hall, A Lukacs, JN Iuliano, GA Jones, GM Greetham, P Donaldson, A Miyawaki, PJ Tonge, SR Meech
Infrared spectroscopy reveals multi-step multi-timescale photoactivation in the photoconvertible protein archetype *dronpa*
 NATURE CHEMISTRY, **10**, 845-852 (2018)

CLA Leung, S Marussi, RC Atwood, M Towrie, PJ Withers, PD Lee
In situ X-ray imaging of defect and molten pool dynamics in laser additive manufacturing
 NATURE COMMUNICATIONS, **9**, 1355 (2018)

G Neri, PM Donaldson, AJ Cowan
In situ study of the low overpotential "dimer pathway" for electrocatalytic carbon dioxide reduction by manganese carbonyl complexes
 PHYSICAL CHEMISTRY CHEMICAL PHYSICS, **21**, 7389-7397 (2019)

PA Summers, BS Adams, N Ibrahim, KE Reynolds, KL Fow, ES Davies, M Towrie, MW George
Photophysical and electrochemical properties of [ReCl] complexes functionalised with pendant pyridyl ligands
 VIBRATIONAL SPECTROSCOPY, **100**, 86-92 (2019)

OCTOPUS

PJ Gallimore, NM Davidson, M Kalberer, FD Pope, AD Ward
1064 nm Dispersive Raman Microspectroscopy and Optical Trapping of Pharmaceutical Aerosols
 ANALYTICAL CHEMISTRY, **90**, 8838-8844 (2018)

G Marucci, A Beeby, AW Parker, CE Nicholson
Raman spectroscopic library of medieval pigments collected with five different wavelengths for investigation of illuminated manuscripts
 ANALYTICAL METHODS, **10**, 1219-1236 (2018)

RH Shepherd, MD King, AA Marks, N Brough, AD Ward
Determination of the refractive index of insoluble organic extracts from atmospheric aerosol over the visible wavelength range using optical tweezers
 ATMOSPHERIC CHEMISTRY AND PHYSICS, **18**, 5235-5252 (2018)

GL Fisher, BC Bateman, TD Craggs, MS Dillingham
The Conformational Landscape of SMC: A FRET Study
 BIOPHYSICAL JOURNAL, **114**, 209a- (2018)

S Roberts, M Hirsch, A McStea, L Zanetti Domingues, D Clarke, J Claus, P Parker, L Wang, M Martin-Fernandez
Cluster Analysis of Endogenous HER2 and HER3 Receptors in SKBR3 Cells
 BIO-PROTOCOL, **8**, e3096 (2018)

D Gutowska-Owsiak, J Bernardino de La Serna, M Fritzsche, A Naeem, EI Podobas, M Leeming, H Colin-York, R O'Shaughnessy, C Eggeling, GS Ogg
Orchestrated control of filaggrin-actin scaffolds underpins cornification
 CELL DEATH & DISEASE, **9**, 412 (2018)

M Lledos, V Mirabello, S Sarpaki, H Ge, HJ Smugowski, L Carroll, EO Aboagye, FI Aigbirhio, SW Botchway, JR Dilworth, DG Calatayud, PK Plucinski, GJ Price, SI Pasqu
Synthesis, Radiolabelling and In Vitro Imaging of Multifunctional Nanoceramics
 CHEMNANOMAT, **4**, 361-372 (2018)

L Wang, B Bateman, LC Zanetti Domingues, AN Moores, S Astbury, C Spindloe, MC Darrow, M Romano, SR Needham, K Beis, DJ Rolfe, DT Clarke, ML Martin-Fernandez
Solid immersion microscopy images cells under cryogenic conditions with 12 nm resolution
 COMMUNICATIONS BIOLOGY, **2**, 74 (2019)

J Claus, G Patel, F Autore, A Colomba, G Weitsman, TN Soliman, S Roberts, LC Zanetti-Domingues, M Hirsch, F Collu, R George, E Ortiz-Zapater, PR Barber, B Vojnovic, Y Yarden, ML Martin-Fernandez, A Cameron, F Fraternali, T Ng, PJ Parker

Inhibitor-induced HER2-HER3 heterodimerisation promotes proliferation through a novel dimer interface
eLIFE, **7**, e32271 (2018)

A Artesani, M Ghirardello, S Mosca, A Nevin, G Valentini, D Comelli

Combined photoluminescence and Raman microscopy for the identification of modern pigments: explanatory examples on cross-sections from Russian avant-garde paintings
HERITAGE SCIENCE, **7**, 17 (2019)

SM King, S Claire, RI Teixeira, AN Dosumu, AJ Carrod, H Dehghani, MJ Hannon, AD Ward, R Bicknell, SW Botchway, NJ Hodges, Z Pikramenou

Iridium nanoparticles for multichannel luminescence lifetime imaging, mapping localization in live cancer cells
JOURNAL OF THE AMERICAN CHEMICAL SOCIETY, **140**, 10242-10249 (2018)

J Owen, S Kamila, S Shrivastava, D Carugo, J Bernardino de la Serna, C Mannaris, V Pereno, R Browning, E Beguin, AP McHale, JF Callan, E Stride

The Role of PEG-40-stearate in the Production, Morphology, and Stability of Microbubbles
LANGMUIR, **35**, 10014-10024 (2018)

DT Clarke, ML Martin-Fernandez

A Brief History of Single-Particle Tracking of the Epidermal Growth Factor Receptor
METHODS AND PROTOCOLS, **2**, 12 (2019)

F Schneider, D Waithe, S Galiani, J Bernardino de la Serna, E Sezgin, C Eggeling

Nanoscale Spatiotemporal Diffusion Modes Measured by Simultaneous Confocal and Stimulated Emission Depletion Nanoscopy Imaging
NANO LETTERS, **18**, 4233-4240 (2018)

LC Zanetti Domingues, D Korovesis, SR Needham, CJ Tynan, S Sagawa, SK Roberts, A Kuzmanic, E Ortiz-Zapater, P Jain, RC Roovers, A Lajevardipour, PMP van Bergen en Henegouwen, G Santis, AHA Clayton, DT Clarke, FL Gervasio, Y Shan, DE Shaw, DJ Rolfe, PJ Parker, ML Martin-Fernandez

The architecture of EGFR's basal complexes reveals autoinhibition mechanisms in dimers and oligomers
NATURE COMMUNICATIONS, **9**, 4325 (2018)

M Compte, SL Harwood, IG Muñoz, R Navarro, M Zonca, G Perez-Chacon, A Erce-Llamazares, N Merino, A Tapia-Galisteo, AM Cuesta, K Mikkelsen, E Caleiras, N Nuñez-Prado, MA Aznar, S Lykkemark, J Martínez-Torrecuadrada, I Melero, FJ Blanco, J Bernardino de la Serna, JM Zapata, L Sanz, L Alvarez-Vallina

A tumor-targeted trimeric 4-1BB-agonistic antibody induces potent anti-tumor immunity without systemic toxicity
NATURE COMMUNICATIONS, **9**, 4809 (2018)

DC Green, MA Holden, MA Levenstein, S Zhang, BRG Johnson, J Gala de Pablo, A Ward, SW Botchway, FC Meldrum

Controlling the fluorescence and room-temperature phosphorescence behaviour of carbon nanodots with inorganic crystalline nanocomposites
NATURE COMMUNICATIONS, **10**, 206 (2019)

AM Santos, A Ponjavic, M Fritzsche, RA Fernandes, J Bernardino de la Serna, MJ Wilcock, F Schneider, I Urbančič, J McColl, C Anzilotti, KA Ganzinger, M Aßmann, D Depoil, RJ Cornall, ML Dustin, D Klenerman, SJ Davis, C Eggeling, SF Lee

Capturing resting T cells: the perils of PLL
NATURE IMMUNOLOGY, **19**, 203-205 (2018)

AR Ahmed, RJ Owens, CD Stubbs, AW Parker, R Hitchman, RB Yadav, M Dumoux, C Hawes, SW Botchway

Direct imaging of the recruitment and phosphorylation of S6K1 in the mTORC1 pathway in living cells
SCIENTIFIC REPORTS, **9**, 3408 (2019)

M Blignaut, B Loos, SW Botchway, AW Parker, B Huisamen
Ataxia-Telangiectasia Mutated is located in cardiac mitochondria and impacts oxidative phosphorylation
SCIENTIFIC REPORTS, **9**, 4782 (2019)

V Kriechbaumer, L Maneta-Peyret, L Fouillen, SW Botchway, J Upson, L Hughes, J Richardson, M Kittelmann, P Moreau, C Hawes

The odd one out: Arabidopsis reticulon 20 does not bend ER membranes but has a role in lipid regulation
SCIENTIFIC REPORTS, **8**, 2310 (2018)

K Sowoidnich, H Kronfeldt

In-situ species authentication of frozen-thawed meat and meat juice using shifted excitation Raman difference spectroscopy
PROCEEDINGS OF SPIE, **10685**, 106850L (2018)

INDIVIDUAL CONTRIBUTIONS AND COLLABORATIVE SCIENCE

- W Schumaker, T Liang, R Clarke, JM Cole, G Grittani, S Kuschel, SPD Mangles, Z Najmudin, K Poder, G Sarri, D Symes, AGR Thomas, M Vargas, M Zepf, K Krushelnick
Making pions with laser light
NEW JOURNAL OF PHYSICS, **20**, 73008 (2018)
- Z Nie, ICE Turcu, Y Li, X Zhang, L He, J Tu, Z Ni, H Xu, Y Chen, X Ruan, F Frassetto, P Miotti, N Fabris, L Poletto, J Wu, Q Lu, C Liu, T Kampen, Y Zhai, W Liu, C Cacho, X Wang, F Wang, Y Shi, R Zhang, Y Xu
Spin-ARPES EUV Beamline for Ultrafast Materials Research and Development
APPLIED SCIENCES, **9**, 370 (2019)
- ICE Turcu, B Shen, D Neely, G Sarri, KA Tanaka, P McKenna, SPD Mangles, T Yu, W Luo, X Zhu, Y Yin
Quantum electrodynamics experiments with colliding petawatt laser pulses
HIGH POWER LASER SCIENCE AND ENGINEERING, **7**, e10 (2019)
- Y Kuramitsu, T Moritaka, Y Sakawa, T Morita, T Sano, M Koenig, CD Gregory, N Woolsey, K Tomita, H Takabe, YL Liu, SH Chen, S Matsukiyo, M Hoshino
Magnetic reconnection driven by electron dynamics
NATURE COMMUNICATIONS, **9**, 5109 (2018)
- J Jarrett, M King, RJ Gray, N Neumann, L Döhl, CD Baird, T Ebert, M Hesse, A Tebartz, DR Rusby, NC Woolsey, D Neely, M Roth, P McKenna
Reflection of intense laser light from microstructured targets as a potential diagnostic of laser focus and plasma temperature
HIGH POWER LASER SCIENCE AND ENGINEERING, **7**, e2 (2018)
- D Kumar, M Šmíd, S Singh, A Soloviev, H Bohlin, K Burdonov, G Fente, A Kotov, L Lancia, V Lédl, S Makarov, M Morrissey, S Perevalov, D Romanovsky, S Pikuz, R Kodama, D Neely, P McKenna, T Laštovička, M Starodubtsev, S Weber, M Nakatsutsumi, J Fuchs
Alignment of solid targets under extreme tight focus conditions generated by an ellipsoidal plasma mirror
MATTER AND RADIATION AT EXTREMES, **4**, 24402 (2019)
- C Conti, A Botteon, C Colombo, M Realini, P Matousek, P Vandenneele, B Laforce, B Vekemans, L Vincze
Contrasting confocal XRF with micro-SORS: a deep view within micrometric painted stratigraphy
ANALYTICAL METHODS, **10**, 3837-3844 (2018)
- JA Griffen, AW Owen, P Matousek
Quantifying low levels of warfarin sodium salts in oral solid dose forms using Transmission Raman Spectroscopy
JOURNAL OF PHARMACEUTICAL AND BIOMEDICAL ANALYSIS, **155**, 276-283 (2018)
- A Botteon, C Colombo, M Realini, S Bracci, D Magrini, P Matousek, C Conti
Exploring street art paintings by microspatially offset Raman spectroscopy
JOURNAL OF RAMAN SPECTROSCOPY, **49**, 1652-1659 (2018)
- CJ Corden, DW Shipp, P Matousek, I Notinger
Fast Raman spectral mapping of highly fluorescing samples by time-gated spectral multiplexed detection
OPTICS LETTERS, **43**, 5733-5736 (2018)
- A Ghita, P Matousek, N Stone
Sensitivity of Transmission Raman Spectroscopy Signals to Temperature of Biological Tissues
SCIENTIFIC REPORTS, **8**, 8379 (2018)
- M Shaikh, AD Lad, D Sarkar, K Jana, GR Kumar, PP Rajeev
Measuring the lifetime of intense-laser generated relativistic electrons in solids via gating their Cherenkov emission
REVIEW OF SCIENTIFIC INSTRUMENTS, **90**, 13301 (2019)
- B Shao, A Eich, C Sanders, AS Ngankeu, M Bianchi, P Hofmann, AA Khajetoorians, TO Wehling
Pseudodoping of a metallic two-dimensional material by the supporting substrate
NATURE COMMUNICATIONS, **10**, 180 (2019)
- SK Mahatha, M Dendzik, CE Sanders, M Michiardi, M Bianchi, JA Miwa, P Hofmann
Quasi-free-standing single-layer WS₂ achieved by intercalation
PHYSICAL REVIEW MATERIALS, **2**, 124001 (2018)
- L Bignardi, D Lizzit, H Bana, E Travaglia, P Lacovig, CE Sanders, M Dendzik, M Michiardi, M Bianchi, M Ewert, L Buß, J Falta, JI Flege, A Baraldi, R Larciprete, P Hofmann, S Lizzit
Growth and structure of singly oriented single-layer tungsten disulfide on Au
PHYSICAL REVIEW MATERIALS, **3**, 14003 (2019)
- SK Mahatha, AS Ngankeu, NF Hinsche, I Mertig, K Guilloy, PL Matzen, M Bianchi, CE Sanders, JA Miwa, H Bana, E Travaglia, P Lacovig, L Bignardi, D Lizzit, R Larciprete, A Baraldi, S Lizzit, P Hofmann
Electron-phonon coupling in single-layer MoS₂
SURFACE SCIENCE, **681**, 64-69 (2019)
- N Holzmann, L Bernasconi, RH Bisby, AW Parker
Influence of charge transfer on the isomerisation of stilbene derivatives for application in cancer therapy
PHYSICAL CHEMISTRY CHEMICAL PHYSICS, **20**, 27778-27790 (2018)
- MM Mang, DT Lloyd, PN Anderson, D Treacher, AS Wyatt, SM Hooker, IA Walmsley, K O’Keeffe
Spatially resolved common-path high-order harmonic interferometry
OPTICS LETTERS, **43**, 5275-5278 (2018)

AG Ghita, N Stone, P Matousek

Characterisation of a novel transmission Raman spectroscopy platform for non-invasive detection of breast micro-calcifications

PROCEEDINGS OF SPIE, **10490**, 104900G (2018)

AS Pirozhkov, TZ Esirkepov, TA Pikuz, AY Faenov, K Ogura, Y Hayashi, H Kotaki, EN Ragozin, D Neely, H Kiriya, JK Koga, Y Fukuda, A Sagisaka, M Nishikino, T Imazono, N Hasegawa, T Kawachi, H Daido, Y Kato, SV Bulanov, K Kondo, M Kando

High-Order Harmonic Generation by Relativistic Plasma Singularities: The Driving Laser Requirements

X-RAY LASERS 2016, 85-92 (2018)

D Rusby, R Gray, N Butler, R Dance, G Scott, V Bagnoud, B Zielbauer, P McKenna, D Neely

Escaping Electrons from Intense Laser-Solid Interactions as a Function of Laser Spot Size

EPJ WEB OF CONFERENCES, **167**, 2001 (2018)

Conference Proceedings

ARTEMIS

DT Lloyd, AS Wyatt, R Chapman, C Thornton, P Majchrzak, A Jones, E Springate, K O'Keeffe

Quantum-Path-Sensitive Inline XUV Interferometry

HIGH INTENSITY LASERS AND HIGH FIELD PHENOMENA 2018 (2018)

ULTRA

SV Lepeshkevich, IV Sazanovich, MV Parkhats, SN Gilevich, BM Dzhagarov

Time-Resolved Multiple-Probe Infrared Spectroscopy Studies of Carbon Monoxide Migration through Internal Cavities in Hemoglobin

2018 INTERNATIONAL CONFERENCE LASER OPTICS, 566 (2018)

VCA Taylor, D Tiwari, M Duchi, DM Donaldson, IP Clark, DJ Fermin, TAA Oliver

Investigating Electron-Phonon Coupling in Formamidinium Lead Iodide Perovskite Using Ultrafast Laser Spectroscopy

2018 IEEE 18TH INTERNATIONAL CONFERENCE ON NANOTECHNOLOGY (2019)

INDIVIDUAL CONTRIBUTIONS AND COLLABORATIVE SCIENCE

YT Li, GQ Liao, D Neely, P McKenna, ZM Sheng, J Zhang
>mJ terahertz radiation sources from intense laser-foil interactions

THE 9TH INTERNATIONAL SYMPOSIUM ON ULTRAFAST PHENOMENA AND TERAHERTZ WAVES (2018)

Theses

ARTEMIS

Aeschlimann, S.

Ultrafast Quasiparticle Dynamics in Graphene and 2D heterostructure

PhD Thesis, MPI Hamburg (2018)

Kliuiev, P.

Reconstruction of Molecular Orbitals from Photoemission Data with Iterative Phase Retrieval Algorithms

PhD Thesis, University of Zurich (2018)

GEMINI

Arran, C.

Techniques for high repetition rate laser wakefield acceleration

PhD Thesis, University of Oxford (2018)

Shaloo, R.

Hydrodynamic Optical-Field-Ionized Plasma Waveguides for Laser Plasma Accelerators

PhD Thesis, University of Oxford (2018)

VULCAN

Mirfayzi, S.

Compact Sources of Fast and Moderated Neutrons using High Power Lasers

PhD Thesis, Queen's University Belfast (2018)

Hadjisolomou, P.

Guiding and Post-Acceleration of TNSA Protons Employing Intense EM Pulse from the Laser-Foil Interaction

PhD Thesis, Queen's University Belfast (2018)

Higginson, A.

Optimisation and Control of Ion Acceleration in Intense Laser-Foil Interactions

PhD Thesis, University of Strathclyde (2018)

Rusby, D.
Study of escaping electron dynamics and applications from high-power laser-plasma interactions
 PhD Thesis, University of Strathclyde (2018)

Oliver, M.
Density, temperature and magnetic field measurements in low density plasmas
 PhD Thesis, University of Oxford (2018)

Rigby, A.
Magnetic effects in astrophysically relevant laboratory plasmas
 PhD Thesis, University of Oxford (2018)

Gwynne, D.
Laser-driven Acceleration of Ions: Biological effects at Ultra-High Dose rates
 PhD Thesis, Queen's University Belfast (2018)

ULTRA

O'Reilly, L.
Synthesis, Characterisation, Time-Resolved and Photocatalytic Studies of Inorganic Assemblies for Hydrogen Generation
 PhD Thesis, Dublin College University (2019)

Cheetham, N.
The Effect of Highly Ordered Molecular Conformations on the Optoelectronic Properties of Conjugated Polymers
 PhD Thesis, Imperial College London (2018)

Belhout, S.
Preparation and Characterisation and Application of Nanoparticle Composite Materials
 PhD Thesis, University College Dublin (2018)

Peeks, M.
Electronic delocalisation in linear and cyclic porphyrin oligomers
 PhD Thesis, University of Oxford (2018)

Adrian, S.
Photophysical and Biological Profiling of Ruthenium(II) Polypyridyl Complex-based Systems
 PhD Thesis, Trinity College Dublin (2019)

Black, F.
Probing Photoinduced Dynamics Within Dye-Sensitised Solar Cells
 PhD Thesis, Newcastle University (2018)

Aucott, B.
Synthesis, Properties, and Evaluation of Mn(I) Tetracarbonyl CO-Releasing Molecules as Therapeutics
 PhD Thesis, University of York (2018)

OCTOPUS

Ahmed, A.
Determining S6K1 localisation and interactions with mTORC1 in live cells using fluorescence lifetime imaging microscopy
 PhD Thesis, Oxford Brookes University (2018)

King, S.
Optical Imaging of Tumour Vasculature using Novel Gold Nanoparticle Probe
 PhD Thesis, University of Birmingham (2018)

Panel Membership and CLF Structure

Laser for Science Facility Access Panel 2018/19

REVIEWERS

Professor J. Molloy (Chair)
Francis Crick Institute, London

Professor C. Bain
Department of Chemistry
Durham University

Dr S. Cox
Randall Division of Cell and Molecular Biophysics
King's College London

Dr I. Dobbie
Department of Biochemistry
University of Oxford

Dr M. Frogley
Diamond Light Source
Harwell Science and Innovation Campus

Professor M. Garcia Parajo
The Institute of Photonic Services
Mediterranean Technology Park

Dr N. Hunt
Department of Physics
University of Strathclyde

Dr M. Kuimova
Department of Chemistry
Imperial College London

Dr S. Leveque-Fort
Institut des Sciences Moléculaires d'Orsay – UMR 8214
Université Paris-Sud

Professor J. Moger
Physics and Medical Imaging
College of Engineering, Mathematics and Physical Sciences
University of Exeter

Dr D. Mulvihill
School of Biosciences
University of Kent

Dr S. Pascu
Department of Chemistry
University of Bath

Professor M. Peckham
Faculty of Biological Sciences
University of Leeds

Dr D. Scott
School of Biosciences
University of Nottingham

Professor K. Vincent
Department of Chemistry
University of Oxford

Dr M. Volk
Department of Chemistry
University of Liverpool

Professor J. Weinstein
Department of Chemistry
University of Sheffield

Professor K. Wynne
School of Chemistry, WestCHEM
University of Glasgow

RESEARCH COUNCIL REPRESENTATIVES

K. Brakspear
MRC

A. Chapman
EPSRC

J. Swarbrick
BBSRC

E. Swain
STFC

L. Garratt
NERC

SCIENCE & TECHNOLOGY FACILITIES COUNCIL REPRESENTATIVES

Dr D.T. Clarke (Head of Laser for Science Facility)
Central Laser Facility
Science & Technology Facilities Council

Prof J.L. Collier (Director)
Central Laser Facility
Science & Technology Facilities Council

Professor M. Towrie (ULTRA Group Leader)
Central Laser Facility
Science & Technology Facilities Council

Dr M. Martin-Fernandez (OCTOPUS Group Leader)
Central Laser Facility
Science & Technology Facilities Council

Dr A. Kaye
ISIS Neutron & Muon Source
Science & Technology Facilities Council

Professor J. Naismith (Director)
Research Complex at Harwell

Professor L. Chapon (Physical Sciences Director)
Diamond Light Source

Dr E. Gozzard
Central Laser Facility
Science & Technology Facilities Council

Artemis Facility Access Panel 2018/19

REVIEWERS

Professor M. Vrakking (Panel Chairman)
Max Born Institute, Berlin

Professor M. Aeschlimann
University of Kaiserslautern, Germany

Dr J. Stahler
Fritz Haber Institute, Germany

Professor H. Fielding
Department of Chemistry, Christopher Ingold Laboratories
University College London

Professor J. Tisch
Department of Physics, Blackett Laboratory
Imperial College London

Professor L. Perfetti
Laboratoire des Solides Irradies, Ecole Polytechnique
Palaiseau Cedex

Professor A. Taleb-Ibrahimi
Synchrotron SOLEIL, L'Orme des Merisiers, France

Dr P. King
School of Physics and Astronomy
University of St. Andrews

SCIENCE & TECHNOLOGY FACILITIES COUNCIL REPRESENTATIVES

Professor J.L. Collier (Director)
Central Laser Facility
Science & Technology Facilities Council

Ms C. Hernandez-Gomez (Head, High Power Laser Programme)
Central Laser Facility
Science & Technology Facilities Council

Dr E. Springate (Artemis Group Leader)
Central Laser Facility
Science & Technology Facilities Council

Dr R.T. Chapman (Artemis, AMO and Imaging)
Central Laser Facility
Science & Technology Facilities Council

Dr D.T. Clarke (Head of Laser for Science Facility)
Central Laser Facility
Science & Technology Facilities Council

Professor M. Towrie (Molecular and Structural Dynamics)
Central Laser Facility
Science & Technology Facilities Council

Vulcan, Astra TA2 & Gemini Facility Access Panel 2018/19

REVIEWERS

Professor N. Woolsey (Panel Chair)
York Plasma Institute
University of York

Professor M. Borghesi
Department of Pure and Applied Physics
Queen's University of Belfast

Professor G. Gregori
Clarendon Laboratory
University of Oxford

Professor A. Thomas
Physics Department
University of Lancaster

Dr J. Pasley
York Plasma Institute
University of York

Professor G. Tallents
York Plasma Institute
University of York

Professor T. Arber
Department of Physics
University of Warwick

Dr R. Kingham
Blackett Laboratory
Imperial College London

Dr A. Klisnick
Institut des Sciences Moléculaires d'Orsay
Université Paris-Sud

Professor M. Tatarakis
TEI Crete

RESEARCH COUNCIL REPRESENTATIVES

M. Rolph
EPSRC

Mr C. Danson
AWE

SCIENCE & TECHNOLOGY FACILITIES COUNCIL REPRESENTATIVES

Professor J.L. Collier (Director)
Central Laser Facility
Science & Technology Facilities Council

Ms C. Hernandez-Gomez (Head, High Power Laser
Programme)
Central Laser Facility
Science & Technology Facilities Council

Dr I.O. Musgrave (Vulcan Group Leader)
Central Laser Facility
Science & Technology Facilities Council

Mr R.J. Clarke (Experimental Science Group Leader)
Central Laser Facility
Science & Technology Facilities Council

Dr R. Pattathil (Gemini Group Leader)
Central Laser Facility
Science & Technology Facilities Council

Dr D. Symes (Gemini Target Area Section Leader)
Central Laser Facility
Science & Technology Facilities Council

Dr N. Booth (Panel Secretary)
Central Laser Facility
Science & Technology Facilities Council

Mr C. Spindloe
Central Laser Facility
Science & Technology Facilities Council

Dr A. Kaye
ISIS Neutron & Muon Source
Science & Technology Facilities Council

E. Swaine
Science Programme Office
Science & Technology Facilities Council



Central Laser Facility Structure



Director

Professor John Collier
john.collier@stfc.ac.uk





Science and
Technology
Facilities Council

